This is to certify that the

dissertation entitled

LOCAL ENERGY FUNCTION METHODS FOR
POWER SYSTEM TRANSIENT STABILITY

presented by

Parviz Rastgoufard

has been accepted towards fulfillment
of the requirements for

Ph.D. degree in Electrical Engineering

Robert Schlueter
Major professor

Date 7/21/83

LOCAL ENERGY FUNCTION METHODS FOR POWER SYSTEM TRANSIENT STABILITY

By

Parviz Rastgoufard

A DISSERTATION

Submitted to
Michigan State University
in partial fulfillment of the requirements
for the degree of

DOCTOR OF PHILOSOPHY

Department of Electrical Engineering
and Systems Science

1983

ABSTRACT

LOCAL ENERGY FUNCTION METHODS FOR
POWER SYSTEM TRANSIENT STABILITY

By

Parviz Rastgoufard

Energy function, the first integral of the accelerating power equation, is used to investigate the problem of power system transient stability. In contrast to the total system (global) energy function, the partial (local) energy function, which is the energy existing <u>between</u> and <u>within</u> an "accelerated" and a "stationary" group of generators, is considered in the analysis. Based on simulation, it has been shown that the local energy function results in a larger region of stability and removes some of the conservativeness of the direct method of Lyapunov.

Furthermore, the concepts of "critical group," the group of generators separating from the system simultaneously, "critical generator," the individual generator the behavior of which dictates the transient stability of the entire power system and the "critical boundary," an appropriate boundary around the critical generator which is used to determine the region of stability (critical clearing time) of the power system have been introduced and investigated. The "Local Kinetic Energy Condition" (LKEC) and the "Local Equal Area Condition"

(LEAC) are two critical boundaries that are based on kinetic and potential energy of the individual generator (critical generator).

The concepts and computational algorithms based on LKEC and LEAC are tested on the 17-generator "Reduced Iowa System." The simulation results verify that the region of stability determined from the individual machine boundaries are accurate and very close to the results obtained from the simulation of the entire power system (the actual region of stability).

FOREWORD

Consumers Power Company support entitled "In Support of an Education and Research Program in Power System at Michigan State University" and the DOE contract entitled "Development of Operations Model for Smaller Utilities Using Wind Electric Conversion Systems" provided the means of research assistantships throughout the completion of this thesis. Both the Consumers Power Company and DOE are gratefully appreciated and acknowledged for their support.

For my wife Hilda

and

my parents Parvin and

Mohammad Mehdi

ACKNOWLEDGEMENTS

I realize that anyone's success is tremendously due to the help and support received from the other members of the society. Sincerely, I would like to appreciate and acknowledge the help of all the people whom I have been associated with throughout my life.

Specifically, I would like to thank the sacrifice, concern and unconditional help of my brothers, sister and my parents.

For the years at Michigan State University, I would like to appreciate and thank Professor R. A. Schlueter, my major advisor, for his continuous material and moral support in the entire course of this study. I would like to extend my appreciation to the members of the advising committee, Professors G. L. Park, R. Rosenberg, H. Khalil and R. A. Schlueter, for reading and correcting the manuscript and sharing their thoughtful and constructive comments. I am also indebted to Professor J. B. Kreer, the chairman of the Department of Electrical Engineering and System Science, for support of the extensive computer cost of the thesis.

I would like to appreciate the thoughtful discussions and moral suppport of my friends Fariborz and Abbas. I wish to express my thanks to Bakhtiar, my dear friend, for his help in preparing the first draft of the thesis.

Most of all, I am forever thankful to Hilda, my wife, for her continuous encouragement, patience, love, understanding and constructive discussions. I also would like to acknowledge Hilda's prompt and excellent typing of the first draft of the dissertation.

Lastly, I appreciate Mrs. Carolyn Samet for her fine typing of the final draft of the dissertation.

TABLE OF CONTENTS

Page

LIST OF TABLES

LIST OF FIGURES

Page

CHAPTER 1

INTRODUCTION

1.1 The Basic Problem

In the interconnected power system, the question of availability of a continuous and an uninterrupted electric energy supply is of main concern. The ever-increasing dependence of society on electric energy requires not only the production of a continuous electric supply but also energy within acceptable quality limits.

The quality (the magnitude and frequency of the voltage at the consumer's terminal) and the continuity of service (lack of interruptions) [1] is most significantly affected by the occurrence of disturbances in the power system. The interconnection of a power system partially guarantees the desired quality and continuity of service. However, as the size of the interconnection grows, the operation and planning of the power system become a challenging task and the questions of security and reliability assume greater importance.

A vital concern for both the planning and operating engineer in their decision making is the transient stability of the power system. The concept of stability arises when the power system is subjected to the occurrence of a disturbance. Depending upon the size of the disturbance, the power system stability is divided into two categories. First, if the size of the disturbance is small, such as a small change in load, then the power system variables, such as the rotor angles, powers, etc., undergo a small deviation from their nominal value if the system is stable around a particular operating point. This type of stability is called steady state stability. Second, if the size of the disturbance is large, a transition from one operating state to another results. The issue of transient stability is related to the second category when the behavior of the system response to occurrence of a large disturbance (electrical fault, loss of a generator, or loss of a part of the transmission network) is of interest.

If during the transition all of the generators maintain synchronous speed, then the transition is considered to be stable. However, if one or more generators lose synchronism, instability results. Loss of synchronism of one or more machines may lead to cascading interruptions and black-outs [2].

The concept of transient stability is used by the planning engineer in both

- long-term planning, and
- short-term planning.

In long-term planning (where the need for additional generation or transmission 5-20 years in the future is of concern), planning engineers consider several alternatives and investigate the behavior of each alternative in response to a set of contingencies. From the planning point of view the loss of one or more transmission lines or the dropping of one or more generators in the power system must be considered a first step in evaluating each expansion alternative. These contingencies should not result in loss of stability or security for any of the alternatives if the alternative is to be considered further. This security analysis is performed for each of the several expansion planning alternatives using a DC load-flow security analysis for possibly all first and second contingencies and several third contingencies. This early approximate analysis is primarily performed to filter out some of the contingencies and select those contingencies which require further analyses using AC load flows or which show a planning alternative meeting certain design requirements. After the early approximate contingency analyses and a more careful load-flow analysis of a few contingencies, a set of transient stability simulation runs is performed to further investigate the performance of each planning alternative under the combinations of possible loading level transfers and line outage contingencies. Clearly, a more reliable expansion plan would result if one is able to apply a larger number of transient stability runs for a wider spectrum of loading and transfers as well as for a larger number of proposed contingencies to each alternative plan. Thus, there is a need for the development of direct methods for assessing transients in expansion planning applications that would reduce computation requirements and allow many hundreds of stability simulations at reasonable cost and memory would significantly improve expansion planning security assessment and reduce its cost.

In operation or short-term planning, the planning of network maintenance, unit commitment and generation dispatch schedules over a day or weeks must be checked to assess whether the system is vulnerable to security or stability problems. Thus, the proposed operation plan must be checked for security or stability violations over that period due to single or multiple line outage, loss of generation contingencies or fault contingencies. The system must be able to survive abnormal disturbances, such as faults and loss of system elements, created by equipment malfunctions, switching surges, lightening strikes, etc. [3]. Hence, in short-term planning a larger number of transient stability simulation runs are desired. However, in recent years this task has become complicated due to [4]:

- size increase of power system interconnections;
- the emphasis on consideration of more detailed power system models;
- the concern to model the components of system such as power system stabilizers, static VAR compensators, DC lines, braking resistors;
- and consideration of the transient stability for more than first-swing behaviors.

The benefits of reduced computation and manpower in applying the direct methods of assessing power system transient stability in both long- and short-term planning is clearly seen. Similarly in on-line operation of the power system, the operating engineer is also interested in investigating the response of the power system for a proposed fault contingency and a network configuration, unit commitment, and generation dispatch not investigated in the operation planning effort. However, in contrast to the operation planning stage, the time frame for study of specific contingencies is very short and at times quick decisions must be made. Moreover, the computation capabilities that are available for transient stability simulation are limited compared to off-line operation and expansion planning. However, there is a need for on-line transient stability analysis, but the transient stability analysis performed must be capable of on-line implementations, which implies rapid and computationally efficient solution such as might be available if direct methods were available.

The most widely used and implemented transient stability analysis is obtained by the time solution of the machine's rotor angles. Then, based on the observation of the swing curves and engineering judgment, the stability or instability of the power system is decided. The disadvantages of this technique are [2]:

- "in each study, stability (or instability) is determined for a given system condition and for a given impact (fault, etc.) only,
- a clear-cut indication of stability (or instability) is not always possible,
- the computation is cumbersome and time consuming for a large system, especially if on-line digital computer analysis is contemplated."

The drawbacks of the time solution and the need for fast, computationally efficient and approximate transient stability analysis made researchers inquire into an alternative approach. As a result, the concept of direct methods of stability was pursued. From the early stages of development, the direct methods of Lyapunov and the energy function analysis showed promise of assessing transient stability rapidly without the computation required to integrate the many system differential equations even though the method remained far from implementation. The use of such a method for contingency analysis in expansion planning, operation planning and on-line operation was exciting. It is clear, however, that such methods would never replace time solution for accurate stability assessment or design of generation controls.

The historical development of the direct methods for transient stability in this area is divided into three distinct but continuous phases. This division is primarily considered to indicate the turning points in the development and does not include all previous work.

Phase One: The work of Magnusson in 1947 [5] considers a classical model representation of the power system. In this representation the transfer conductance is omitted and an energy function for the system is evaluated. Then the critical energy, by which the region of stability is identified, is determined by the energy of the lowest saddle point, V_{1s}. The work of Aylett in 1958 [6] is devoted to finding an energy integral. The kinetic (KE) and potential (PE) components of energy are identified and the stability of the power system is decided by determining whether $KE < PE$.

Phase Two: The work in phase one, although outstanding in the elaboration of the concept, was far from implementation. The main issues remaining were:

- to resolve the difficulty in obtaining all singular points,
- to be able to identify the correct singular point,
- to be able to include the transfer conductances in the model,
- to have the ability to identify the critical value of energy at clearing which if exceeded would result in loss of stability.

The work of El-Abiad et al. [7] and Prabhakara et al. [8] was devoted to finding the appropriate saddle points and hence the critical energy. The work of Uyemura et al. [9] was devoted to approximating the transfer conductance term, while Smith and Tavora [10] initiated the first work toward considering the critical energy which was related to the faulted trajectory.

Phase Three: The work in references [4,11,12] in development of the Potential Energy Boundary Surface (PEBS) and [13,14,15] in development of energy accounting by using the transient energy function mark the latest advances of algorithms for direct assessment of transient stability. A main characteristic of this phase is that the critical value evaluated is directly related to the fault trajectory and hence a larger region of stability is obtained. The work in this phase will be discussed in detail in Chapter 2.

However, in spite of these encouraging results, it is believed that the true region of stability is identified by consideration of local kinetic and potential energy of an individual machine rather than global kinetic and potential energies of all generators in the system. This investigation attempts to identify the particular individual machine whose behavior dictates the stability of the entire system. Furthermore, it is shown that the region of stability obtained by the algorithms based on these concepts is the most accurate attained to date.

To achieve the goals, the content of Chapter 2 is devoted to describing the behavior of the power system and the concept of transient stability analysis. The historical development of the direct methods for transient assessment is revisited in further detail. The concepts and algorithms based on potential energy boundary surface [4,11,12] and global energy accounting [13,14,15] are explained.

Chapter 3 considers the presence of energy within and between coherent groups of generators that swing together due to the fault energy. Based on this division of energy, an analogy to the "equal area criterion" of a one-machine infinite bus system is obtained by aggregating the energy function without aggregating the power system model used for simulation. The analysis of within-group and between-group potential and kinetic energies of the system was used as a foundation to develop a reasonably accurate algorithm for estimating the critical clearing time of the entire power system. This algorithm is based on the assumption that the kinetic energy between groups (the accelerated group and the rest of the system) will approach zero at some time after fault clearing only when the system is stable. If the system is not stable, the minimum of the between-group kinetic energy over time after fault clearing is a measure of the excess energy at clearing that caused the loss of stability.

Chapter 4 proposes and justifies two hypotheses that (a) the stability of a group of machines and thus the system is dictated by a region of stability for one machine in that group and (b) that this region of stability is reflected in the kinetic and potential energy of this machine. The individual machine energy function is then presented and shown not to be a Lyapunov function. An algorithm [16] is then justified that utilizes the maximum individual generator potential energy as a function of time for a fault on trajectory as a critical energy threshold for deciding whether the system is or is not stable. This threshold energy value is compared with the sum of the individual generator kinetic and potential energy at fault clearing to decide retention or loss of stability. This justification is based on the assumption that the transmission network connected to the generator has a maximum magnetic energy available for decelerating the generators' initial fault acceleration. This maximum potential energy over time for a fault on trajectory is further assumed to be a measure of this maximum energy for deceleration.

A second criterion for determining the boundary of stability for this individual generator is then justified based on the kinetic energy of the individual generator. This criterion suggests that the individual generator kinetic energy minimum over time after the fault is cleared will only approach zero if the system is stable. The zeroing of kinetic energy indicates a reversal of initial direction of motion caused by the fault which in turn suggests stability for this generator.

A justification of the hypothesis that one generator in the fault-accelerated group of machines dictates the stability of the group is then made. An explanation based on physical reasoning is offered for why this will occur and then this explanation is justified based on the simulation of the energy of individual generators in an accelerated group for a particular fault case on the Reduced Iowa System.

Chapter 5 presents two algorithms based on the kinetic and potential energy conditions discussed above. These conditions indicate a crossing of the boundary of stability for the individual generators. Simulation results are then presented that indicate these algorithms are extremely accurate and hold significant promise for future development of both accurate and computationally efficient procedures.

Finally, in Chapter 6 the contribution of this investigation and the avenues for future inquiry are considered.

CHAPTER 2

THE ENERGY FUNCTION AND ITS USE IN POWER SYSTEM TRANSIENT STABILITY

2.1 Power System Behavior During A Transient

When the power system is operating in its normal state, all the equality and inequality constraints are satisfied, there is negligible imbalance between supply and demand, and all the generators are operating at synchronous speed. In this situation the system is said to be operating at its stable equilibrium operating point $\underline{X}^{sl}$ (s.e.p.) defined by

$$\dot{\underline{X}} = \underline{f}_o(\underline{X}^{sl},\underline{P}^o) = \underline{0} \tag{2.1}$$

where $\underline{f}_o(\underline{X}^{sl},\underline{P}^o)$ is the transient stability model of the power system with parameters P^o of the pre-fault system. Upon the occurrence of an electrical fault, the power system undergoes two new phases: (a) during the fault, and (b) post-fault (after clearance of the fault).

The dynamic behavior of the power system during the fault phase is governed by a set of nonlinear differential equations of the form

$$\dot{\underline{X}} = \underline{F}_1(\underline{X},P_i^f) \qquad 0 < t < t_c \tag{2.2}$$

where $\underline{P}_i^f$ is the parameter vector of the system for the i^{th} disturbance.

Once the fault is cleared (post-fault phase), the system will assume a new configuration and thus its behavior will be governed by another set of nonlinear differential equations of the form [23]

$$\dot{\underline{X}} = \underline{F}_2(\underline{X},\underline{P}^{pf}) \qquad t > t_c \qquad (2.3)$$

If, after the transition from the fault phase to the post-fault phase, synchronism for all the generators in the system is maintained, then transient stability results and the system trajectory will converge toward a post-fault s.e.p.

$$\underline{F}_2(\underline{X}^{s2},\underline{P}^{pf}) = 0 \qquad (2.4)$$

If, after this transition, synchronism of all the generators is not maintained, the trajectory will pass close to an unstable equilibrium point (u.e.p.) that satisfies

$$\underline{F}_2(\underline{X}^{u},\underline{P}^{pf}) = \underline{0} \qquad (2.5)$$

For understanding the transient stability, it is essential to comprehend the interaction between the input and output power of the generators during these two phases. The following example is an attempt to clarify the point.

Consider the CIGRE 225 Kv system [17] depicted in Figure 2.1. Prior to the occurrence of the fault at $t(\bar{0})$,

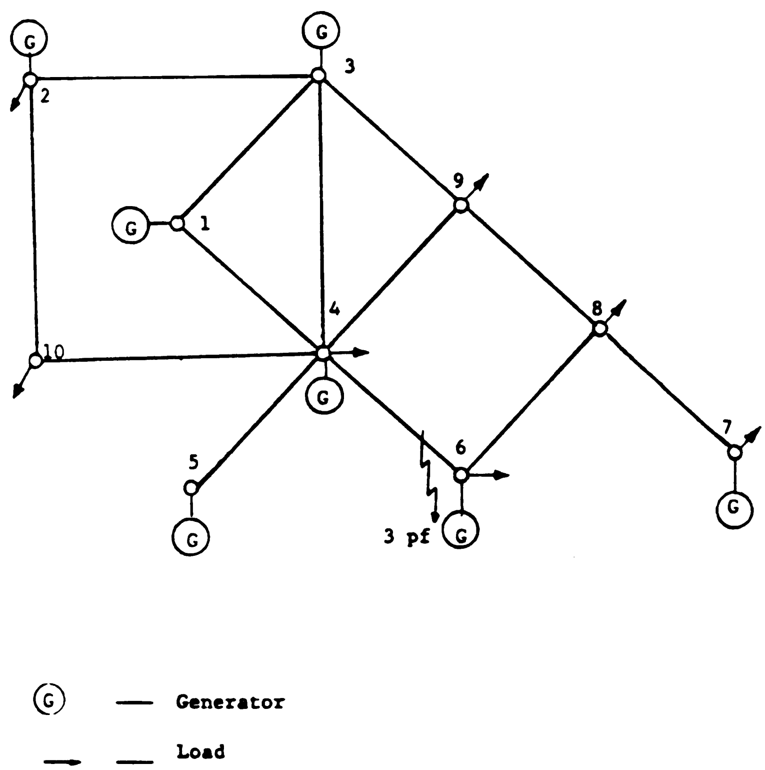

Figure 2.1 CIGRE 225 kV system

the system is operating at the pre-fault s.e.p. Due to the distribution of the load, let us assume that there is a large power flow from bus 6 to bus 4, through line 6-4. Let us further assume that all the electric power needed on load bus 8 is supplied through line 7-8 and from generator 7, so that there is no flow of power from bus 6 to bus 8 by line 6-8.

At the time t(0) a 3-phase fault is applied to the line 6-4 near bus 6. After a fraction of a second at time t_c, the fault is cleared by tripping out line 6-4.

The outage of line 6-4 introduces a mismatch between the input (mechanical) and the output (electrical) power of bus 6 which is electrically closest to the location of the disturbance. Depending upon the period of the fault clearing time t_c, two events may happen. If t_c is less than a critical time t_{cc}, generator 6 may accelerate initially but return to synchronous speed eventually. In contrast, for t_c longer than t_{cc}, generator 6 will accelerate and pull out of step from the rest of the system.

Once the fault is cleared and the voltage on bus 6 is recovered, the excess electric power of bus 6 will be transferred to bus 8 via line 6-8. This power flow will reduce the flow of energy from bus 7 to bus 8 and thus cause another power mismatch at bus 7. The second power mismatch forces generator 7 to accelerate and pull out of step. Similar arguments indicate that some of the generators in the system would decelerate and fall out of synchronism.

Note that in this example generators 6, 7 or both 6 and 7 may pull out of step and thus result in different modes of instability, and hence different unstable equilibrium points (u.e.p.). For a multi-machine power system all the singular points are identified by the solution $\underline{X}^{u}$ of the equation $\underline{0} = F_2(\underline{X}^{u}, \underline{P}^{pf})$. Among the singular points one is the post-fault (s.e.p.) $\underline{X}^{s2}$, and the rest are either (u.e.p.) $\underline{X}^{u}$ or saddle points. Theoretically once the trajectory of the system passes one of these u.e.p.'s or saddle points, then instability is resulted and it is impossible to return to a normal operating state.

In this section the concepts of transient stability and critical clearing time were discussed based on the mismatch between the input and output powers of the generators. An alternative approach investigates this concept by comparison of energy at two different instants of time. The energy produced in the "during fault phase" is compared to a "critical energy" and transient stability or instability is concluded. The next section is devoted to the transient stability analysis from the energy point of view.

2.2 Transient Energy Analysis

2.2.1 Discussion

Before the occurrence of the fault, the power system is residing at the pre-fault s.e.p. and the machine velocities are zero. As was discussed previously, the fault changes the network configuration of the system and some of the generators accelerate (or decelerate). During the fault period the machine velocities will increase, thus increasing kinetic energy. This increase in kinetic energy moves the system from its pre-fault s.e.p. $\underline{X}^{s1}$. At clearing time t_c, the fault is removed and a new network configuration results. The excess kinetic energy produced during the fault period is distributed in the post-fault network according to the load and network requirements. If the motion of the accelerated (or decelerated) generators is reversed--due to the kinetic energy distribution, then the system converges toward the post-fault s.e.p. where again the machine velocities are zero. If the motion of the accelerated generator is not reversed, a loss of stability occurs. The restoring forces of the post-fault network are proportional to relative rotor position of generators and thus the electro-magnetic forces of the post-fault network could be considered as producing or recovering stored potential energy in the network elements.

The mechanism by which the disturbed system assumes a new equilibrium point is one of converting the kinetic energy (produced during the fault) to potential energy (produced after the fault clearing). Comparison of the kinetic and potential energy of the system enables one to draw some conclusion on the transient stability of the system. If all the kinetic energy is converted to potential energy, then stability is resumed and a new s.e.p. is obtained. In this case the post-fault network was able to slow down the accelerated generators and in the transition from pre-fault s.e.p. to post-fault s.e.p. the synchronism was maintained.

In contrast, if the kinetic energy exceeded the potential energy capacity of the network, then instability resulted. This situation implies that some of the generators at clearing time have accelerated considerably and the restoring energy is not able to slow them down. In this case synchronism is lost.

There are several approaches for transient energy analysis, but what they all have in common is that the energy at clearing V_{c1} is compared to a critical value V_{cr} which solely depends on the post-fault configuration. Evaluation of an accurate critical value has been the goal of many researchers in this area. Further investigation on the subject requires a mathematical model representing the dynamic behavior of the power system. In section 2.4.2 the system model is introduced and the latter part of this chapter is then devoted to the discussion of the direct methods that evaluate both clearing and critical energies.

2.2.2 Mathematical Formulation

The dynamic behavior of the power system is described by a set of nonlinear differential equations. The order of these differential equations depends upon two factors, the time frame of interest and the inclusion of the components of the power system. Fouad [2] states that the mathematical model of a synchronous machine with amortisseur windings, exciter and turbine-governor can be a set of fourteen first-order differential equations. Other controls such as power system stabilizer, boiler, etc., increase the complexity.

The complexity will become more apparent if a multi-machine power system is considered. Even for modern computing facilities, the solution of several thousand nonlinear coupled differential equations is a challenging task. For the purpose of investigation of stability for short clearing times and for approximate and easily computed transient security assessment, a simplified classical model will determine the dynamic behavior of the power system. The classical model is valid and useful if the time frame of investigation is limited to order of one second.

The classical model used in this dissertation is characterized by [18]:

(1) Mechanical power input from the turbine is constant.

(2) Damping coefficient, both mechanical and electrical, is neglected.

(3) The voltage behind transient reactance of the synchronous machine is assumed to be constant.

(4) The mechanical rotor angle of a machine coincides with the angle of the voltage behind the transient reactance.

(5) The dynamic behavior of the load is neglected. Loads are represented by constant impedances.

Using the classical model, the equation of motion for machine i is represented as 2.6

$$M_i \dot{\omega}_i = P_i - P_{ei} \tag{2.6}$$

$$\delta_i = \omega_i \qquad\qquad i = 1,2,\ldots,n$$

where:

$$P_{ei} = \sum_{\substack{j=1 \\ j \neq i}}^{n} C_{ij} \mathrm{Sin}(\delta_i - \delta_j) + D_{ij} \mathrm{Cos}(\delta_i - \delta_j)$$

$P_i = P_{mi} - E_i^2 G_{ii}$

$C_{ij} = E_i E_j B_{ij}$

$D_{ij} = E_i E_j G_{ij}$

P_{mi} = mechanical input power

E_i = constant voltage behind transient reactance

δ_i = rotor angle

ω_i = rotor speed

M_i = moment of inertia

G_{ij} = real part of the reduced bus admittance matrix connecting bus i to j

B_{ij} = imaginary part of the reduced bus admittance matrix connecting bus i to j

G_{ii} = Sum of negative of G_{ij}'s for row i and columns $j=1,2,\ldots,i-1,i+1,\ldots,n$

The <u>transient energy function</u> proposed by Athay et al [4] is obtained from equation (2.6) by first evaluating the relative accelerating equations of machines i and j

$$M_i M_j (\dot{\omega}_i - \dot{\omega}_j) = (M_j P_i - M_i P_j) - (M_j P_{ei} - M_i P_{ej}) \tag{2.7}$$

Then, multiplying both sides of (2.7) by relative velocity $(\omega_i - \omega_j)$ and summing the resulting equations for all possible $n(n-1)/2$ combinations, (2.8) is produced

$$\sum_{i=1}^{n-1} \sum_{j=i+1}^{n} M_i M_j (\dot{\omega}_i - \dot{\omega}_j)(\omega_i - \omega_j) = \sum_{i=1}^{n-1} \sum_{j=i+1}^{n} (M_j P_i - M_i P_j)(\omega_i - \omega_j)$$

$$- \sum_{i=1}^{n-1} \sum_{j=i+1}^{n} (M_j P_{ei} - M_i P_{ej})(\omega_i - \omega_j) \tag{2.8}$$

By integrating (2.8) from an arbitrary reference (a s.e.p.) to a variable upper limit, the transient energy function V of (2.9) is obtained

$$V = \sum_{i=1}^{n-1} \sum_{j=i+1}^{n} \frac{1}{2M_T} M_i M_j (\omega_i - \omega_j)^2 - \frac{1}{M_T} (P_i M_j - P_j M_i)(\delta_{ij} - \delta_{ij}^s)$$

$$-C_{ij}(\mathrm{Cos}\ \delta_{ij} - \mathrm{Cos}\ \delta_{ij}^s) + \int_{\delta_i^s + \delta_i^s - 2\delta_o}^{\delta_i + \delta_j - 2\delta_o} D_{ij} \mathrm{Cos}\ \delta_{ij}\, d(\delta_i + \delta_j - 2\delta_o) \tag{2.9}$$

where:

$$M_T = \sum_{i=1}^{n} M_i$$

$$\delta_o = \frac{1}{M_T} \sum_{i=1} M_i \delta_i \tag{2.10}$$

The terms in the transient energy function are physically identifiable. The first term corresponds to the total kinetic energy of the system, the second term is the energy produced from rotor angle disposition and thus the position energy, the third term relates to the magnetic energy and finally the fourth term is related to the real part of the post-fault reduced admittance matrix and thus the conductance (dissipative) energy. The last three terms constitute the total potential energy of the system.

The transient energy function of (2.9) is derived from the equation of motions of synchronous machines which are referenced with respect to a synchronously moving frame. This representation is particularly valuable if the interaction of energy between generators is of interest. It is, however, possible to formulate the swing equations with respect to a fictitious center of inertia reference frame. Let

$$\omega_o = \frac{1}{M_T} \sum_{i=1}^{n} M_i \omega_i \tag{2.11a}$$

$$\delta_o = \frac{1}{M_T} \sum_{i=1}^{n} M_i \delta_i \tag{2.11b}$$

$$M_T \dot{\omega}_o = \sum_{i=1}^{n} M_i \dot{\omega}_i = \sum_{i=1}^{n} (P_i - P_{ei}) \triangleq P_{COA} \tag{2.11c}$$

The machine rotor angle and velocity with respect to the center of inertia is defined as

$$\vartheta_i = \delta_i - \delta_o$$
$$\tilde{\omega}_i = \omega_i - \omega_o \tag{2.12}$$

From (2.6), (2.11) and (2.12) the dynamic behavior of the machines with respect to the center of inertia is

$$M_i\dot{\tilde{\omega}}_i = P_i - P_{ei} - \frac{M_i}{M_T} P_{COA}$$
$$\dot{\vartheta}_i = \dot{\tilde{\omega}}_i \qquad i=1,2,\ldots,n \tag{2.13}$$

Applying the steps in obtaining the transient energy function of (2.9) on (2.13) and noting that

$$\sum_{i=1}^{n} M_i\vartheta_i = \sum_{i=1}^{n} M_i\omega_i = 0$$

results in the transient energy function of (2.14)

$$V = \frac{1}{2}\sum_{i=1}^{n} M_i\tilde{\omega}_i^2 - \sum_{i=1}^{n} (P_i(\vartheta_i-\vartheta_i^s) - \sum_{i=1}^{n-1}\sum_{j=i+1}^{n} C_{ij}(\mathrm{Cos}\vartheta_{ij}-\mathrm{Cos}\vartheta_{ij})$$
$$-\int_{\vartheta_i^s+\vartheta_j^s}^{\vartheta_i+\vartheta_j} D_{ij}\mathrm{Cos}\ \vartheta_{ij}d(\vartheta_i+\vartheta_j) \tag{2.14}$$

where $\vartheta_{ij} = \vartheta_i-\vartheta_j$.

Equations (2.9) and (2.14) define the system transient energy from a s.e.p. (pre-fault or post-fault) to an arbitrary position. If the lower and upper limits are chosen as pre-fault s.e.p., ϑ^{s1} and the angle at clearing time ϑ^{c}, respectively, then the transient energy identifies the energy of the system accumulated in the fault period, $\underline{V}_{c1}$.

Similarly, if the transient energy is evaluated between the post-fault s.e.p., ϑ^{s2} and a critical angle, say, an appropriate unstable equilibrium point, ϑ^{u}, the critical energy V_{cr} is obtained.

Note that the integration of the conductance term in (2.9) and (2.14) requires the knowledge of the trajectory of the system. Since the clearing time is relatively short, the system trajectory can be simulated up to this point using an appropriate numerical integration technique, and thus V_{c1} can be evaluated. However, a closed-form expression for transient energy function is required if V_{cr} is to be evaluated without significant computation.

In order to use the transient energy function as a direct method for assessing transient stability, an approximation to the conductance energy term is necessary. By assuming a linear trajectory in the angle space, the integral term is expressed as (2.15) [4]

$$I_{ij} = \int_{\vartheta_i^s+\vartheta_j^s}^{\vartheta_i+\vartheta_j} D_{ij} \cos \vartheta_{ij} \, d(\vartheta_i+\vartheta_j)$$

$$= \frac{\vartheta_i+\vartheta_j-\vartheta_i^s-\vartheta_j^s}{\vartheta_i-\vartheta_j-\vartheta_i^s+\vartheta_j^s} \left[\sin \vartheta_{ij} - \sin \vartheta_{ij}^s\right] \cdot D_{ij} \qquad (2.15)$$

Based on (2.15), the transient energy function of (2.9) and (2.14) will become

$$V = \sum_{i=1}^{n-1} \sum_{j=i+1}^{n} \frac{1}{2M_T} M_i M_j (\omega_i - \omega_j)^2 - \frac{1}{M_T} (P_i M_j - P_j M_i)(\delta_{ij} - \delta_{ij}^s)$$

$$-C_{ij}(\text{Cos } \delta_{ij} - \text{Cos } \delta_{ij}^s) + \frac{\delta_i + \delta_j - \delta_i^s - \delta_j^s}{\delta_{ij} - \delta_{ij}^s} \left[\text{Sin } \delta_{ij} - \text{Sin } \delta_{ij}^s \right] D_{ij}$$

$$(2.16)$$

$$V = \frac{1}{2} \sum_{i=1}^{n} M_i \tilde{\omega}_i^2 - \sum_{i=1}^{n} P_i (\vartheta_i - \vartheta_i^s)$$

$$- \sum_{i=1}^{n-1} \sum_{j=i+1}^{n} \Bigg[C_{ij} (\text{Cos } \vartheta_{ij} - \text{Cos } \vartheta_{ij}^s)$$

$$- \frac{\vartheta_i + \vartheta_j - \vartheta_i^s - \vartheta_j^s}{\vartheta_{ij} - \vartheta_{ij}^s} \left[\text{Sin } \vartheta_{ij} - \text{Sin } \vartheta_{ij}^s \right] D_{ij} \Bigg] \qquad (2.17)$$

According to (2.16) or (2.17), the clearing energy V_{c1} and the critical energy V_{cr} are

$$V_{c1} = V \Big|_{\vartheta^{s1}}^{\vartheta^c} \; , \qquad V_{cr} = V \Big|_{\vartheta^{s2}}^{\vartheta^u} \qquad (2.18)$$

This concludes the formulation of the transient energy function. However, the identification of clearing and critical energies by transient energy function is one of dispute; section 2.2.3 is devoted to the further clarification and physical interpretation of this concept.

2.2.3 Transient Stability Assessment by Direct Method

(I) Two-Machine Case: The Equal Area Criterion

The motivation for multi-machine transient stability assessment is provided by the concept of the "equal area criterion" where the swing equations of two machines, or equivalently one machine against an infinite bus with zero transfer conductance, is considered.

The pre-fault, fault, and post-fault nonlinear differential equations are

$$\dot{\underline{X}} = \begin{bmatrix} \dot{\delta} \\ \dot{\omega} \end{bmatrix} = \underline{F}_0(\underline{X},\underline{P}^o) = \begin{bmatrix} \omega \\ \frac{1}{M} \frac{|E|\,|E_\infty|}{X^o} \operatorname{Sin} \delta \end{bmatrix} \tag{2.19}$$

$$\dot{\underline{X}} = \begin{bmatrix} \dot{\delta} \\ \dot{\omega} \end{bmatrix} = \underline{F}_1(\underline{X},\underline{P}^f) = \begin{bmatrix} \omega \\ \frac{1}{M} \frac{|E|\,|E_\infty|}{X^f} \operatorname{Sin} \delta \end{bmatrix} \tag{2.20}$$

$$\dot{\underline{X}} = \begin{bmatrix} \dot{\delta} \\ \dot{\omega} \end{bmatrix} = \underline{F}_2(\underline{X},\underline{P}^{pf}) = \begin{bmatrix} \omega \\ \frac{1}{M} \frac{|E|\,|E_\infty|}{X^{pf}} \operatorname{Sin} \delta \end{bmatrix} \tag{2.21}$$

where:

$|E|$ = voltage magnitude of the internal generator bus

$|E_\infty|$ = voltage magnitude at the infinite bus

δ = angle difference between the generator internal bus and the infinite bus

M = inertia constant

$$\frac{|E| \; |E_\infty|}{X^{o}} \text{ Sin } \delta, \quad \frac{|E| \; |E_\infty|}{X^{f}} \text{ Sin } \delta, \text{ and } \frac{|E| \; |E_\infty|}{X^{pf}} \text{ Sin } \delta$$

are the power angle curves for the pre-fault, fault, and post-fault system differential equations.

Figure 2.2 illustrates the power angle curves for pre-fault, during-fault and post-fault situations. Prior to the occurrence of the fault, the system is residing at ϑ^{s1}, satisfying (2.19), the pre-fault stable equilibrium point, at which the system velocity is zero. Upon occurrence of the fault, the system will accelerate and moves away from ϑ^{s1}. In this motion the system gains an amount of energy proportional to area A_1. By clearance of the fault at ϑ^{c}, the system resumes a new configuration (post-fault power curve on Figure 2.2). The new network attempts to compensate for the energy produced during the fault and moves the system toward the post-fault s.e.p. ϑ^{s2} satisfying (2.20). The remaining restorative energy of the post-fault network is proportional to the area A_2. Note that area A_2 is evaluated from the instant of fault clearing to the unstable equilibrium point ϑ^{u}, satisfying (2.21) and thus resulting in the maximum remaining restorative energy. If the clearing time is such that the area A_1 does not exceed area A_2, then stability is maintained. In contrast, if for a larger clearing time A_1 exceeds A_2, then instability results. That particular clearing time which equates A_1 and A_2 is denoted by the critical clearing times t_{cc}. The prediction of this time is of interest to the power engineer.

The transient energy function of section 2.2.2 for a two-machine system with the assumption of zero transfer conductance is analogous to the equal area criteria.

Considering the situation at clearing time, the transient energy function, using the post-fault network and ϑ^{s1} as reference, is given by [13]:

$$V_{c1} = V\Big|_{\vartheta^{s1}}^{\vartheta^{c}} = \frac{1}{2} M (\tilde{\omega}^{c})^{2} - C(\text{Cos } \vartheta^{c} - \text{Cos } \vartheta^{s1}) - P_{max}(\vartheta^{c} - \vartheta^{s1}) \tag{2.22}$$

where $C = E_1 E_2 B_{12}$, $P_{max} = (P_M - V_1^2 G_{11})$.

The first term in the right-hand side of (2.22) is the kinetic energy produced during the fault and is proportional to the area Oabf of Figure 2.2. The second and third terms add up to the potential energy of the system during the fault which is associated with the (area cdf - area Oed). It is worthwhile to note that, if ϑ^{s2} is used as a reference, then the potential energy term is equal to the area cdf. The clearing energy of (2.21) is thus the area dcfbaed.

The critical energy is evaluated from post-fault s.e.p. ϑ^{s2} to the u.e.p., ϑ^{u}. At both ϑ^{s2} and ϑ^{u} the velocity of the system is zero and thus the critical energy consists of only potential energy,

$$V_{cr} = -C(\text{Cos } \vartheta^{u} - \text{Cos } \vartheta^{s2}) - P_{max}(\vartheta^{u} - \vartheta^{s2}) \tag{2.23}$$

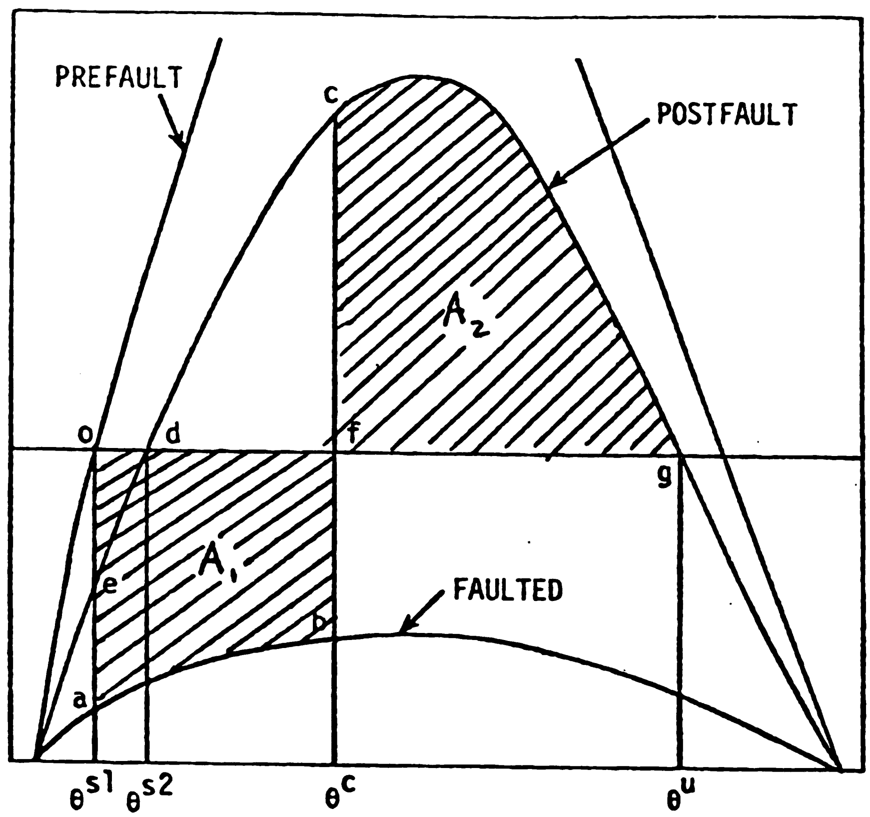

Point o: prefault operating point; $\vartheta = \vartheta^{s1}$, $t = t_o^-$

Point a: electrical power at $t = t_o^+$, $\vartheta = \vartheta^{s1}$

Point b: electrical power at $t = t_c^-$, $\vartheta = \vartheta^{c}$

Point c: electrical power at $t = t_c^+$, $\vartheta = \vartheta^{c}$

Point d: operating point when transient subsides, $t \to \infty$, $\vartheta = \vartheta^{s2}$

Figure 2.2 Power angle curves for one-machine infinite-bus system (transfer conductances neglected) [13]

From Figure 2.2 it is clearly seen that area dgcd corresponds to the right-hand side of (2.23).

When both V_{c1} and V_{cr} use ϑ^{s2} as a reference (which is the case for the investigation of Athay et al. in [4]), the transient energy function is not analogous to the equal area criteria. However, Fouad et al. in [13] argue that the clearing energy should be evaluated from ϑ^{s1} and thus a correction term of

$$V_{cor} = V\Big|_{\vartheta^{s1}}^{\vartheta^{s2}} \tag{2.24}$$

must be added to the critical value, V_{cr}.

$$V'_{Cr} = V_{cr} + V_{cor} = V\Big|_{\vartheta^{s2}}^{\vartheta^{u}} + V\Big|_{\vartheta^{s1}}^{\vartheta^{s2}} = V\Big|_{\vartheta^{s1}}^{\vartheta^{u}} \tag{2.25}$$

V'_{Cr} then corresponds to the area dgcd - Oed and contains the area cdfc - Oed in addition to A_2. The V_{C1} in (2.22) contains area dcfd - Oed in addition to A_1. Thus, the condition

$$V_{C1} \le V'_{Cr}$$

with the correction V_{cor} in V'_{Cr} corresponds to the equal area criterion. The V_{Cr} can be found for multi-machine power systems by computing the proper u.e.p. ϑ^{u} and knowing ϑ^{s2}. Thus, Fouad [13] performed the above analysis to show that it is improper to compare the easily computed $V_{C\ell}$

(2.22) with V_{cr} (2.23) but rather V'_{cr} with the V_{cor} term as in (2.25) to assess whether the system is stable.

In a multi-machine power system the unstable u.e.p. can be computed by minimizing

$$J = \underline{F}_2^T(\underline{X},\underline{P}^{pf})\underline{F}_2(\underline{X},\underline{P}^{pf})$$

based on a proper initial guess for $\underline{X}^u$ where $\underline{F}_2(\underline{X},\underline{P}^{pf})$ are the equations given in equations (2.21).

(II) Three-Machine Case: Potential Energy Surface

The "potential energy surface" is an abstraction which extends the concept of equal area criterion of two-machine to a multi-machine power system. Consider the case where the power system consists of three machines. Taking one machine, ϑ_3, as reference, the maximum ability of the system to absorb the fault energy depends on the relative rotor position ϑ_{13}, ϑ_{23} and thus the potential energy of the remaining machines.

Figure 2.3 [4,14] illustrates a three-machine energy terrain where the horizontal axes are the rotor positions, ϑ_{13}, ϑ_{23} and the vertical axis represents the system's energy. The post-fault s.e.p. could be considered as the bottom of the valley where the potential energy of the system is zero. The valley is surrounded by mountains with different summit and pass elevations (the summits and passes represent the u.e.p.'s and saddle points, respectively). Finally, the system could be thought of as a ball traveling around the s.e.p. and on the potential energy surface.

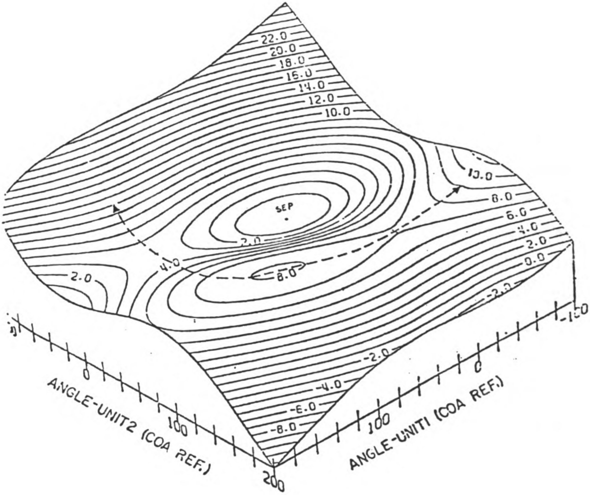

Figure 2.3 Potential energy surface (solid lines) and the boundary surface (dotted line) for three-machine system [4]

The fault energy motivates the ball to climb up the potential surface. At any given time two forces will act on the rolling ball: a force produced by the fault kinetic energy V_{c1}, which pushes the ball in an upward direction, and a force produced by the torque (potential energy) V_{cr}, which pulls the ball downward.

If the moving ball reaches zero velocity before hitting the potential energy boundary surface, PEBS (the boundary which connects the u.e.p.'s and saddle points and is perpendicular to the energy contours), the trajectory is stable and the ball will eventually settle down at $\underline{\vartheta}^{s2}$. In contrast, if the trajectory reaches this boundary, then the ball will escape from the valley and instability results.

The three-dimensional energy terrain is generalized to n-dimensional and the transient energy function of section 2.2.2 mathematically represents this concept. The total potential energy of the system is visualized as an n-dimensioned potential energy terrain where $\underline{\vartheta}^{s2}$ represents the minimum energy point of this surface. Also, there is a one-to-one correspondence between the energy points of this surface and the possible positions of the generators [14].

(III) Evaluation of Clearing and Critical Energies

The determination of the region of stability (critical clearing time) by direct methods has been recently investigated by [4,11,12,13,16]. Athay et al. [4] compare the <u>total</u> transient energy function at clearing with a critical energy and estimate the region of stability. The critical energy V_{cr} is evaluated by two methods. First, it is argued that the critical trajectory passes through an appropriate u.e.p., $\underline{\vartheta}^u$. At $\underline{\vartheta}^u$ the system's velocity is zero, resulting in elimination of the kinetic energy term in the transient energy function. The potential energy term evaluated at $\underline{\vartheta}^u$ will determine the critical value V_{cr}. Hence, the main task involved in this approach is the identification of the appropriate u.e.p. (a u.e.p. which depends on the trajectory of the system).

In their second method, the potential energy boundary surface (Figure 2.3) is identified and the total potential energy of the system at the crossing of PEBS and the trajectory constitutes V_{cr}. This approach was also pursued in [12].

Fouad et al. [13] estimate the critical clearing time by again considering the total energy at the instants of clearing and a boundary. It is argued that not all the kinetic energy at clearing contributes to instability. The kinetic energy contributing to system separation is equal to the energy produced from the relative motion of the center of inertia of the accelerated group in regard to the inertial center of the rest of the system. Thus, the kinetic within the accelerated group and in the group representing the rest of the system at clearing time t_c must be subtracted from V_{C1}. Examining equation (2.18), it is also claimed that V_{c1} and V_{cr} must be evaluated from the same reference and thus V_{cr} must be used with correction V_{cor} (2.24). Hence, in estimating the critical clearing time, these two corrections must be made. However, in spite of the previous discussion, it is the kinetic and potential energies of the individual machines (and not the total energy) which must be considered for accurately estimating the stability boundary (critical clearing time). A very recent work [16] does also support this idea mathematically. Chapter 3 is devoted to analyzing the transient energy function and investigating the partial energies in contrast to total energies.

CHAPTER 3

AGGREGATION AND LOCALIZATION OF ENERGY FUNCTION

3.1 Coherent Group Energy

3.1.1 Discussion

As was discussed in the previous chapter, the fault energy breaks the system into groups of generators that swing together and form coherent groups. The generators of a coherent group approximately possess identical rotor angle positions and angular velocity and thus could be replaced by an equivalent generator.

Accurate simulation of the response of a power system is possible when the coherent generator groups for a particular fault are aggregated to form single-generator equivalents and thus a reduced-order power system transient stability model. This ability to aggregate coherent groups before the simulation of a particular fault is performed to determine whether or not a system is stable suggests that the stability of the system is dictated by the components of the model that govern the coherent group against coherent group dynamics. The components of the power system transient stability model that determine the dynamic response within coherent groups appear to have little or no effect on the retention or loss of stability for a particular fault.

It is believed that the total system energy function can be broken into within-group and between-group components. The within-group kinetic and potential energy components are hypothesized to have little or no effect on stability based on the observation that within-group dynamics can be aggregated without much effect on the accuracy of the simulation model in prediction of retention or loss of stability for a particular fault. This chapter is devoted to the determination of expressions for the within- and between-group kinetic and potential energy components in the total system energy function. The within-group kinetic and potential energy components are then eliminated to form an aggregated transient energy function (ATEF). This ATEF attempts to preserve between-group kinetic and potential energy components. This representation is especially of interest where the fault separates the system into two groups where the fault energy accelerates a group of generators with respect to the others. In this situation the ATEF is analogous to the well-known "equal area criterion" and thus the transient stability of a multi-machine could be approximately estimated by the "equal area criterion" of two equivalent machines that represent the two coherent groups.

The motion of coherent groups is shown to be dictated by the "center of inertia" rotor angle position and angular velocity that are represented by the motion of the equivalent inertial center machine. The aggregation of the coherent group into an equivalent machine requires obtaining parameters of the equivalent machine model, aggregated mechanical input power and an aggregated network model. This aggregation procedure has been applied to produce dynamic equivalents for transient stability studies. A crucial point worth noting in this analysis is that the aggregation of the power system parameters does not reduce the order of the system, i.e., the dynamic behavior of the power system is not <u>approximated</u> by a lower order model. The aggregation is solely applied to the energy components in the transient energy function and thus results in an <u>approximate</u> stability condition.

The "Equal Area Stability Condition" obtained for multi-machine systems is shown to obtain an optimistic (too large) region of stability and critical clearing times because the aggregation of the energy function is shown through analysis and simulation to stiffen the network between groups. The derivation and discussion of the equal area condition for multi-machine power systems is given in section 3.2.

A second effort is made to show that between-group kinetic and potential energy contains the information about whether the system is or is not stable for a particular fault. An algorithm is developed in section 3.4 based on the observation that the kinetic energy between groups will approach zero at some time instant after fault clearing if the system is stable. If the system is unstable, the minimum kinetic energy over time after the fault is cleared is considered to be the excess kinetic energy at clearing that caused the loss of stability. This algorithm is shown to obtain a more accurate estimate of the region of stability and thus the critical clearing time than the u.e.p. method [13] discussed in section 3.3. However, this u.e.p. method is shown to be a computationally attractive approximation of this new algorithm. The encouraging results of this algorithm led to the effort in Chapters 4 and 5 to determine if a particular generator in the accelerated group of generators would even more accurately determine the region of stability for the system.

The remainder of this first subsection of Chapter 3 is devoted to deriving expressions for the between- and within-group potential and kinetic energy components of the total system energy function. The assumption and procedure required to aggregate the generators within a coherent group are then reviewed in subsection 3.1.3 so they can be applied to the total system energy function divided into within- and between-group components.

3.1.2 Between-Group and Within-Group Energy Function Components

The transient energy function of (2.16) (presented in (3.1) for convenience) could alternatively be written in terms of energy components residing within and between coherent groups.

$$V = \sum_{i=1}^{n-1} \sum_{j=i+1}^{n} \left[\frac{1}{2M_T} M_i M_j (\omega_i - \omega_j)^2 \right.$$

$$- \frac{1}{M_T} (P_j M_i - P_i M_j)(\delta_{ij} - \delta_{ij}^s)$$

$$\left. - C_{ij}(\text{Cos } \delta_{ij} - \text{Cos } \delta_{ij}^s) + I_{ij} \right] \tag{3.1}$$

In order to achieve our objective, the following nomenclature is considered and then applied to (3.1) to obtain (3.2):

N = total number of generator

K = number of groups

N_i = number of generators in group i where $i=1,2,\ldots,K$

n_o = A constant equal to zero

$n_j = \sum_{i=1}^{j} N_i \qquad j = 1,2,\ldots,K$

Expressing (3.1) in terms of the preceding terminologies results in

$$V = \sum_{k=1}^{K} \sum_{i=n_{k-1}+1}^{n_k-1} \sum_{j=i+1}^{n_k} A_{ij} + \sum_{k=1}^{K-1} \sum_{\ell=k+1}^{K} \sum_{i=n_{k-1}+1}^{n_K} \sum_{j=n_{\ell-1}+1}^{n_\ell} A_{ij} \tag{3.2}$$

where A_{ij} is the argument of the double summation in (3.1). The first and second terms in (3.1) represent the kinetic and potential energy residing within and between K coherent groups. From this derivation, the between-group kinetic and potential energies for all K groups are

$$KE_{BG} = \sum_{k=1}^{K-1} \sum_{\ell=k+1}^{K} \sum_{i=n_{k-1}+1}^{n_k} \sum_{j=n_{\ell-1}+1}^{n_\ell} \frac{1}{2M_T} M_i M_j (\omega_i - \omega_j)^2 \qquad (3.3a)$$

$$PE_{BG} = -\sum_{k=1}^{K-1} \sum_{\ell=k+1}^{K} \sum_{i=n_{k-1}+1}^{n_k} \sum_{j=n_{\ell-1}+1}^{n_\ell} + \frac{1}{M_T} (P_j M_j - P_j M_i)(\delta_{ij} - \delta_{ij}^s)$$
$$+ C_{ij}(\text{Cos } \delta_{ij} - \text{Cos } \delta_{ij}^s) - \int_{\delta_i^s+\delta_j^s-2\delta_o}^{\delta_i+\delta_j-2\delta_o} D_{ij} \text{Cos}\delta_{ij} d\delta_{ij} \qquad (3.3b)$$

The within-group kinetic and potential energies can be similarly defined from (3.2).

3.1.3 Assumptions and Procedures for Aggregating A Coherent Group

The assumptions and methodology of obtaining the aggregated transient energy function are:

(i) to replace rotor angle position and angular velocity of all generators in a specific coherent group by the center of inertia variables of the same group, so that each group is represented by a center of inertia center machine;

(ii) to model the mechanical input power of the inertial center machine that represents the coherent group by the sum of the mechanical input powers of the generators contained in the same group;

(iii) to develop a transmission network representation that connects the center of inertia of equivalent machines that represent the coherent group's generators.

In order to develop an appropriate mathematical representation of the equivalent transmission network connecting the coherent groups, the power flow between generators is considered.

The real transmitted power from bus i to bus j of a power system through line i-j consisting of resistance and reactance r_{ij}, x_{ij}, respectively, is given by (3.4).

$$P_{ij} = \frac{1}{r_{ij}^2+x_{ij}^2}\left[r_{ij}|V_i|^2 - r_{ij}|V_i||V_j| \text{ Cos } \delta_{ij} + x_{ij}|V_i||V_j| \text{ Sin } \delta_{ij}\right] \quad (3.4)$$

The change in transmitted power due to a change in the relative rotor angle position of buses i and j is the synchronizing torque coefficient or stiffness of the line T_{ij} given by

$$T_{ij} = \frac{|V_i|\ |V_j|}{r_{ij}^2+x_{ij}^2}\left[r_{ij}\text{Sin}\delta_{ij}+x_{ij}\text{Cos}\delta_{ij}\right] \quad (3.5)$$

Consider the case depicted in Figure 3.1 where the power system includes two coherent groups and it is desired to produce an equivalent line representation of the power system connecting group 1 (G_1) to group 2 (G_2). The transmission lines connecting a specific gnerator $i \varepsilon G_1$ to all the generators $j \varepsilon G_2$, $j=n_1+1$, $n_1+2,\ldots,n$, are constrained by the synchronizing torque coefficient T_{ij}. Therefore, an equivalent line connecting bus $1 \varepsilon G_1$ to the fictitious center of inertia of the second group (δ_{o2}) must maintain the same constraint, i.e.,

$$\sum_{j=n_1+1}^{n} T_{ij} = T_{i,II} \tag{3.6}$$

where $T_{i,II}$ is the synchronizing torque coefficient of the equivalent line connecting bus $1 \varepsilon G_1$ to the center of inertia of G_2, δ_{o2}.

Without loss of generality let us assume that the transmission line consists of reactive components, x_{ij}, only. In this case

$$\sum_{j=n_1+1}^{n} \frac{|V_i|\ |V_j|}{X_{ij}} \operatorname{Cos} \delta_{ij} = T_{i,II}$$

$$= \frac{|V_i|\ |V_{II}|}{X_{i,II}} \operatorname{Cos} \delta_{i,II} \tag{3.7}$$

where V_{II}, $X_{i,II}$, δ_{II} are the variables of the equivalent line of interest.

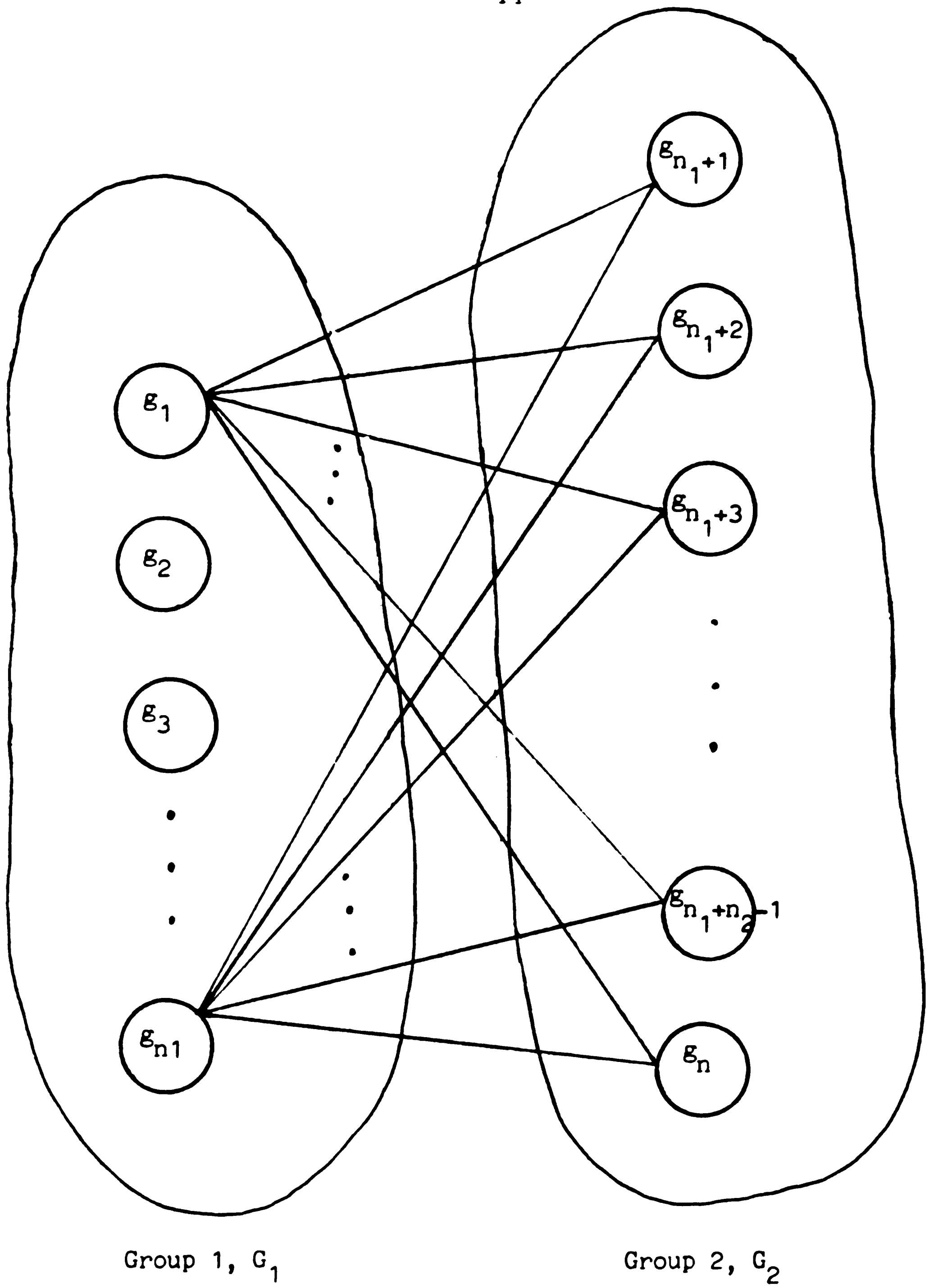

Figure 3.1 Representation of power system consisting of two coherent groups

Expanding the cosine terms in (3.7) and equating the coefficients of the known variable $i \in G_1$ reveals

$$\sum_{j=n_1+1}^{n_2} \frac{|V_i|\,|V_j|}{X_{ij}} (\cos\delta_i \cos\delta_j + \sin\delta_i \sin\delta_j) =$$

$$\frac{|V_i|\,|V_j|}{X_{i,II}} (\cos\delta_i \cos\delta_{II} + \sin\delta_i \sin\delta_{II}) \tag{3.8a}$$

$$\sum_{j=n_1+1}^{n_2} \frac{|V_i|\,|V_j|}{X_{ij}} \cos\delta_j = \frac{|V_i|\,|V_{II}|}{X_{i,II}} \cos\delta_{II} \tag{3.8b}$$

By implementing the assumption that the rotor angle positions of generators of a specific group are equal to their center of inertia, (3.8b) becomes

$$\sum_{j=n_1+1}^{n_2} \frac{|V_i|}{X_{ij}} = \frac{|V_{II}|}{X_{i,II}} \tag{3.8c}$$

$$\delta_{II} = \delta_{o2} = \frac{\sum_{j=n_1+1}^{n_2} M_j \delta_i}{M_{T_2}}, \quad M_{T_2} = \sum_{j=n_1+1}^{n_2} M_j \tag{3.8d}$$

where δ_{o2} is the center of inertia rotor angle position of G_2.

Continuing the same analysis but now considering a generator j, $j \in G_2$ with respect to all the generators $i \in G_1$, following similar steps as found in equation (3.8a,b,c,d) and finally summing over all possible $i \in G_1$, $j \in G_2$, (3.9) is obtained.

$$\sum_{i=1}^{n_1} \sum_{j=n_1+1}^{n_2} \frac{|V_i|\,|V_j|}{X_{ij}} \cos\delta_{ij} = \frac{|V_I|\,|V_{II}|}{X_{I,II}} \cos\delta_{o12} \qquad (3.9a)$$

where

$$\delta_{o12} = \delta_{o1}-\delta_{o2}, \quad \delta_{o1} = \frac{1}{M_{T_1}} \sum_{i=1}^{n_1} M_i\delta_i, \quad M_{T_1} = \sum_{i=1}^{n_1} M_i$$

$$\frac{|V_I|\,|V_{II}|}{X_{I,II}} = \sum_{i=1}^{n_1} \sum_{j=n_1+1}^{n_2} \frac{|V_i|\,|V_j|}{X_{ij}} \qquad (3.9b)$$

Equations (3.9a,b) identify the parameters of an equivalent line connecting the center of inertia of G_1 to the center of inertia of G_2. Representing the power system by an equivalent line will introduce some approximation which will be the subject of the following section.

The one-line equivalent representation of the power system is applied to the transient energy function to produce the ATEF. Section 3.2 obtains the ATEF and will show the analogy between the equal area criteria and the ATEF when the power system consists of only two coherent groups.

3.2 Equal Area and Energy Function Relationship and Approximation

3.2.1 Formulation and Discussion

Implementation of the assumption of equal rotor angle positions and speeds (assumption (i) in 3.1.3) for the generators of an identical group eliminates the first term--which represents within-group energy--in equation (3.2) and consequently (3.2) reduces to

$$V \approx \hat{V} = \sum_{k=1}^{K-1} \sum_{=k+1}^{k} \sum_{i=n_{k-1}+1}^{n_k} \sum_{j=n_{\ell-1}+1}^{n_\ell} A_{ij}$$

or

$$\hat{V} = \sum_{k=1}^{K-1} \sum_{\ell=k+1}^{K} \frac{M_{T_k} M_T}{2M_T} (\omega_{ok} - \omega_{o\ell})^2 - \frac{1}{M_T} (P_{T_k} M_{T_\ell} - P_{T_\ell} M_{T_k}) \cdot$$

$$(\delta_{ok\ell} - \delta_{ok\ell}^s) - (T_{T_{k\ell}} - T_{T_{k\ell}}^s) + (I_{T_{k\ell}} - I_{T_{k\ell}}^s) \qquad (3.10)$$

where

$$M_{T_k} = \sum_{i=n_{k-1}+1}^{n_k} \qquad k=1,2,\ldots,K \qquad (3.10a)$$

$$P_{T_k} = \sum_{i=n_{k-1}+1}^{n_k} P_i \qquad k=1,2,\ldots,K \qquad (3.10b)$$

$$M_T = \sum_{i=1}^{N} M_i \qquad (3.10c)$$

$$\omega_{ok} = \frac{1}{M_{T_k}} \sum_{i=n_{k-1}+1}^{n_k} M_i \omega_i \qquad (3.10d)$$

$$\delta_{ok} = \frac{1}{M_{T_\ell}} \sum_{i=n_{k-1}+1}^{n_k} M_i \delta_i \tag{3.10e}$$

$$\omega_{ok\ell} = \omega_{ok} - \omega_{o\ell} \tag{3.10f}$$

$$\delta_{ok\ell} = \delta_{ok} - \delta_{o\ell} \tag{3.10g}$$

$$T_{ij}\ ,\ (T^s_{ij}) = \frac{|V_i||V_j|}{X_{ij}} \operatorname{Cos} \delta_{ij}\ ,\ (\frac{|V_i||V_j|}{X_{ij}} \operatorname{Cos} \delta^s_{ij}) \tag{3.10h}$$

$$T_{T_{k\ell}}\ ,\ (T^s_{T_{k\ell}}) = \sum_{i=n_{k-1}+1}^{n_k} \sum_{j=n_{\ell-1}+1}^{n_\ell} T_{ij}\ ,\ (T^s_{ij}) \tag{3.10i}$$

$$I_{T_{k\ell}} = \sum_{i=n_{k-1}+1}^{n_k} \sum_{j=n_{\ell-1}+1}^{n_\ell} \frac{|V_i||V_j|}{r_{ij}} \frac{\delta_i-\delta^s_i+\delta_j-\delta^s_j}{\delta_{ij}-\delta^s_{ij}} \cdot (\operatorname{Sin} \delta_{ij}-\operatorname{Sin} \delta^s_{ij}) \tag{3.10j}$$

When the fault energy separates the system into two coherent groups, then (3.10) is <u>almost analogous</u> to the equal area criterion of the two-machine system, i.e., when K=2 the (ATEF) is

$$\hat{V} = (\frac{M_{T_1} M_{T_2}}{2(M_{T_1}+M_{T_2})})(\omega_{o1}-\omega_{o2})^2 - \frac{1}{(M_{T_1}+M_{T_2})}(P_{T_1}M_{T_2}-P_{T_2}M_{T_1}) \cdot (\delta_{o12}-\delta^s_{o12}) - (T_{T_{12}}-T^s_{T_{12}}) + (I_{T_{12}}-I^s_{T_{12}}) \tag{3.11}$$

$$\delta_{ok} = \frac{1}{M_{T_\ell}} \sum_{i=n_{k-1}+1}^{n_k} M_i \delta_i \tag{3.10e}$$

$$\omega_{ok\ell} = \omega_{ok} - \omega_{o\ell} \tag{3.10f}$$

$$\delta_{ok\ell} = \delta_{ok} - \delta_{o\ell} \tag{3.10g}$$

$$T_{ij}\ ,\ (T_{ij}^s) = \frac{|V_i||V_j|}{X_{ij}} \text{Cos}\ \delta_{ij}\ ,\ \left(\frac{|V_i||V_j|}{X_{ij}} \text{Cos}\ \delta_{ij}^s\right) \tag{3.10h}$$

$$T_{T_{k\ell}}\ ,\ (T_{T_{k\ell}}^s) = \sum_{i=n_{k-1}+1}^{n_k} \sum_{j=n_{\ell-1}+1}^{n_\ell} T_{ij}\ ,\ (T_{ij}^s) \tag{3.10i}$$

$$I_{T_{k\ell}} = \sum_{i=n_{k-1}+1}^{n_k} \sum_{j=n_{\ell-1}+1}^{n_\ell} \frac{|V_i||V_j|}{r_{ij}} \frac{\delta_i - \delta_i^s + \delta_j - \delta_j^s}{\delta_{ij} - \delta_{ij}^s} \cdot (\text{Sin}\ \delta_{ij} - \text{Sin}\ \delta_{ij}^s) \tag{3.10j}$$

When the fault energy separates the system into two coherent groups, then (3.10) is <u>almost analogous</u> to the equal area criterion of the two-machine system, i.e., when K=2 the (ATEF) is

$$\hat{V} = \left(\frac{M_{T_1} M_{T_2}}{2(M_{T_1} + M_{T_2})}\right)(\omega_{o1} - \omega_{o2})^2 - \frac{1}{(M_{T_1} + M_{T_2})} (P_{T_1} M_{T_2} - P_{T_2} M_{T_1}) \cdot (\delta_{o12} - \delta_{o12}^s) - (T_{T_{12}} - T_{T_{12}}^s) + (I_{T_{12}} - I_{T_{12}}^s) \tag{3.11}$$

The parameters $T_{T_{12}}$ and $I_{T_{12}}$ defined in (3.10h) represent an equivalent line connecting the equivalent inertial center generators 1 and 2 with angle position (δ_{o1}, δ_{o2}) and velocities (ω_{o1}, ω_{o2}), respectively. Thus, the ATEF in (3.11) could be used to measure the energies A_1 and A_2 to produce an equal area criterion. The equal area criterion based on (3.11) would not be accurate based on the analyses and simulation results which follow.

To obtain the exact analogy with the equal area criterion, the last term in (3.11), which represents the conductance term in the system, must be eliminated. In applying a direct method stability criterion, such as the equal area criterion, it is assumed that the total system energy remains constant after the fault period (only conservative systems could be analyzed). However, for a qualitative view, it is possible to analyze the systems with losses.

Examining the terms in V of (3.11), it is revealed that the first term represents the kinetic energy produced by relative motion of the center of inertia of G_1 and G_2. The work of Fouad et al. [13] points out that not all the kinetic energy at clearing contributes to instability. The kinetic energy responsible for system separation is equal to the kinetic energy associated with the relative motion of the center of inertia of the groups at fault-clearing time. This kinetic energy that contributes to instability in [13] is exactly equal to the first term of (3.11).

The potential energy term, however, introduces some errors. The ATEF in (3.11) suggests that the potential energy term within the coherent groups must be eliminated but the potential energy existing between the coherent groups must be retained. By this elimination, it seems that the ability of the overall system to absorb kinetic energy due to the fault will be increased rather than reduced as might at first be thought. The requirement that all generators have the same motion effectively stiffens the effective network connecting the two groups. Stiffening connections between the two groups would clearly occur if the network in between generators in a group is shorted together to produce a network equivalent. The assumption that the angles at every generator in the group are identical effectively assumes the network between these generators is shorted and would stiffen the effective network between the groups as indicated. The effective stiffening of the network caused by assuming identical angles in a group and the resulting errors in the equal area criterion based on the ATEF in (3.11) is indicated by the simulation results on an example test system in the next subsection.

3.2.2 Research Test System

The test network used in the simulation studies of this research consists of 17 generators, 163 busses, 304 lines and transformers. This network (Reduced Iowa System Model) is an equivalent to the real generation network of Iowa State consisting of 862 busses and 1323 lines [14]. Figure 3.2 shows a one-line diagram of the Reduced Iowa System.

The study done at Iowa State confirms that this reduction preserves the dynamic behavior of the system for "first swing" stability. In references [13,14], a detailed investigation of the matter is performed. The data for this model were provided by Iowa State University and the generator initial conditions and data are presented in Table 3.1.

Two different fault cases are considered in this investigation.

(i) RAUN CASE

A three-phase fault is applied to the high side of the transformer connected to generator 6 (Raun) and is removed by clearing line 372-193.

(ii) COOPER CASE

A three-phase fault is applied to generator 2 (Cooper) and is removed by clearing line 6-439.

From Figure 3.2 the generators electrically close to the fault location (Raun Case) are generators 5, 16, 10, 12, 17 and 2. For different fault clearing times the system trajectory was simulated and it was observed that generator 5 was electrically closest to the fault location and thus possesses similar behavior as generator 6. The fault energy separated the system into two groups, one consisting of the accelerated generators (5 and 6) and the second by the rest

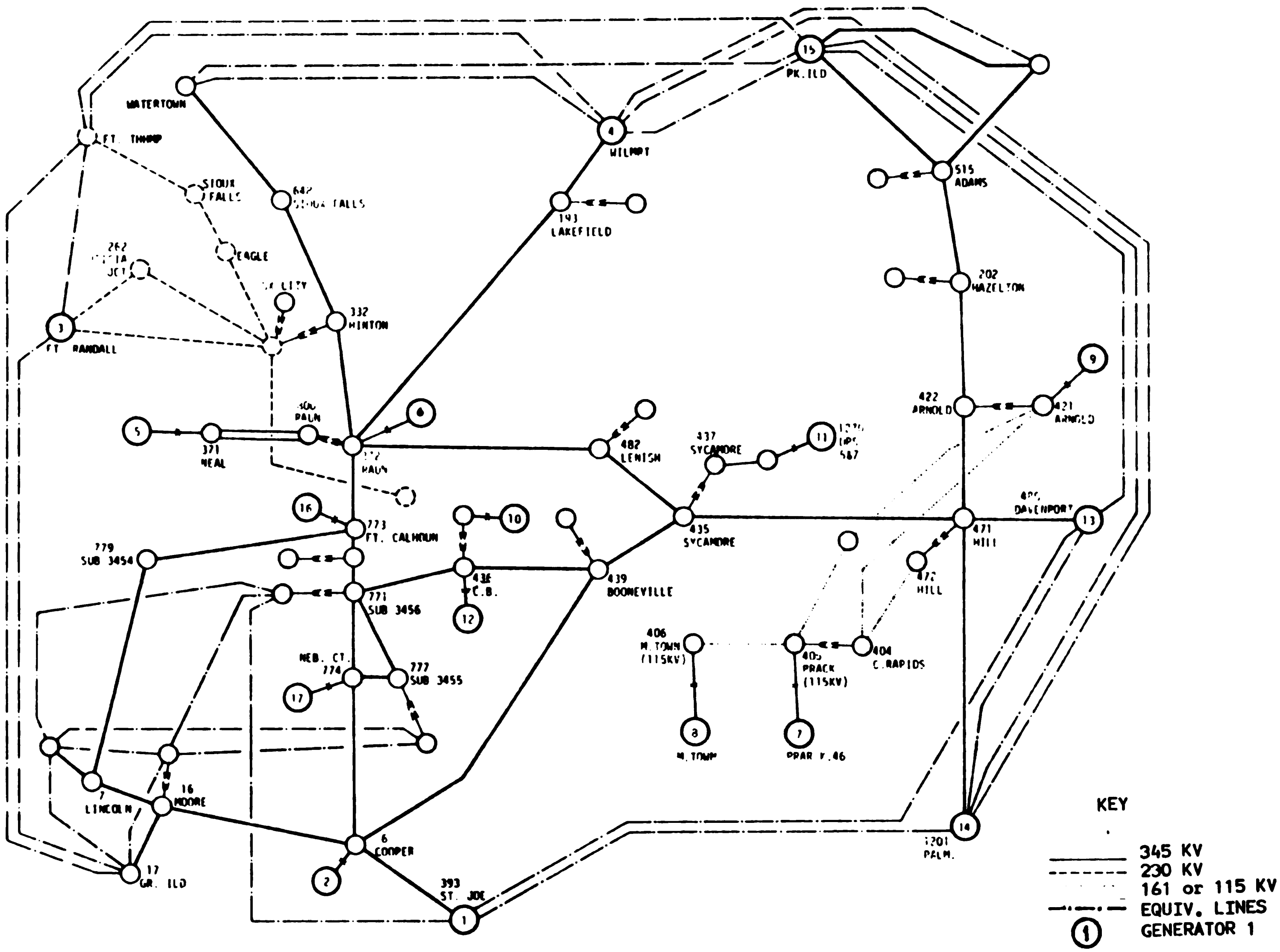

Figure 3.2 17-generator system (Reduced Iowa System) [13]

Table 3.1 Reduced Iowa System Generator Data and Initial Conditions

Generator Number	Generator Parameters[a] H (MW/MVA)	x'_d (pu)	Initial Conditions P_{mo}[a] (pu)	Internal Voltage E (pu)	(degrees)
1	100.00	0.004	20.000	1.0032	-27.92
2	34.56	0.043	7.940	1.1333	-1.37
3	80.00	0.0100	15.000	1.0301	-16.28
4	80.00	0.0050	15.000	1.0008	-26.09
5	16.79	0.0507	4.470	1.0678	-6.24
6	32.49	0.0206	10.550	1.0505	-4.56
7	6.65	0.1131	1.309	1.0163	-23.02
8	2.66	0.3115	0.820	1.1235	-26.95
9	29.60	0.0535	5.517	1.1195	-12.41
10	5.00	0.1770	1.310	1.0652	-11.12
11	11.31	0.1049	1.730	1.0777	-24.30
12	19.79	0.0297	6.200	1.0609	-10.10
13	200.00	0.0020	25.709	1.0103	-38.10
14	200.00	0.0020	23.875	1.0206	-26.76
15	100.00	0.0040	24.670	1.0182	-21.09
16	28.60	0.0559	4.550	1.1243	-6.70
17	20.66	0.0544	5.750	1.116	-4.35

[a] on 100-MVA base

of the system. Figures 3.3 and 3.4 show the swing curves of generators for fault clearing times, t_c, of .19 and .1925 seconds, respectively. For t_c=.19 (s) all the rotor positions do not exceed the stability limit and do not accelerate indefinitely. However, it is clear that the behavior of generators 5 and 6 is different from that of the other generators. Figure 3.4, where the fault was cleared at t_c=.1925 (s), also indicates the similarity in behavior of generators 5 and 6, but here they are both accelerated and thus pull out of step from the rest of the system causing instability. For the stable case, the components of energy, i.e., position, conductance and magnetic, is illustrated in Figure 3.5a. These energy components, for example position energy, may exceed the total energy of the system but the sum of these components (potential energy) will always remain below the upper bound imposed by total energy which is constant after t_c. Figure 3.5b illustrates the relationship between kinetic, potential and the total system energy. The total energy increases up to the clearing time indicating the accumulation of energy during the fault period. After clearing time, it is seen that there is an interchange between potential and kinetic energy but constant total energy is maintained.

Based on simulation results, it was concluded that the system may consist of either: (a) two groups (5, 6) and the rest of the system, or (b) three groups; 5, 6, rest of the system. For each of these cases the center of inertia rotor

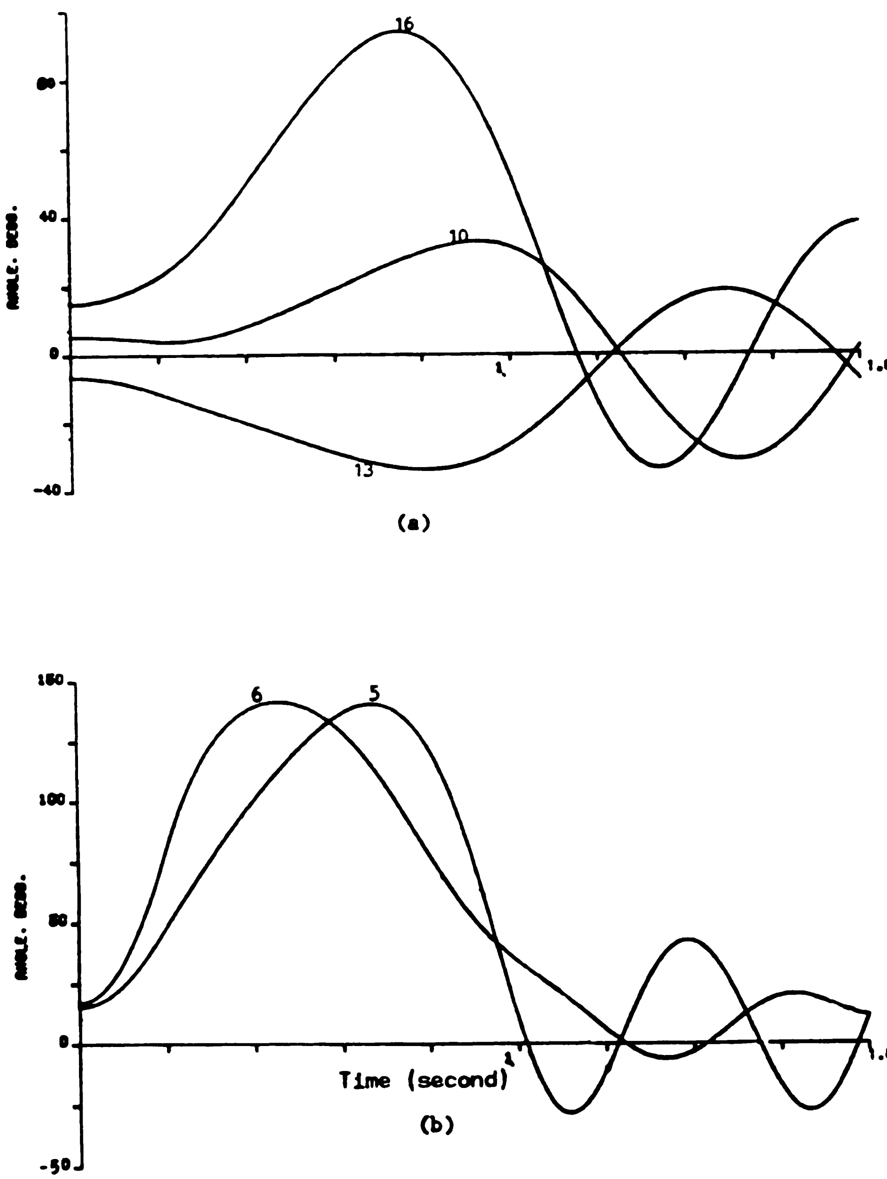

Figure 3.3 Swing curves. Clearing time = .1900 seconds.
a) Generators 10, 13, 16
b) Generators 5, 6

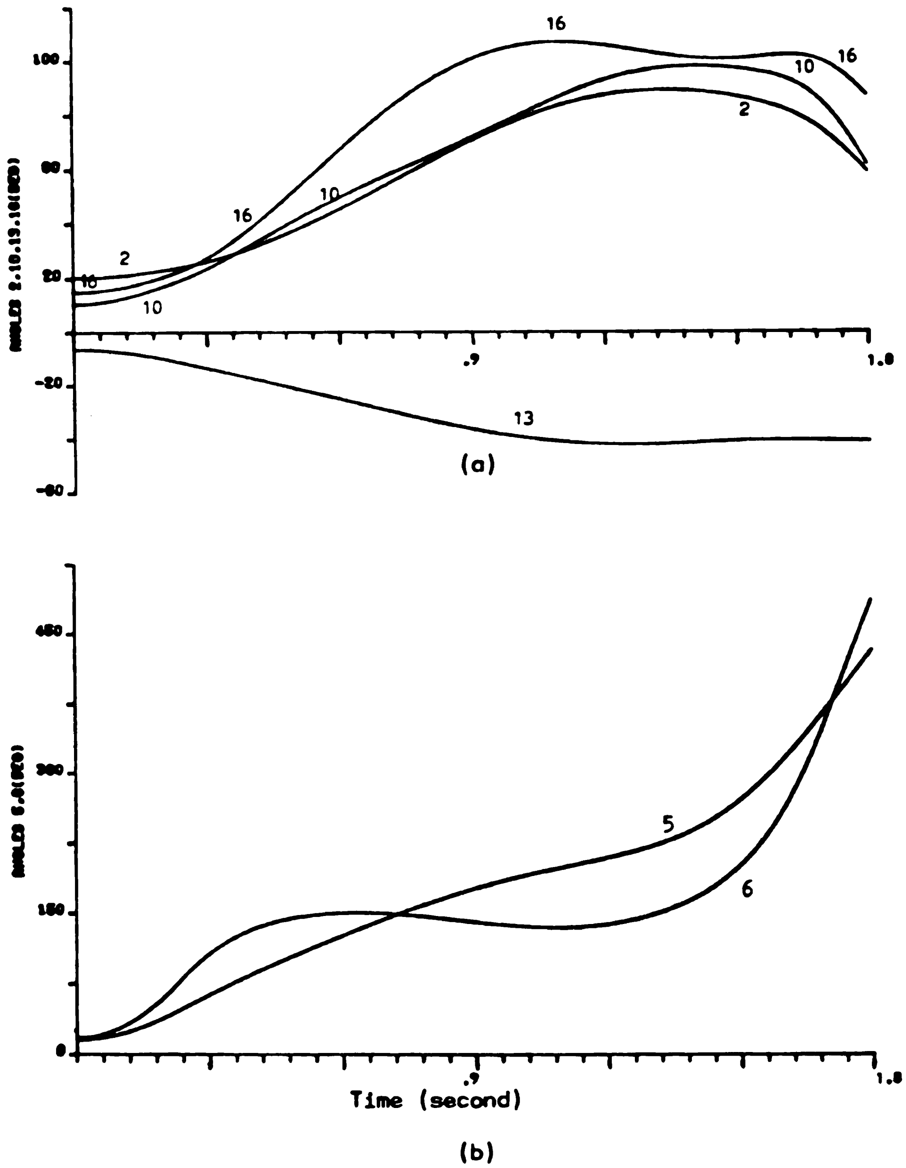

Figure 3.4 Swing curves. Clearing time = .1925 seconds.
a) Generators 2, 10, 13, 16
b) Generators 5, 6

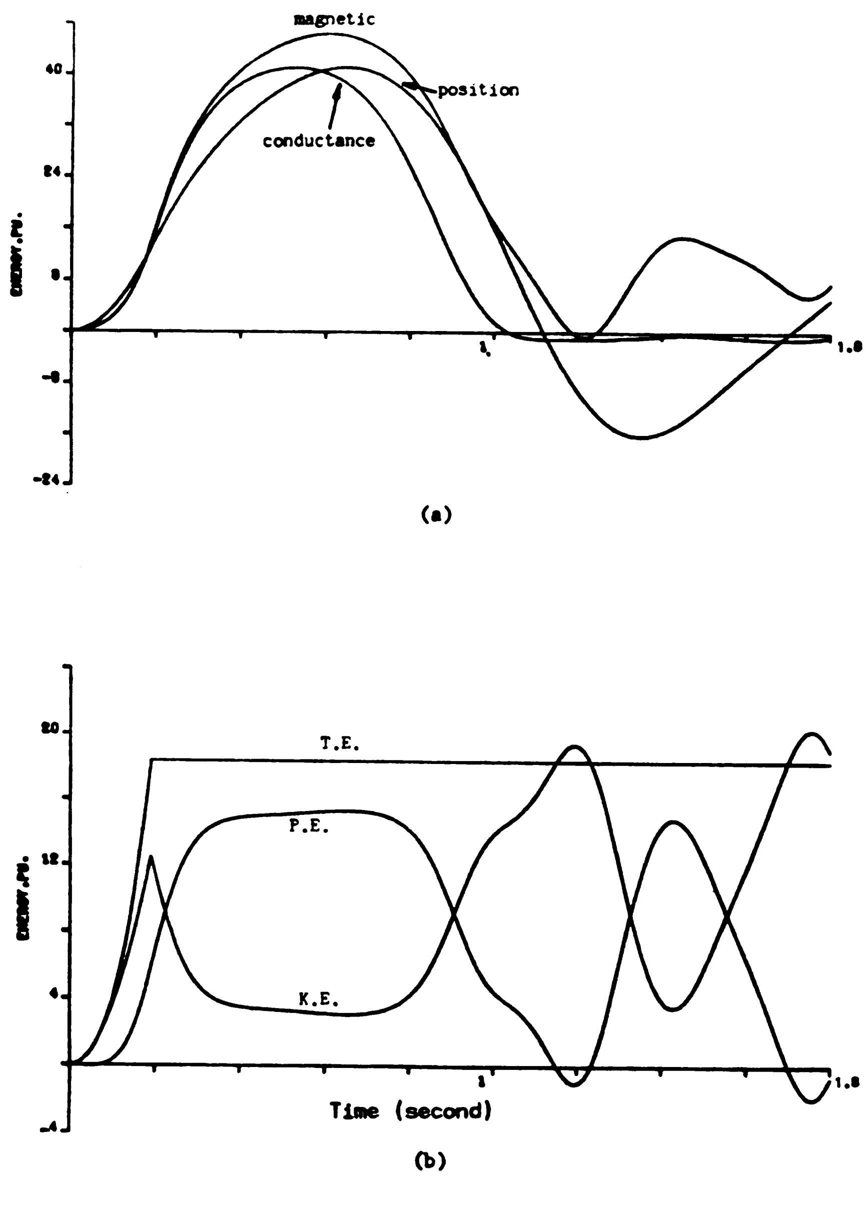

Figure 3.5 Energy analysis of 17-generator system. Clearing time = .1900 seconds.
a) Magnetic, position and conductance energy
b) Kinetic (K.E.), potential (P.E.) and total energy (T.E.)

angle position and velocity of each group and the parameters of the equivalent line connecting these centers of inertia was evaluated. Finally, the ATEF of (3.10) for different clearing times was computed.

Figures 3.6 and 3.7 depict the aggregated-unaggregated transient energy function comparisons. In both figures it is observed that the aggregated kinetic energy at any given time is smaller than the unaggregated kinetic energy indicating the elimination of within-group energy. In contrast, the maximum of aggregated potential energy exceeds that of the unaggregated case. This discrepancy is due to the effective stiffening of the connections between the groups by assuming all generator angles are identical in each group, which allows representing the connection between the two groups by one equivalent line. The direct consequence of this fact is that a more optimistic critical clearing time will be obtained. This is to say that a larger aggregated maximum potential energy implies a larger energy-absorbing capability of the system and thus a longer critical clearing time. For power system transient stability, a conservative critical clearing time, t_{cc}, is preferable over an optimistic region of stability, i.e., for a conservative t_{cc} the power system integrity is assured while for the optimistic t_{cc}, the actual region of stability is crossed and thus instability has resulted.

In spite of the foregoing discussion, the consideration of <u>within</u>- and <u>between</u>-group energies (without--one-line

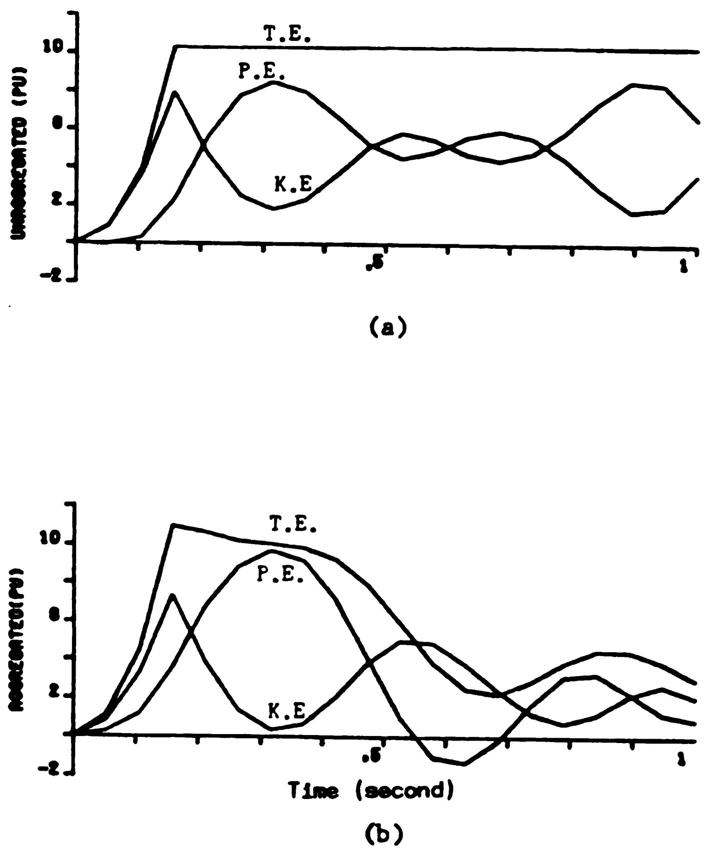

Figure 3.6 Energy analysis when the system consists of three groups, generator 5, generator 6 and the rest of the system.
a, b) Unaggregated, aggregated kinetic (K.E.), potential (P.E.) and total (T.E.) energies, respectively

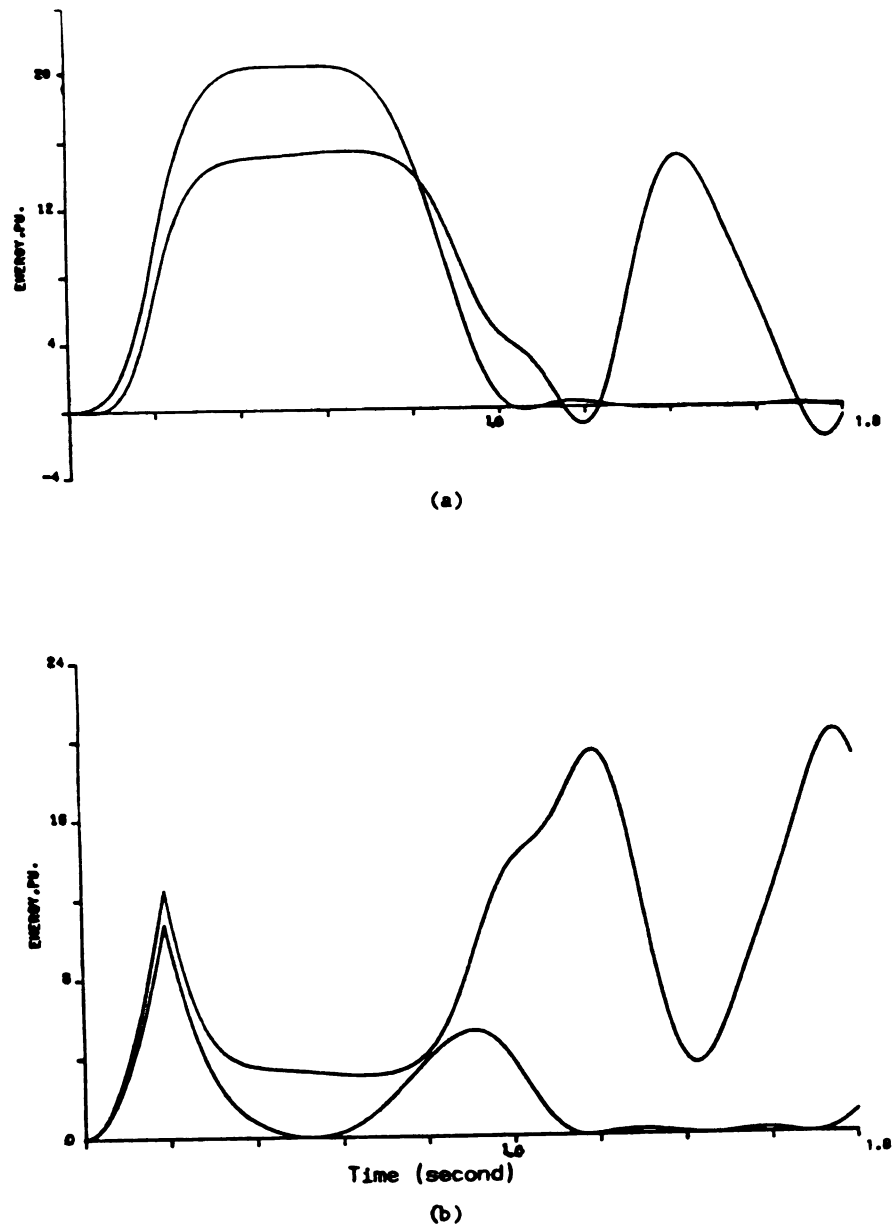

Figure 3.7 Energy analysis when the system consists of two groups, (5,6) and the rest of the system. Clearing time = .1900 seconds.
a, b) Potential and kinetic energy, respectively.

equivalent representation) is a valuable tool in assessing a realistic region of stability. The algorithms represented in the latter part of this chapter and also the following chapters will confirm the idea.

3.3 A u.e.p. Method Based on Coherent Group Energies

In direct methods based on an unstable equilibrium point (u.e.p.), it is argued that in response to fault energy, the critical system trajectory will move toward a particular u.e.p., $\underline{\vartheta}^u$, and will reach $\underline{\vartheta}^u$ with zero velocity vector $\underline{\omega}=\underline{0}$. At $\underline{\vartheta}^u$, the system energy $V=V_k(\underline{\omega})+V_p(\underline{\vartheta})$ is solely potential, i.e., $V=V_p(\underline{\vartheta}^u)$. For a given fault clearing time, t_c, the total energy at the instant of clearing V_{c1} is compared with a critical value, $V_{cr}=V_p(\underline{\vartheta}^u)$. If $V_{c1}\leq V_{cr}$, stability is preserved whereas if $V_{c1}>V_{cr}$ stability is lost. In summary, the steps taken in this procedure are

- evaluation of an appropriate u.e.p., $\underline{\vartheta}^u$
- evaluation of the critical energy $V_{cr}=V_p(\underline{\vartheta}^u)$
- comparison of clearing energy V_{c1} with V_{cr}

For the Raun case discussed in the previous section, the critical group, the group pulling away from the system, consisted of generator 5 or 6 or both 5 and 6, so that, if the critical group contains n_1 generators, the number of possible combinations in which generators could lose synchronism and thus <u>interesting</u> u.e.p.'s is

$$\sum_{i=1}^{n_1} \binom{n_1}{i} = 2^{n_1}-1 \tag{3.12}$$

Determination of the appropriate u.e.p., the one that the faulted trajectory passes by, among all interesting u.e.p.'s, is not an easy task. This task is extremely difficult if the critical group consists of 10's of n_i generators. However, the establishment of the n_i generators in the critical group restricts the number of u.e.p.'s to 2^{n_i-1} rather than 2^{N-1} which is the total number of u.e.p.'s in an N generator system. The system potential energy $V_p(\underline{\vartheta}^u)$ at a u.e.p., $\underline{\vartheta}^u$, in general will be different for different interesting u.e.p.'s $\underline{\vartheta}_i^u$. Depending upon the choice of the appropriate u.e.p., the critical energy will differ and thus produce different estimates, t_{cc_i}, of critical clearing times at which $V_c(t_{c_i})=V_p(\underline{\vartheta}_i^u)$. Without determining the proper u.e.p. $\underline{\vartheta}^u$ and thus the appropriate estimate of critical clearing time t_{cc}^*, there is no precise estimate of the region of stability. The proper u.e.p. was usually chosen [13] as the one that gives the most accurate estimate of stability after evaluating all 2^{n_i-1} u.e.p.'s.

Following the approach proposed by Fouad et al. [13], the critical group for Raun case consists of both generators 5 and 6. The potential energy at the 5,6 unstable equilibrium point is estimated to be

$$V_{cr} = V_u = V\Big|_{\underline{\vartheta}^{s2}}^{\underline{\vartheta}^u} = V_p(\vartheta_{5,6}^u) = 17.16 \quad \text{p.u.}$$

where $\underline{\vartheta}^{s2}$ is the stable equilibrium point of the post-fault network.

The authors claim that if V_{cr} is to be compared to a clearing energy V_{c1} which is evaluated from $\underline{\vartheta}^{s1}$

$$V_{c1} = V\Big|_{\underline{\vartheta}^{s1}}^{\underline{\vartheta}^{c}}$$

where $\underline{\vartheta}^{s1}$ is the stable equilibrium point of the pre-fault network and $\underline{\vartheta}^{c}$ is the rotor angle at clearing, a correction term due to change of reference from $\underline{\vartheta}^{s1}$ to $\underline{\vartheta}^{s2}$ must be added to the critical value, i.e.,

$$(V_{cr})_{corrected}=V_p(\underline{\vartheta}^{u})+V\Big|_{\underline{\vartheta}^{s1}}^{\underline{\vartheta}^{s2}}=17.16+(-.498)=16.662 \text{ p.u.}$$

It is also suggested that the kinetic energy responsible for system separation is the kinetic energy produced by the relative motion of the center of inertia of groups, and not the total kinetic energy of the system, at the instant of fault clearing. According to the terminologies developed for the coherent groups, the kinetic energy correction that does not contribute to instability and thus must be subtracted from clearing energy is exactly equal to the within-group kinetic energy evaluated at critical clearing time; hence, Based on this procedure, a critical clearing time, $t^*_{cc} \varepsilon$ (.189, .191) seconds, is estimated. From simulation of the system trajectory, it is observed that actual $t_{cc} \varepsilon$ (.1922, .1925).

It is possible to obtain a larger region of stability by estimating the total potential energy plus the kinetic energy which does not contribute to instability at a critical boundary for stability. The kinetic energy not responsible in system separation is that amount of kinetic energy remained within groups at the critical boundary. The u.e.p. methods assume that the kinetic energy at the critical boundary, i.e., at a u.e.p., is zero. Although this argument may be correct, at $t=\infty$, practically the system trajectory does not reach the unstable equilibrium point in finite time and at best first passes near an appropriate u.e.p. To clarify the point, let us consider a critically stable case, i.e., the Raun fault for t_c=.1922 seconds. The maximum total potential energy, i.e., the maximum absorbing capability of the system is $V_p(t^*_B)$=18.56952 p.u. and coincides with the minimum of total kinetic energy which is $K.E.(t^*_B)$=.30908 p.u., at $t=t^*_B$. At t^*_B, a portion of kinetic energy resides within groups and this amount of energy (.12916 p.u.) does not contribute to instability and can be deducted from the total energy at the estimated clearing time. Alternately this group kinetic energy $K.E._{group}(t^*_B)$ can be added to $V_p(t^*_B)$ to produce an estimate of V_{cr}

$$V_{cr} = V_p(t_B^*) + K.E._{(Group)}(t_B^*)$$

$$V_{cr} = 18.56952 + .12916 = 18.698681 \quad \text{p.u.}$$

The clearing energy

$$V_{c1} = V_p\Big|_{\underline{\vartheta}^{s1}}^{\underline{\vartheta}^{c}} + K.E.\Big|_{\underline{\omega}^{s1}=0}^{\underline{\omega}^{c}} = V_p(t_c) + K.E.(t_c)$$

and the estimate of critical energy

$$V_{cr}(t_B) = V_p\Big|_{\underline{\vartheta}^{s1}}^{\underline{\vartheta}(t_B)} + K.E._{Group}\Big|_{\underline{\vartheta}^{s1}}^{\underline{\vartheta}(t_B)} = V_p(t_B) + K.E._G(t_B)$$

both have the same reference $\underline{\vartheta}^{s1}$ and thus there is no need for correction $V\Big|_{\underline{\vartheta}^{s2}}^{\underline{\vartheta}^{s2}}$ to $V_{cr}(t_B)$.

The procedure for estimating the critical clearing time presented in the next section requires

$$V_{c1}(t_{cc}) < V_{cr}(t_B) = 18.698$$

and would produce a $t_{cc}^* \in (.191, .192)$.

This modified procedure gives a larger t_{cc}, V_{cr} and region of stability than the u.e.p. method. Before discussing this new method, the difference in calculating kinetic energy correction at t_c in the u.e.p. method and at t_B in this new method should be explained. The total energy for all $t > t_c$ including $t=t_B$ is constant and the kinetic and potential energy components at t_c or t_B can be broken into <u>within-group</u> (group) and <u>between-group</u> (boundary) components and therefore

$$V_{CR}(t_B) = V_{PG}(t_B) + V_{PB}(t_B) + K.E._G(t_B) + K.E._B(t_B) =$$
$$V_{CL}(t_c) = V_{PG}(t_c) + V_{PB}(t_c) + K.E._G(t_c) - K.E._B(t_c)$$

$V_{PG}(t)$ - potential energy within groups from $\underline{\vartheta}^{s1}$ to $\underline{\vartheta}(t)$

$V_{PB}(t)$ - potential energy between groups from $\underline{\vartheta}^{s1}$ to $\underline{\vartheta}(t)$

$K.E._G(t)$ - Kinetic energy within groups from $\underline{\omega}^{s1}=0$ to $\underline{\omega}(t)$

$K.E._B(t)$ - Kinetic energy between groups from $\underline{\omega}^{s1}$ to $\underline{\omega}(t)$

The total kinetic energy $K.E._B(t_B)+K.E._G(t_B)$ at t_B does not become zero; hence the trajectory just passes near the u.e.p. in finite time and never exactly reaches it. The kinetic energy between the group, which measures the kinetic energy associated with the relative motion of inertial centers of these groups, does approach zero if the system is stable. Thus, if the system is stable $K.E._B(t_B)$ is approximately zero, but if unstable, $K.E._B(t_B) > 0$. The best estimate of V_{CL} for an unstable trajectory is to subtract $K.E._B(t_B)$ and thus estimate V_{CL} as

$$V_{CL} = V_{PG}(t_B) + V_{PB}(t_B) + K.E._G(t_B)$$

where t_B is the time at which the K.E.(t) reaches a minimum and $V_p(t)$ is maximum. Note that the kinetic energy correction would in this case be $K.E._G(t_B)$ since it is the kinetic energy that must be added to the potential energy at the boundary to equal the clearing energy estimate.

The proper theoretical estimate of the kinetic energy correction is the group kinetic energy at some boundary where stability is actually determined and not the kinetic energy within the group at the clearing time $K.E._G(t_c)$, which from simulation results is larger than $K.E._G(t_B)$. However, in the u.e.p. method the use of the group kinetic energy at clearing is quite appropriate from a practical standpoint since

(1) the correction $K.E._G(t_c)$ is easily calculated by approximations without simulation where $K.E._G(t_B)$ requires simulation which is to be avoided,

(2) the kinetic energy correction at t_c is larger than at t_B from simulation results and compensates for the fact that $V_p(\underline{\theta}^u)$ is smaller than $V_p(t_B)$.

Discussing the energy accounting at t_B rather than t_c required a new computation procedure. The procedure is presented and applied to the Raun case on the Reduced Iowa System in the next subsection.

3.4 Global KINETIC ENERGY Stability Criterion

Among the components of energy, i.e., the magnetic, kinetic, position and conductance energy, the system kinetic energy is directly related to the fault energy and reaches its peak at the instant of fault clearing. It assumes a minimum at a later time and then oscillates back and forth until the system resumes an equilibrium point where the kinetic energy becomes zero. Thus, the observation of the global and group kinetic energy may reveal valuable information on determination of the region of stability. Based on this observation, an algorithm for estimation of critical clearing time is developed and will be pursued along with the concept of potential energy boundary surface (PEBS).

In Chapter 2 it was discussed that the PEBS is a surface passing through all the u.e.p.'s and saddle points. Figure 3.8 illustrates a PEBS for a three-machine system where one generator is considered as reference. The dotted line connects all the u.e.p.'s and saddle points of the system (mountain summits and passes of Figure 2.5) and thus a PEBS. Consider the following two cases

Unstable trajectories: If the fault is cleared at t_s, $t_s \geq t_{cc}$ (critical clearing), the faulted trajectory would go over the ridge and crosses the boundary at a point, BC (Figure 3.8). At BC, the total kinetic energy is minimum but not necessarily zero. The excessive fault energy does not allow the velocity vector at BC to approach zero. Note also that the smaller the amount of fault energy, the smaller the minimum of kinetic energy.

Stable trajectories: If the fault is cleared at $t_c < t_{cc}$, the faulted trajectories do not reach the boundary but the kinetic energy will reach its minimum. However, the minimum kinetic energy between groups is zero but there is a substantial amount of kinetic energy within groups. Thus, the total kinetic energy has a minimum which never approaches zero.

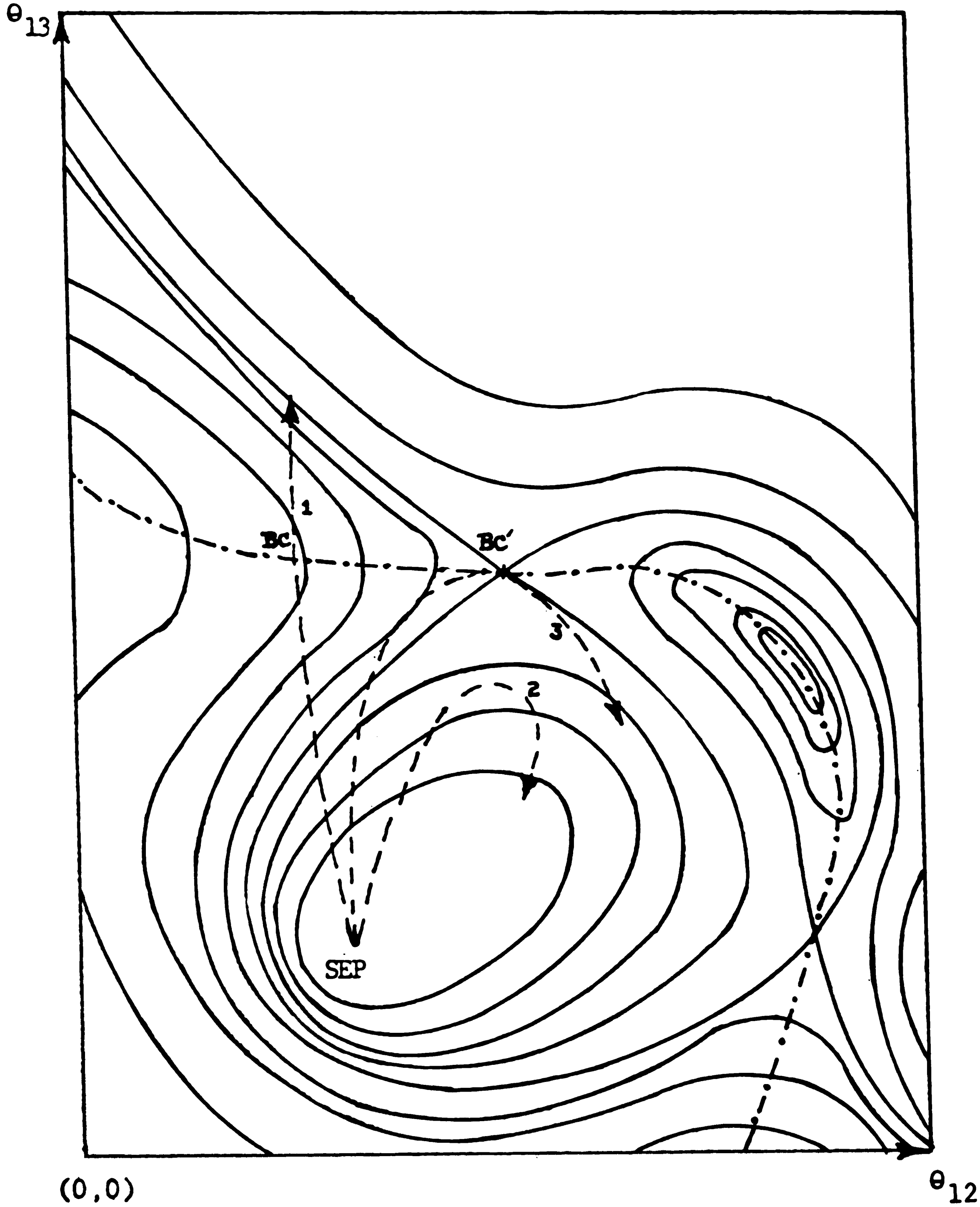

Figure 3.8 Stable, unstable and critical trajectory for a 3-machine system

Besides the two types of trajectories, stable and unstable, there is a critical trajectory. The critical trajectory touches the boundary at BC', and at this point, the between-group kinetic energy is almost zero and the total and group kinetic energies are both minimum. Therefore, the potential energy plus the group kinetic energy at the instant where the critical trajectory has minimum kinetic energy could be considered as the critical energy, V_{cr}. The between-group kinetic energy when total kinetic energy is minimum is then considered to be the excess energy at clearing that causes loss of stability. Note that, if one was able to identify the true critical trajectory, then both group and global kinetic energies would also be identically zero. The steps followed in this algorithm are:

Initialization:

- $t_{c_i} \gg t_{cc}$, sustained fault
- V_{c1} - energy at t_{c_i}
- $\mathrm{Min(KE)}_i$ - minimum of kinetic energy KE(t), for given clearing time t_{c_i}
- t_i - time at which $\mathrm{Min(KE)}_i$ occurs
- $KE_G(t_i)$ - group kinetic energy at t_i
- ε - a prespecific small number

STEPS:

(1) Evaluate $V_{c1} - K.E._G(t_i) = V'_{c1}$

(2) Clear the fault when $V = V'_{c1}$ at $t_{c_{i+1}}$, and find $\mathrm{Min(K.E.)}_{i+1}$, t_{i+1}, $K.E._G(t_{i+1})$

(3) Monitor

$$E = \mathrm{Min}(K.E.)_i - \mathrm{Min}(K.E.)_{i+1}$$

(a) If $E \leq \varepsilon$, the potential energy at t_{i+1}, i.e., $PE(t_{i+1}) = V_{cr}$ identifies the critical energy and $t_{cc} = t_{c_{i+1}}$. Terminate the algorithm when appropriate t_{cc} is obtained.

(b) if $E > \varepsilon$, set $i=i+1$ and go to step 1.

Based on this algorithm, the Raun case was analyzed and the results of Table 3.2 were obtained. The critical clearing time predicted is $t_{cc} \varepsilon (.191, .1922)$ for $\varepsilon = .25$. The predicted critical clearing time very well matches the actual critical clearing time of $t_{cc} \varepsilon (.1922, .1925)$ obtained by simulation of the system trajectory.

Based on the analysis of Table 3.2, the following remarks are made:

- For $t_c = .2$, the minimum of kinetic energy is 5.2541 p.u. and the peak of potential energy is 15.51829 p.u. Based on the algorithm, the next clearing energy is approximately 18.4013 at time interval t_c (.19, .2).
- When the fault is cleared at $t_c = .1925$, the minimum of kinetic energy is reduced by 91.5% (from 5.25411 to .50262) and the potential energy increased by 15.8%. Columns 3 and 4 show that before critical clearing time the kinetic and potential energy

Table 3.2 Global kinetic energy criterion for Raun

i	t_{c_i}	$\mathrm{Min}(KE_i) = KE(t)\big\rvert_{t=t_i}$	$\mathrm{Max}(PE_i) = PE(t)\big\rvert_{t=t_i}$	$V_{c1}=V(t_{c_i})$	$KE_G(t_i)$	V'_{c1}	$t_{c_{i+1}}$
1	.2	5.25411	15.51829	20.77103	2.36973	18.4013	(.19, .2)
2	.1925	.50262	18.44726	18.94950	.2470	18.7025	(.19, .1925)
3	.1922	.30908	18.56952	18.87818	.12916	18.74902	(.19, .1922)
4	.192	.72049	18.10973	18.82204	.84460	17.97744	
5	.190	3.06077	15.29901	18.35819	1.56539		

decrease and increase, respectively, and after the t_{cc} the process is reversed.

- Investigation of the fourth and fifth columns reveals that the critical energy (Max (PE)) is getting closer to the clearing energy V_{c1}, up to the instant of critical clearing. Recall that in the equal area criterion, $A_1=A_2$ at the critical clearing time. Past the critical clearing time these two values diverge from each other.
- The estimated critical energy V_{cr} is at least 18.56952 (if t_{cc} is considered to be .1922 seconds). By the u.e.p. method of the previous section, the critical energy was estimated to be 17.18 p.u.

In spite of the large region of stability obtained by previous algorithm, it is believed that the actual boundary of stability is dictated by the behavior of the individual machines rather than the overall power system. In other words, the mechanism of stability is a local phenomenon rather than a global phenomenon. More specifically, the boundary of stability for the Raun case hinges upon the behavior of generators 5 and 6 rather than all the generators in the power system. The content of the following chapters is an attempt at clarification of the subject.

CHAPTER 4

LOSS OF STABILITY DUE TO SEQUENTIAL DECOUPLING OF THE INDIVIDUAL GENERATORS IN THE CRITICAL GROUP

4.1 Discussion

In Chapter 2 an attempt was made to investigate the recent development in assessment of transient stability by direct methods. The concept of potential energy boundary surface [4,11] and energy accounting of the total system energy [13] was introduced. Several stability criteria [7] based on total system energy were also identified. However, it was pointed out that the region of stability evaluated based on total system energy produces conservative results. For larger and more accurate regions of stability and thus critical clearing times the stability problem must be investigated in terms of the potential and kinetic energies components that truly reflect retention or loss of stability for a particular fault and post-fault network. As a first step, the separation of the system energy into "within" and "between" coherent group energies was considered.

A "Kinetic Energy Stability Criterion" was proposed based on the within-group and between-group potential and kinetic energy components. This stability criterion was based on the assumption that the kinetic energy representing motion between the group of accelerated generators and those in the rest of the system would approach a minimum close to zero at some instant after the fault is cleared as long as the system is stable. This between-group kinetic energy minimum over time would itself be minimized as a function of clearing time if the clearing time equaled the critical clearing time. This minimum between-group kinetic energy would increase as a function of clearing time if the clearing time exceeded the critical clearing time since there is excess kinetic energy that cannot be absorbed in potential energy. The "Kinetic Energy Stability Criterion" was applied to a single-fault case on the Reduced Iowa System and the prediction of critical clearing time and region of stability was more accurate than a u.e.p. method applied to the same fault case. The result produced by the new algorithm was quite encouraging even though it was not exhaustively tested on other fault cases.

The testing of this algorithm based on the "Kinetic Energy Stability Criterion" was not pursued because the algorithm is still based on accounting for the <u>total</u> system kinetic and potential energy even though it was for the first time properly separated into between- and within-group kinetic and potential energies. The following two hypotheses concerning stability of the system is the basis of the research that follows in this chapter and Chapter 5 and why algorithms based on the within-group and between-group kinetic and potential energy were not pursued.

It is believed that

(1) a single generator can be identified for each fault case that determines whether a group of one or more generators and thus the system will remain stable or lose stability. This single generator is one of the members of this group of generators whose stability is in question for the particular fault.

(2) The kinetic and potential energy between this single generator and the rest of the system contains all the information necessary to determine the stability of this group of generators and thus the stability of the system. The kinetic and potential energy is thus hypothesized to contain no information about whether the group will remain stable or lose stability. Moreover, it is hypothesized that the between-group kinetic and potential energy that contains the essential information about stability is not that between the entire group of generators that are accelerated and the rest of the system but the kinetic and potential energy between an individual generator in this accelerated group and the rest of the system including other members of the accelerated group.

The kinetic energy and potential energy of this individual generator is obviously contained in the total system energy function. If the region of stability of the group of generators and thus the stability of the entire system is dictated by a region of stability of the single generator that is totally captured in the kinetic and potential energy of this single generator, then the total system between and within group potential and kinetic energy also contains this essential information about stability. However, the total system energy function also contains information about kinetic energy and between every other generator in the accelerated group and the rest of the system which is not essential to assessing stability and cannot be filtered out to obtain criteria based on the kinetic and potential energy of the individual generator that assesses if the boundary of the region of stability of this individual generator is crossed and thus whether the system is or is not stable.

The total system kinetic and potential energy is sometimes strongly dominated by the individual machine kinetic and potential energy, which explains the partial success of stability criteria and methods based on the total system kinetic and potential energy found in Chapter 3 and [13], respectively. The stability criteria based on the individual generator potential and kinetic energy for assessing the region of stability of this individual generator could then clearly be applied to the total kinetic and potential energy function to assess whether the region of stability of the individual generator has been crossed. This discussion suggests that if the hypotheses (that

(a) stability of the system is dictated by the stability of a single generator and (b) that the region of stability for this generator is captured solely in the kinetic and potential energy function for this generator) are true, then the methods and criteria developed for the total system kinetic and potential energy could also be applied to the individual machine kinetic and potential energy functions with hopefully more accurate results. This will be confirmed in the next chapter.

It should be noted that the kinetic and potential energy of the individual generator depends on the rotor position and velocity of all the generators in the system. Thus, the stability criteria to be developed depend on the dynamic behavior of the total system even if it does not depend on the total energy in the entire system.

This chapter will define the individual generator energy function and then show that it is not a Lyapunov function for the system if the system is sufficiently weakly damped. The total system energy function with conductance energy terms has not been proven to be a Lyapunov function but certainly was assumed to be a Lyapunov function. The fact that the individual generator energy function is not a Lyapunov function may at first be quite disturbing. However, the stability criteria to be developed in Chapter 5 and their justification is not based on Lyapunov stability theory but observation of the minimum of kinetic energy and the maximum of potential energy of the individual generator as a function of time after the fault is cleared. The individual generator kinetic energy minimum as a function of time after the fault is cleared should approach zero if the generator reverses direction after its initial acceleration due to the fault. This reversal of the individual generator's rotor velocity direction would indicate the generator would remain stable. A kinetic energy minimum after the fault is cleared that is not zero indicates there is excess kinetic energy due to the fault's acceleration. This excess kinetic energy cannot be absorbed in the magnetic field in the transmission network connecting this generator to the rest of the system, which implies that the rotor motion at the fault clearing time will never be reversed, which in turn implies loss of stability.

Observation of the maximum of the individual generator potential energy as a function of time, after the fault is cleared, is another indicator of whether stability is retained or lost. This individual generator potential energy maximum stability indicator is also not dependent on Lyapunov stability theory and thus is not diminished in usefulness by the fact that the individual generator energy function is not a Lyapunov function. The maximum of the individual generator potential energy function after the fault is cleared is a measure of the effect of the magnetic coupling of the transmission network in decelerating the individual generator. As the fault clearing time is increased, toward critical clearing time, the larger will be the magnetic coupling energy that decelerates and reverses the direction of rotor velocity. The increase in magnetic coupling energy required for deceleration at clearing time increases; the larger should be the maximum of potential energy that in part measures this magnetic coupling energy. It is clear that for any clearing time that exceeds the critical clearing time, the maximum magnetic coupling energy has been utilized in an attempt to decelerate the individual generator. The maximum potential energy after the fault is cleared is in part a measure of this maximum magnetic energy if the clearing time exceeds critical clearing time. Thus, it can be argued that the maximum potential energy as a function of time may well be approximately equal for any clearing time that exceeds the critical clearing time. A very recent paper [16] utilizes the maximum individual generator potential energy for a fault on trajectory as the critical energy value V_{cr_i}, which is compared to the individual generator's energy at clearing V_{c1_i} to assess whether the system is stable. This algorithm is not justified based on the above understanding of maximum magnetic coupling energy but rather based on the assumption that the individual generator energy function is Lyapunov function and thus Lyapunov stability theory.

The development and justification of stability criteria based on the understanding of the physical implications of the minimum kinetic energy and the maximum potential energy after the fault is cleared as a function of the fault clearing time is pursued in Chapter 5. The remainder of this chapter is devoted to

(1) presenting and discussing the form and properties of the individual generator potential and kinetic energy function

(2) proving that the individual generator energy function is not a Lyapunov function

(3) justifying the hypothesis that the stability or instability of the accelerated group of generators is determined by whether an individual generator in the group crosses its region of stability and that this individual generator's region of stability is measured by observing the maximum of the individual generator potential energy and the minimum of the individual generator's kinetic energy after the fault is cleared.

The individual generator energy function will now be presented and discussed. Consider the equation of motion of a single machine written with respect to center of inertia, (2.13). From multiplication of both sides of (2.13) by $\dot{\vartheta}_i$, (4.1) is obtained

$$M_i \dot{\tilde{\omega}}_i \dot{\vartheta}_i = (P_i - P_{ei} - \frac{M_i}{M_T} P_{COA}) \dot{\vartheta}_i \tag{4.1}$$

Integrating Eq. (4.1) from a s.e.p., ϑ_i^s to an arbitrary angle, ϑ_i, results in

$$\frac{1}{2} M_i \tilde{\omega}_i^2 = P_i(\vartheta_i - \vartheta_i^s) - \sum_{\substack{j=1 \\ j \neq i}}^{n} \int_{\vartheta_i^s}^{\vartheta_i} C_{ij} \operatorname{Sin}\vartheta_{ij} d\vartheta_i$$

$$- \sum_{\substack{j=1 \\ j \neq i}}^{n} \int_{\vartheta_i^s}^{\vartheta_i} D_{ij} \operatorname{Cos}\vartheta_{ij} d\vartheta_i - \frac{M_i}{M_T} \int_{\vartheta_i^s}^{\vartheta_i} P_{COA} d\vartheta_i \qquad (4.2)$$

or equivalently the total energy of the i^{th} unit is,

$$V_i = \frac{1}{2} M_i \tilde{\omega}_i^2 - P_i(\vartheta_i - \vartheta_i^s) + \sum_{\substack{j=1 \\ j \neq i}}^{n} \int_{\vartheta_1^s}^{\vartheta_1} C_{ij} \operatorname{Sin}\vartheta_{ij} d\vartheta_i$$

$$+ \sum_{\substack{j=1 \\ j \neq i}}^{n} \int_{\vartheta_i^s}^{\vartheta_i} D_{ij} \operatorname{Cos}\vartheta_{ij} d\vartheta_i + \frac{M_i}{M_T} \int_{\vartheta_1^s}^{\vartheta_i} P_{COA} d\vartheta_i \qquad (4.3)$$

Considering the definitions of the center of inertia variables,

$$\vartheta_i = \left(\delta_i - \frac{1}{M_T} \sum_{i=1}^{n} M_i \delta_i\right) \text{ and } \tilde{\omega}_i = \left(\omega_i - \frac{1}{M_T} \sum_{i=1}^{n} M_i \omega_i\right)$$

reveals that the individual machine energy of Eq. (4.3) depends on the angular velocity and rotor angle position of the entire system. It is clear that, if the individual generator function is to be capable of assessing the region of stability for the individual generator and the system, it must be a function of the angle position and velocity of the entire system as shown above.

The very recent work of Michel et al. [16] discusses direct methods for determining stability based on the individual machine energy function. The individual machine energy function argued to be a Lyapunov function is partially based on simulation results and partially on proof. It is also argued that this energy function will satisfy additional conditions based on the invariance principle of ordinary differential equations. The following section will show that this individual energy function is not a Lyapunov function.

4.2 Application of Invariance Theory in Power System Transient Stability

Recall that one way of assessing the transient stability of a power system is by comparison of the critical energy, the energy at the lowest saddle point, with the clearing energy V_{c1}. A second method was based on the concept of potential energy boundary surface (PEBS), the collection of hypersurfaces which are orthogonal to equipotential surfaces and pass through the saddle points. In this method the critical energy is considered to be the potential energy at the crossing of the total system trajectory and the PEBS. It was pointed out previously that the region of stability obtained by the application of the PEBS is larger than the one resulting by consideration of the energy at the lowest saddle point. Theoretically speaking, these different approaches are based on similar Lyapunov stability theorems but with different (smaller or larger) regions of definiteness. For clarification, consider theorem (4.1) [4,20,24].

Theorem 4.1

> Let $V(\underline{x})$ be a scalar function. Suppose that the region $R = \{\underline{x} \mid V(\underline{x}) < k\}$ is bounded. Let $\dot{V}(\underline{x})$ be the derivative of $V(\underline{x})$ along the solutions of $\dot{\underline{x}}=f(\underline{x})$; $f(\underline{0})$. If $V(\underline{x})$ is positive definite and $\dot{V}(\underline{x})$ negative definite in R, then the origin is an asymptotically stable equilibrium state and all motions starting in R converge to the origin as $t\to\infty$.

The region R in theorem 4.1 could be the entire state space, and if this is the case, the equilibrium point will be called asymptotically stable in the <u>large</u>. However, this condition cannot be met and thus for power systems, one is able to speak at most of <u>local</u> asymptotic stability. Thus, it is desired to identify the largest region of stability (R). When the energy of the lowest saddle point, V_{1s}, is chosen as the critical energy, the value of k in theorem (4.1) is equated to V_{1s} and thus a region of stability (R_1) is identified. On the other hand, when the critical energy is chosen as the potential energy of the saddle point closest to the system trajectory, then another region of stability, R_2, is such that $R_2 > R_1$ is found.

The regions R, R_1 and R_2 are by definition the invariant sets; i.e., for any initial condition of the post-fault system contained in the set, the post-fault trajectory converges to the post-fault stable equilibrium point as $t \to \infty$. Note that if the initial condition contained in the invariant set, then $V_{c1} \leq V_{cr}$. The initial conditions of the post-fault dynamics are rotor position and angular velocity of all units at the instant of fault clearing, which is represented in terms of energy by V_{c1}.

Michel et al. [16] propose that the concept of invariance theory and potential energy boundary surface is extendable to the individual machine energy. The maximum potential energy of a specific individual machine, i, for a sustained fault is chosen as the critical energy, $V_{cr} = PE_i\big|_{max}$. Then the region of stability for the entire power system is identified by an invariant set $R_i = \{x: V_i(\underline{x}) \leq PE_i\big|_{max}\}$, when $V_i(\underline{x})$ is the kinetic plus potential energy of the i^{th} unit. Note that, in order to apply an invariance theorem, it is first required to show that the individual machine energy function is a Lyapunov function, i.e., $V_i(\underline{x}) \geq 0$ and $\dot{V}_i < 0$ on the region of interest (refer to theorem 4.1). Before proceeding to the proof for the individual generator energy function, it is worthwhile to show how the conditions of theorem (4.1) are indicated to be satisfied for the total system energy function. The sign definiteness of the total system energy function V and its derivative $\dot{V}$ cannot be proven when the transfer conductance term is included in V. However, the total system energy function restricted to a suitably small region of interest can be shown to be positive. The derivative of this total system energy function without mechanical damping is zero based on simulation results in [4,13,14,15,21], for all system trajectories and all $t \geq t_c$. This observation is then coupled with a proof that the effect of the mechanical damping is negative definite to suggest that $\dot{V}(x) < 0$.

Consider the mathematical model including the mechanical damping

$$M_i \dot{\omega}_i = P_i - P_{ei} - D_i \omega_i$$

where D_i presents the mechanical damping for i=1,2,...,n.

Writing the equation of motion in terms of center of angle results in (4.4)

$$M_i \dot{\tilde{\omega}}_i = (P_i - P_{ei} - D_i \omega_i) - \frac{M_i}{M_T} P_{COA} + \frac{M_i}{M_T} \sum_{j=1}^{n} D_j \omega_j$$

$$= (P_i - P_{ei} - \frac{M_i}{M_T} P_{COA}) - (D_i \omega_i - \frac{M_i}{M_T} \sum_{j=1}^{n} D_j \omega_j) \qquad (4.4)$$

From (4.4) the contribution of the mechanical damping to the time derivative of the energy function is

$$- \sum_{i=1}^{n} \left[D_i\omega_i - \frac{M_i}{M_T} \sum_{j=1}^{n} D_j\omega_j \right] \tilde{\omega}_i$$

$$= -\left[\sum_{i=1}^{n} D_i\omega_i\tilde{\omega}_i - 0 \right] = -\left[\sum_{i=1}^{n} D_i\omega_i^2 - \sum_{i=1}^{n} D_i\omega_i\omega_{COA} \right] \tag{4.5}$$

The right-hand side of (4.5), i.e., the contribution of the mechanical damping to the time derivative, is negative, if [4]

$$\omega_{COA} < \omega_i \qquad i=1,2,3,\ldots,n \tag{4.6}$$

Condition (4.6) and the fact that (from simulation) the time derivative of energy function of a model without mechanical damping is zero results in $\dot{V} < 0$. Under these conditions and simulation observation, one is able to apply an invariance theory to theoretically estimate a larger region of stability. In summary, the steps taken in the analysis are (a) to show that the energy function is positive in a suitable small subregion, (b) to suggest that the constant energy of the undamped system in simulation results indicates the time derivative of the energy function is zero and (c) to suggest that the contribution of damping under certain conditions is negative and thus result in a negative time derivative of the energy function. However, when the individual machine energy is considered, one is not able to make any judgment on the sign definiteness of the time derivative of the individual machine energy. In contrast to the case of the total system energy, the individual machine energy does not maintain a constant value after the fault clearing time. There is always a transfer of energy back and forth between machines. Figure 4.1 shows the potential, kinetic and the sum of these energies for generator 6 of the Reduced Iowa System. Generator 6 belongs to the accelerated coherent group and as individual energy is of particular interest. The oscillatory nature of the sum of the potential and kinetic energy of this individual machine in Figure 4.1a clearly displays the nondefinite behavior of the time derivative of the energy. Thus, the individual energy function is not a Lyapunov function for weakly damped systems and thus theorem (4.1) cannot be used as the theoretical bases of the algorithm developed in [16] or the algorithms developed in Chapter 5 for the individual energy functions.

These algorithms need not be justified based on Lyapunov stability theory because there are sound physical arguments for justifying these algorithms. The algorithm in [16] selects the critical energy to be the maximum potential energy over time after the fault is cleared. This potential energy maximum is in part of the maximum magnetic coupling that attempts to reverse the direction of motion of the individual generator due to the fault acceleration. The maximum magnetic coupling and the maximum potential energy as a function of time after the fault is cleared varies only

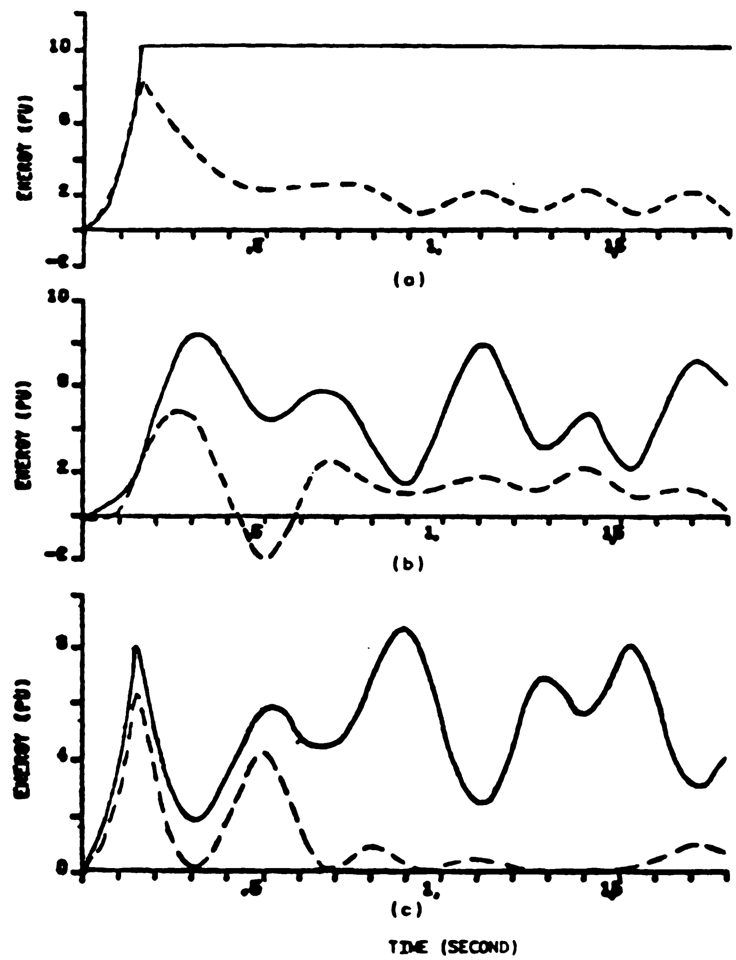

Figure 4.1 Individual machine energy analysis. Clearing time = .15 seconds.
a, b, c) Total, potential and kinetic energy

slightly for any fault clearing time that exceeds critical clearing time based on exhaustive simulation results. The decision that the system will be stable or unstable based on $\underline{V}(\underline{x}(t_c)) < PE_i$ and $\underline{V}(\underline{x}(t_c)) > PE_i$, respectively, assumes that the energy of the individual generator energy function does change as a function of time and that the kinetic energy of the individual generator approaches zero for some instant after the fault is cleared for clearing times less than the critical clearing time. This kinetic energy of generator 6 is shown to approach zero for an instant after the fault is cleared when $t_c < t_{cc}$ as shown in Figure 4.1c, indicating the second assumption is true. The assumption that the individual generator energy does not change as a function of time after clearing is not true based on the energy of generator 6 shown in Figure 4.1a. The energy of generator 6 decreases after clearing thus indicating the stability criterion $\underline{V}(\underline{x}(t_c)) < PE_i$ is conservative and would predict slightly smaller clearing times than if the individual generator energy function did not change as a function of time. The results in [16] predicted a .1920 clearing time that is indeed conservative but comparable to simulation results that indicate the critical clearing time lies in (.1922, .1925). The very high accuracy of the algorithm in predicting critical times based on application to several fault cases on three different power system data bases [16] further justifies the algorithm and stability criteria based on the individual generator energy function.

A very important but unanswered question for applying this algorithm based on the individual energy function is which of the accelerated generators will dictate the stability of the group. This particular problem is of particular interest for the Raun case on the Reduced Iowa System since three different critical clearing times are given in [16] based on selecting generators 6, 5 and group (5,6) as the individual or group energy function. This same problem existed in selecting the proper u.e.p. in [13]. The following section proposes a procedure for identifying this individual generator that dictates stability of the accelerated group of generators and thus the system.

4.3 Critical Group, Generator and Boundary

In the latter part of Chapters 2 and 3 it was suggested that the accurate transient stability assessment of the entire power system depends on the analysis of the individual machines. To show the legitimacy of using the individual machine energy, it was also argued in section 4.1 that the individual machine energies are related to the entire system rotor angle position and angular velocity, and thus could be used to estimate the critical clearing time of the entire system. Knowing that it is possible to predict the critical clearing time by an individual machine raises the argument that one has to identify a particular individual machine whose behavior dictates most accurately the stability of the entire power system.

In response to occurrence of a fault, those generators of the power system which are electrically closer to the fault location are the ones which are most affected by the fault energy. These generators deviate drastically from their pre-fault conditions and consequently gain a substantial acceleration. The group of generators consisting of the generators which are most affected and disturbed by the fault energy is called the accelerated group. The generators of the accelerated group are then those generators which are electrically close to the location of the disturbance. Hence, the candidacy of this group depends on two factors: (a) the system configuration, i.e., the resistance and reactance of the transmission line connecting these generators to the rest of the system, and (b) the fault duration. The longer the fault remains on the system, the larger will be the number of generators in this group. For example, in the Cooper case where the fault is applied to the high side of the transformer connected to generator 2 and the fault is cleared at t_c=.21 seconds, only generator 2 is contained in the accelerated group. On the other hand, if the fault is kept on for a longer time and cleared at t_c=.3 seconds, then generator 17 also enters the accelerated group (to be shown in Chapter 5). Note that from Figure 3.2 generator 17 (Neb. CT, bus 774) is close to the fault location and thus would logically enter the accelerated group as the fault clearing time increases. Setting aside the generators of the accelerated group, the rest of the system constitutes the <u>stationary</u> group. Generators of the stationary group are least affected by the fault energy and remain relatively close to their pre-fault conditions and thus have very similar dynamic behavior for the particular fault being experienced. In contrast, the behavior of the generators of the accelerated group are very different from that of their pre-fault condition. This observation leads one to believe that the specific generator dictating the transient stability of the entire system is contained in the accelerated group. A point worth noting is that the generators initially forming the accelerated group do not necessarily remain in this group. Some of the generators may initially accelerate and diverge from their pre-fault condition but at a later time decelerate and join the generators of the stationary group. This situation particularly happens if a large number of generators are located in a small area and the disturbance is applied inside this area. In this case a number of generators are accelerated initially and form a large accelerated group but at a later time the transmission network and inertia of generators decelerate some of these generators and force them to join the generators of the stationary group. These generators will be considered as part of the stationary group in this discussion since they will remain stable.

Further investigation of the generators of the accelerated group reveals that there are two types of generator behavior present in this group. For a given clearing time a generator or a group of generators acceleerates and pulls out of the system simultaneously. If the fault cleared with a longer fault clearing time, then other generators also pull out from the system and thus a different mode of instability results. However, the group of interest is that group of generators which pull out from the system initially for the smallest clearing time among all the clearing times which cause instability. This group is called the critical group. For example, the critical group for the Cooper case consists of generator 2 and not generators 2 and 17. Recall that generator 17 joined the accelerated group when the fault was at t_c=.3 seconds rather than .21 seconds. As another example, the critical group for the Raun case consists of both generators 5 and 6. These two generators pull out of the system simultaneously. A more detailed discussion for practically identifying the critical group will be presented in Chapter 5 where the simulation results are considered.

Once the critical group is identified, the dynamic behavior and energy transfers between the individual machines in this group must be investigated. Although all of the generators of the critical group pull out of synchronism with the system, there is only one particular generator whose stability or loss of stability accurately indicates the stability or instability of the critical group and thus the system. This particular generator in the critical group, which dictates the stability or instability of the critical group, is called the critical generator. The appropriate boundary encircling the critical generator is called the critical boundary. The critical transmission boundary determines a potential or kinetic energy boundary surface whose violation or crossing results in instability. The kinetic energy boundary crossing is evidenced by a minimum in kinetic energy of the critical generator after the fault is cleared that does not approach zero. The crossing of a potential energy boundary for the critical generator is evidenced by a maximum in potential energy of the critical generator after the fault is cleared that does not increase with an increase in fault clearing time.

Generators of the critical group will each cross their own potential or kinetic energy boundary with respect to the generators of the stationary group one at a time and the critical generator is the last generator in the critical group which crosses a potential or kinetic energy boundary. If the critical generator crosses its potential or kinetic energy boundary, then the entire critical group loses synchronism with the stationary group. If this critical generator never crosses its potential or kinetic boundary, the critical group will remain stable. To clarify the loss of synchronism between the critical generator and the generators of the stationary group, a very simplified example is in order. Consider the real power transmitted between two generators i and j connected by a lossless line with reactance X_{ij},

$$P_{ij} = \frac{|V_i| \; |V_j|}{X_{ij}} \text{ Sin } \delta$$

where $\delta = \delta_i - \delta_j$ and V_i , V_j are the magnitude of voltage at buses i and j. If V_i and V_j are kept constant, then

$$P_{ij} = P_{max} \text{Sin } \delta \tag{4.7}$$

where $P_{max} = \dfrac{|V_i||V_j|}{X_{ij}}$.

The real power transmitted from bus i to bus j through line ij clearly depends on the phase angle difference between buses i and j. When the phase angle difference (due to load increase or a change in generation due to a fault) is forced to attain a value near 90°, the power transmitted will reach P_{max}, the maximum value, and any additional phase angle difference (beyond 90°) will decrease the transmitted power. At the point where $\delta = 90°$ (the static stability limit), the system "pulls apart electrically" and the synchronism between buses i and j is lost [22] if buses i and j are only connected through this one path. If buses i and j are operating in such a way that the phase angle difference is small, then these two generators are said to be operating in synchronism or <u>strongly coupled</u>. In contrast, if the angle difference exceeds 90°, buses i and j are <u>weakly coupled</u>. If there are several paths connecting two sets of buses I and J, then all buses $i_k \in I$ and $j_\ell \in J$ must be weakly coupled for I and J to lose synchronism. One can now argue that, once the potential energy of the line connecting bus i_k to bus j achieves its maximum capacity, then generators i_k and j_ℓ become weakly coupled. In a dynamic sense, if all of the generators i_k belonging to the critical group and all generators j_ℓ belonging to the stationary group exceed the potential energy capacity of the equivalent line connecting them, the two groups lose synchronism and thus the critical group goes unstable. The last generator in the critical group which approaches its potential energy boundary of the lines connecting it to the stationary group decides the stability of the critical group and hence the entire system.

The above simplified example can be generalized to investigate the loss of synchronism between any generator in the critical group with respect to all the generators of the stationary group. The potential energy produced between the generators of the critical group and that of the stationary group is investigated via extensive simulation runs. For the Raun case, generators 5 and 6 constitute the critical group and the rest of the generators are then considered to be in the stationary group. Based on simulation, it was observed that for clearing time of t_c=.1922 seconds the system was critically stable. For this situation, Figures 4.2a and 4.2b illustrate the swing curves of some of the generators of the stationary and all of the generators of the critical group, respectively. Note that the peak of the swing curves of the stationary group is somewhere around 90°-100° while that of the critical group is about

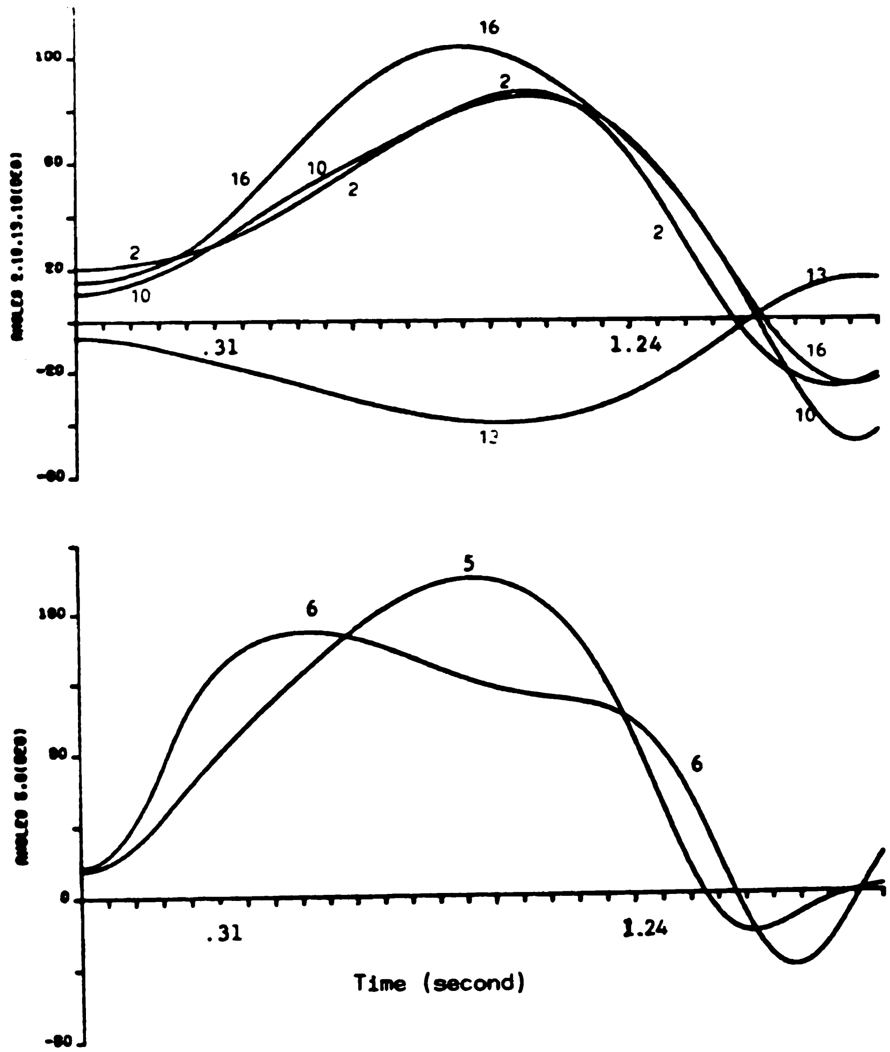

Figure 4.2 Swing curves. Clearing time = .1922 seconds.

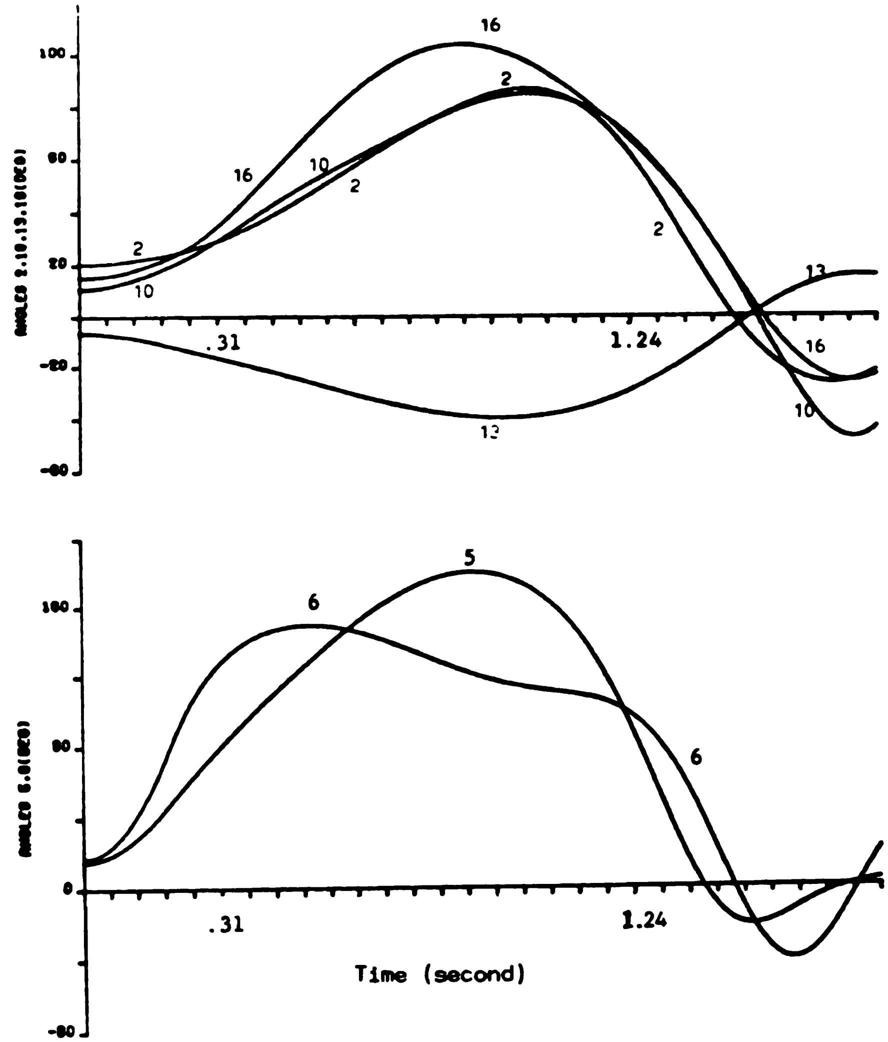

Figure 4.2 Swing curves. Clearing time = .1922 seconds.

160°-170°, confirming the fact that the critical group is initially pulling away from the stationary group but at a later time all of the generators (both in the critical and stationary groups) resume a relatively small angle indicating stability. For the same clearing time, i.e., t_c=.1922 seconds, Figure 4.3a illustrates the sum of the potential energy produced between generators 5 and 6 (critical group) and all of the generators of the stationary group. Figure 4.3b depicts two plots: one for the potential energy produced between generator 5 and the stationary group (partial potential energy) and a similar one for the partial potential energy between generator 6 and the stationary group. From Figure 4.3b it is clearly seen that the 6-partial potential energy increases up to t=.25 seconds and decreases afterward. The peak of 6-partial potential energy indicates the maximum energy capacity of the transmission network connecting generator 6 to the stationary group. To confirm the fact that the peak at t=.25 seconds is indeed the maximum energy capacity between generator 6 and the stationary group, several simulation runs were performed for different clearing times ($t_c > t_{cc}$). The maximum of 6-partial potential energy maintained a constant value for all $t_c > t_{cc}$ indicating the limit on the potential energy capacity of all lines connecting 6 and the stationary group is achieved at t_c=.1922 < t_{cc} (the simulation results will be shown in Chapter 5). The maximum potential energy capacity, recalling the simplified example,

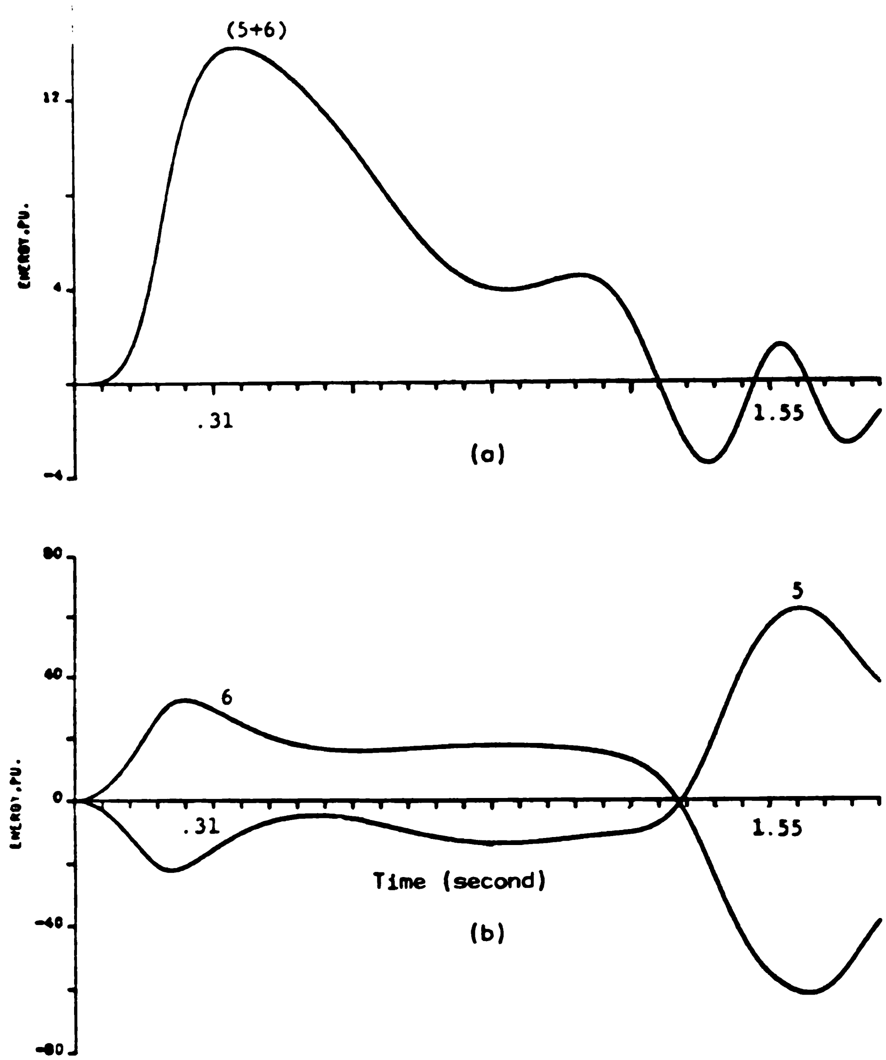

Figure 4.3 Partial energy analysis. Clearing time = .1922 seconds.
a) Sum of partial energies for generators 5 and 6
b) Partial energy for generators 5 and 6

depends on the transmission line parameters, the bus voltages and the angle difference between generator 6 and all of the generators of the stationary group. Before reaching the peak of potential energy, there is a strong coupling between generator 6 and the stationary group, and after the energy exceeds the maximum potential energy capacity of all lines connecting 6 and the stationary group, the magnetic coupling between generator 6 and the stationary group become weakly coupled. If generator 6 was the only machine in the critical group, then upon observation of the maximum energy capacity of the 6-partial potential energy one could conclude that generator 6 would pull away from the system and thus lose synchronism. However, for this particular case, where generator 5 is also in the critical group, one cannot yet make any decision on the loss of stability. A crucial point to note is the difference between the peak of 6-partial potential energy and the "maximum potential energy capacity" between generator 6 and the stationary group. It is true that at some instant of time the partial potential energy peaks; however, this peak may or may not be the "maximum energy capacity." If the peak of partial potential energy and the maximum energy capacity coincide (which is the case for generator 6), then one can conclude that this particular generator is weakly coupled (or electrically pulled apart) from the stationary group. The peak of partial potential energy is always less than or at most equal to the maximum energy capacity. Now considering the energy behavior of generator 5 reveals that the peak of 5-partial potential energy is reached at a later time, indicating the fact that, although generator 6 is trying to pull away from the system, generator 5 is holding on to the stationary group and maintains a strong coupling. Thus, among the generators of the critical group (5 and 6) generator 5 is the last generator to exceed its potential energy boundary capacity and therefore by definition the critical generator. Figure 4.3a, which displays the sum of partial potential energies of generator 5, shows a very pronounced peak in potential energy at t=.31 indicating the network connecting generator 5 to the stationary group decelerates generator 5 and causes it to reverse direction and thus causes 5 and 6 to remain stable.

To further pursue the matter, let us investigate the Raun case where the fault is cleared at t_c=.1925 seconds. Figures 4.4a and 4.4b again illustrate the swing curves of some of the generators of the stationary and the generators of the critical group, respectively. It is clear that the swing curves of generators 5 and 6 swing away from their initial operating condition and reach a value of several hundred degrees. Clearly this is an unstable case. In contrast, the swing curves of the generators of the stationary group remain below 100° and ultimately reside at an angle close to their initial condition. Investigation of Figures 4.5a and 4.5b where the partial potential energies are illustrated reveals that again generator 6 reaches its

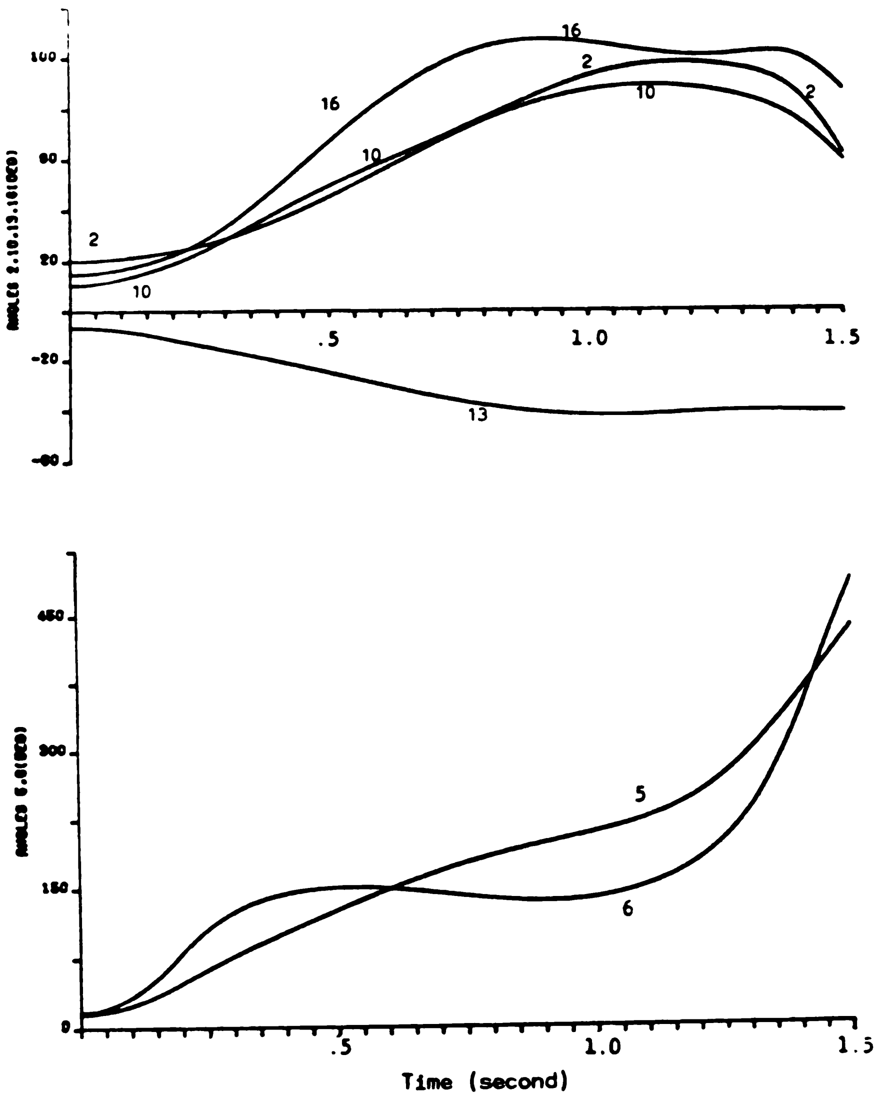

Figure 4.4 Swing curves. Clearing time = .1925 seconds.

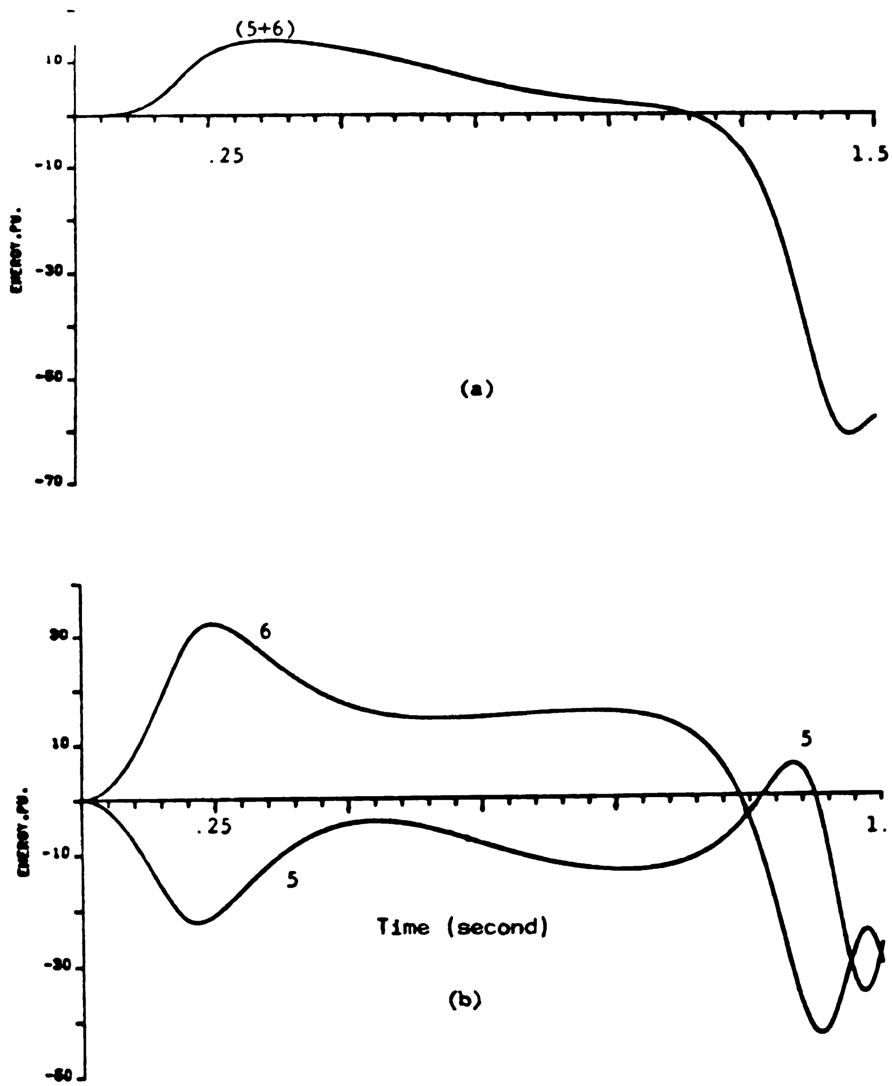

Figure 4.5 Partial energy analysis. Clearing time = .1925 seconds.

a) Sum of partial energies for generators 5 and 6

b) Partial energy for generators 5 and 6 maximum energy capacity and becomes weakly coupled with respect to the stationary group. At a later time the partial potential energy of generator 5 peaks and attempts to prevent generator 6 from pulling away from the system. However, it is observed that due to large angle deviations between the angles of generators 5, 6 and those of the stationary group, this attempt is not successful, critical generator 5 also becomes weakly coupled, and both pull away from the system.

From these observations it is confirmed that for both a critically stable and critically unstable case, generator 5 is the critical generator. Note that the fault was applied on the high side voltage of the transformer connected to generator 6, but generator 5 was shown as the critical generator.

Now that the critical generator is identified, it still remains to identify a boundary of stability. As was discussed before, the boundary of stability is an appropriate boundary encircling the critical generator. As a candidate one can investigate the quantity

$$A = \frac{1}{2M_T} \sum_{\substack{j=1 \\ j \neq i}}^{n} M_i M_j (\omega_i - \omega_j)^2$$

where i is the critical generator.

This quantity is an indication of the velocity deviation existing between the critical generator and the rest of the system. In Chapter 5, two boundary conditions are investigated and the accuracy of the critical clearing time estimates which are based on these stability boundaries will be discussed. It is worth noting that the observations made based on swing curves of this chapter are only true for short time spans. This is a limitation of the classical model used in this investigation. However, for the short clearing times of fractions of a second and simulation period of approximately two seconds the applications of the classical model for transient stability analysis is believed to be appropriate.

CHAPTER 5

LOCAL STABILITY BOUNDARIES AND COMPUTATIONAL RESULTS

5.1 Discussion

In the previous chapter the concept of individual machine energy, the critical group and critical machine were defined. Once the last generator in the critical group, the critical generator, was decoupled from the stationary group then the two groups produced by the fault energy will disconnect and all of the generators of the critical group lose synchronism with respect to the rest of the system. Thus, the true region of stability of the entire system or the critical clearing time depends on the energy behavior of the critical generator.

The energy behavior of the critical generator is investigated by consideration of a boundary encircling this generator. One such boundary is observed in the sum of the relative kinetic energy between the critical generator and the rest of the generators in the system (both the generators of the stationary group and the remaining generators of the critical group). This boundary, the "Local Kinetic Energy Condition" (LKEC), is crossed when the critical trajectory reaches a point where the critical generator kinetic energy is minimum as a function of time after the fault is cleared. The crossing of this kinetic energy boundary indicates a crossing of the region of stability of the individual generator and thus a loss of stability for the critical generator, critical group, and system. It is quite clear that in the fault period $t \in (0,t_c)$ the critical machines accelerate and hence the sum of the kinetic energies (LKEC) increase. Upon the clearance of the fault, the post-fault network decelerates the critical generator and the LKEC decreases until it reaches a minimum. The increase of LKEC during the fault and the decrease until reaching a minimum is true for every clearing time.

When the fault is cleared at $t_{c_1} > t_{cc}$ (critical clearing time), the fault energy accelerates the critical generator so much that the absorbing capability of the post-fault transmission lines connecting the critical generator to the rest of the system is consumed rapidly and the minimum of LKEC, occurring at time t_{B_1}, is achieved quickly. Once this minimum is achieved, the LKEC increases sharply. Now if the fault is cleared at $t_{c_2} > t_{cc}$ such that $t_{c_2} < t_{c_1}$, then a smaller amount of energy is contributed to the acceleration of the critical generator, and thus the absorbing capability of the post-fault network existing between the critical generator and the rest of the system is consumed at a longer time and hence the minimum of LKEC occurs at $t_{B_2} > t_{B_1}$. As the fault is cleared at a clearing time closer to the actual critical clearing time, the minimum of LKEC occurs at a longer time, and furthermore, the level of this minimum LKEC is reduced indicating the existence of a smaller amount of excess kinetic energy between the critical generator and all of the generators in the rest of the system. Among all the minimum of the LKEC, the absolute minimum corresponds to the critical clearing time and has a value near zero. A minimum of individual generator kinetic energy over time after clearing near zero indicates the direction of motion of the critical generator with respect to the other generators has reversed indicating the critical generator and system remain stable. The minimum kinetic energy over time after clearing for $t_c < t_{cc}$ will be near zero indicating stability, but when $t_c = t_{cc}$, the kinetic energy minimum is less than for $t_c < t_{cc}$ from simulation results to be presented suggesting that at $t_c = t_{cc}$ more of the kinetic energy is drained from the critical generator at $t_c = t_{cc}$. An algorithm based on the LKEC will be pursued further in the next section.

The second approach in estimation of the critical clearing time uses the concept of the equal area criterion. Recalling the method of "Equal Area Criterion" of two machine, the region of stability is defined by comparison of energy in two different periods of time, i.e., the potential energy (A_1) obtained during the fault period that is a measure of acceleration between critical generator and the generators in the rest of the system and the potential energy in the post-fault period that measures the deceleration energy. The sum of the partial energy of the system existing between the critical generator and the rest of the system over the two periods is the basis of a "Local Equal Area Condition." This LEAC condition requires that the sum of the partial potential energy function must be zero indicating the initial acceleration energy during the fault period is absorbed by the post-fault network resulting in deceleration to a near-zero kinetic energy. The partial potential energy over the fault period is evaluated by the use of the <u>during-fault</u> network configuration and the partial potential energy is evaluated by using the reduced post-fault admittance matrix. Hence

$$A_k = \frac{1}{M_T} \sum_{\substack{j=1 \\ j \neq i}}^{n} (P_i M_j - P_j M_i)(\delta_{ij} - \delta_{ij}^s) + \sum_{\substack{j=1 \\ j \neq i}}^{n} C_{ij}^{pf_k} (\mathrm{Cos}\,\delta_{ij} - \mathrm{Cos}\,\delta_{ij}^s)$$

$$- \int_{\delta_i^s + \delta_j^s - 2\delta_o^s}^{\delta_i + \delta_i - 2\delta_o} D_{ij}^{pf_k} (\mathrm{Cos}\,\delta_{ij})\, d(\delta_i + \delta_j - 2\delta_o)$$

where k=1,2: identifies the during-fault and post-fault parameters $(C_{ij}^{pf_1}, D_{ij}^{pf_1})$ and $(C_{ij}^{pf_2}, D_{ij}^{pf_2})$, the during-fault and post-fault quantities A_1 and A_2, respectively. Section 5.3 is devoted to the investigation of the properties associated with this concept.

5.2 Local Kinetic Energy Condition

As the first criterion for assessment of the transient stability of the entire power system, the kinetic energy of the critical generator is investigated. Considering the one-machine infinite bus case, the boundary of stability is identified by the comparison of the energy gained during the fault on period and the amount of energy at an instant of time where the relative velocity of the machine with respect to the infinite bus, ω, reaches zero. In transition from one state to another, there are two states where the relative velocity of the machine with respect to the infinite bus becomes identically zero, i.e., at the post-fault stable equilibrium state and/or at the unstable equilibrium state. A zeroing of kinetic energy at some instant after fault clearing which then again increases is a necessary and sufficient condition for stability for the single generator infinite bus system. If the system is unstable, the kinetic energy never approaches zero after fault clearing, and if critically stable, the kinetic energy remains zero after it becomes zero.

Based on the foregoing observation and the fact that the generators of the critical group decouple from the rest of the system one at a time, it is intuitively appealing to consider the generators of the critical group (and particularly the critical generator) against the rest of the system analogous to the one machine-infinite bus case. Hence the kinetic energy produced by the relative motion of the generators of the critical group with respect to the rest of the system is monitored.

The quantity

$$KE_i = \frac{1}{2M_T} \sum_{\substack{j=1 \\ j \neq i}}^{n} M_i M_j (\omega_i - \omega_j)^2 \tag{5.1}$$

where i represents a unit in the critical group, is a quantitative measure of the kinetic energy produced from the relative motion of generator i with respect to the motion of the rest of the system. It can be viewed as a normed measure of the velocity of the generator with respect to all other generators in the system.

At the pre-fault stable equilibrium point, the acceleration of the entire system, i.e., $\dot{\underline{\omega}}=0$, and thus there is no kinetic energy produced by the relative movement of the generators. When the fault is applied, the state of the system deviates from the equilibrium state and the fault energy in part becomes kinetic energy. Because of the fault energy, the generators of the critical group and hence the critical generator are accelerated with respect to the rest of the system resulting in an increase of the kinetic energy of the critical generator with respect to the rest of the generators in the system. The maximum kinetic energy of the critical generator is achieved at the instant of fault clearing. After the fault clearing, the post-fault network decelerates the accelerated generators and the kinetic energy of the generators of the critical group start to decrease and reach a minimum.

For any clearing time, the kinetic energy of the critical generator attains a minimum but what is of interest is the fact that for the clearing times $t_c > t_{cc}$, not all the kinetic energy is absorbed by the post-fault network. Thus, even though the kinetic energy reaches a minimum after the fault clearing time, the amount of the minimum of the kinetic energy is relatively large. At a clearing time less than or equal to the critical clearing time, almost all of the kinetic energy of the system is absorbed in potential energy of the transmission network. A minimum of kinetic energy after fault clearing indicates a reversal of the direction of motion of the critical generator (or critical group) from that caused by the fault acceleration. A reversal of direction of motion on the first swing in the critical group has traditionally been interpreted as a necessary and sufficient indication that stability is preserved. The minimum of kinetic energy after fault clearing near zero is just a measure that can but does not necessarily reflect this traditional indication of stability. However, if multi-machine systems behave as the single-machine infinite bus, a zeroing of kinetic energy that increases afterwards is a necessary and sufficient condition for retention of stability.

The "Kinetic Energy Stability Criterion" in Chapter 3 was based on this principle and assumed that the kinetic energy of the accelerated group would approach zero sometime after fault clearing. The algorithm based on this condition cleared the fault when the total system energy at clearing $V_C(t_c)$ approaches a critical value V_{CR}. For an initial choice of V_{Cr} such that $V_C(t_c)=V_{Cr}$ where $t_c > t_{cc}$, the between-group minimum kinetic energy $KE_{BG}(t_B)$ at $t_B > t_c$ was assumed to be the excess energy in V_{Cr} that caused loss of stability. Thus the revised choice for V_{Cr} is

$$V'_{Cr} = V_{Cr} - KE_{BG}(t_B)$$

The algorithm proposed in this chapter replaces $KE_{BG}(t_B)$ by the minimum kinetic energy between the critical generator i and the rest of the generators (5.1) at $t'_B > t_c$. The kinetic energy boundary based on (5.1) is a measure of the kinetic energy between a generator in the critical group with respect to the rest of the system. This kinetic energy is exactly the "between group" kinetic energy introduced in Chapter 3 if the individual machine (a member of the critical group) is considered as one group and the rest of the system as a second group. Recall that the total kinetic energy was split into two parts,

$$KE = KE_{BG} + KE_{WG} \tag{5.2}$$

where KE_{BG} and KE_{WG} are the between- and within-group kinetic energies. Also from Chapter 3

$$KE_{BG} = \frac{1}{2M_T} \sum_{k=1}^{K-1} \sum_{\ell=k+1}^{K} \sum_{\substack{i=n+1 \\ k-1}}^{n_k} \sum_{\substack{j=n+1 \\ \ell-1}}^{n_\ell} M_i M_j (\omega_i - \omega_j)^2 \tag{5.3}$$

where K, n_k, n_ℓ are the number of groups, number of generators in the k^{th} and ℓ^{th} group, respectively. For the assumption that the power system consists of two groups and further that one of the groups contains only one of the generators of the critical group, then (5.3) will become the LKEC of (5.1). It is hypothesized then that the true region of stability is related to the Local Kinetic Condition based on (5.1). Furthermore, for every generator in the critical group, there exists a kinetic energy condition between this generator and the rest of the system. Among all these LKEC's the one existing between the critical generator and the rest of the system, i.e.,

$$KE_{BG_i} = \frac{1}{2M_T} \sum_{\substack{j=1 \\ j \neq i}}^{n} M_i M_j (\omega_i - \omega_j)^2$$

where i is the <u>critical generator</u>, dictates the true region of stability.

COOPER CASE: Consider the Cooper Case where a three-phase fault is applied near generator 2. The generators electrically close to the faulted generator are generators 1, 17, 12 and 16. For several fault clearing times the behavior of all of the generators in the power system was investigated. Figures 5.1, 5.2 and 5.3 depict

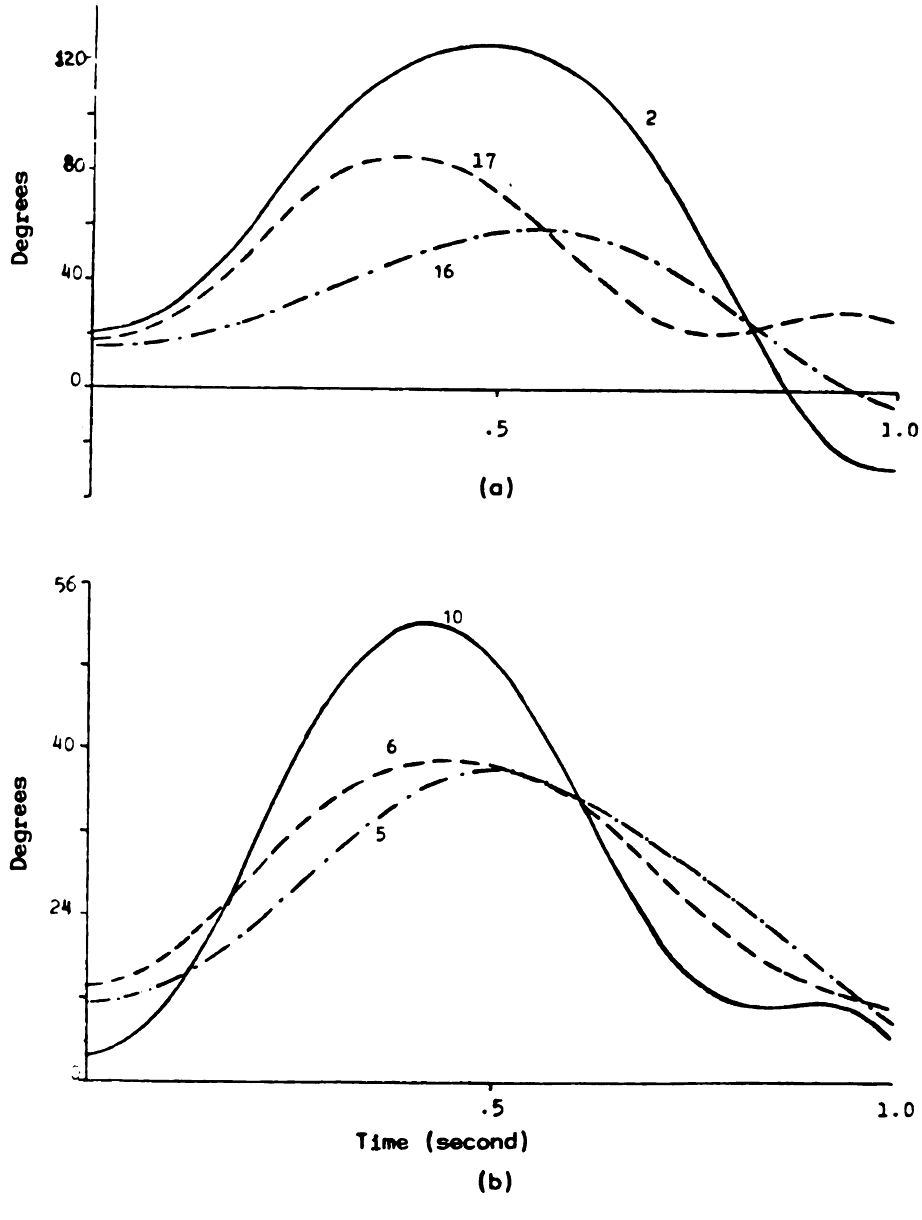

Figure 5.1 Swing curves. Clearing time = .2100 seconds.
a) Generators 2, 16 and 17
b) Generators 5, 6 and 10

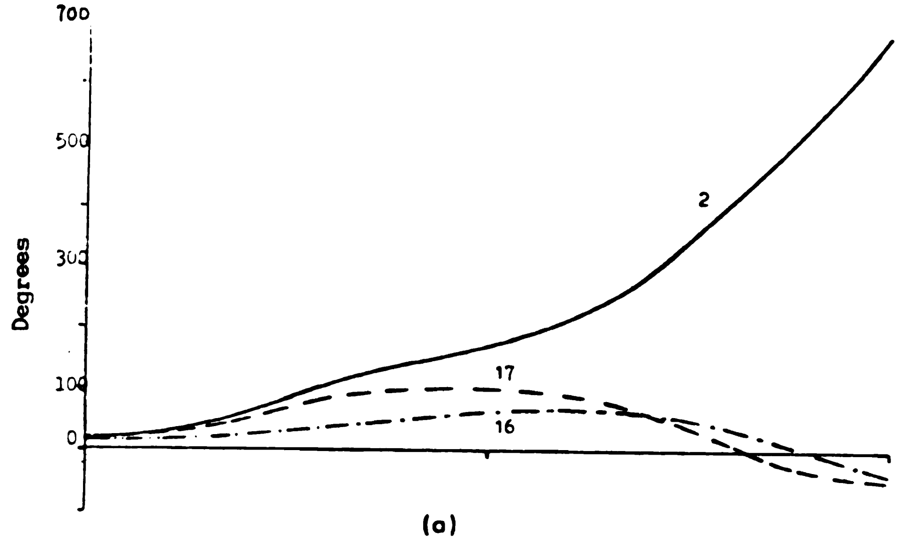

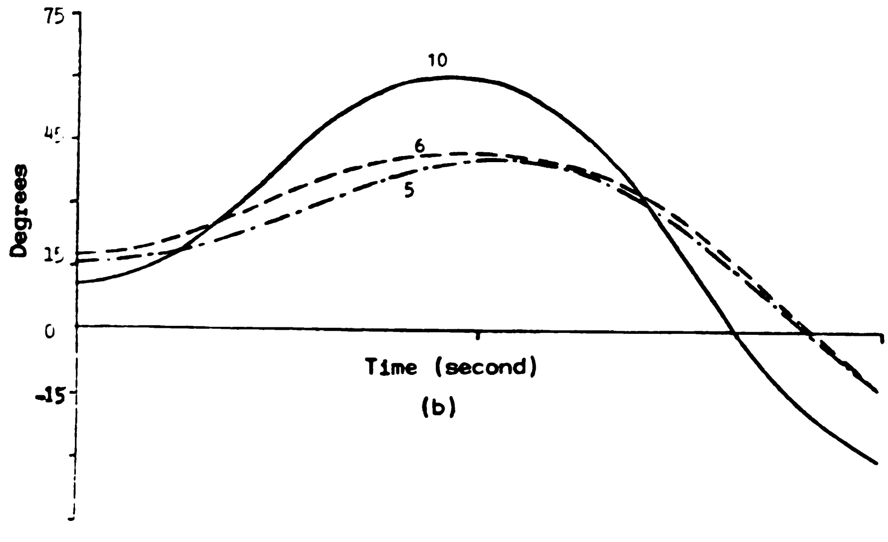

Figure 5.2 Swing curves. Clearing time = .2400 seconds.
a) Generators 2, 16 and 17
b) Generators 5, 6 and 10

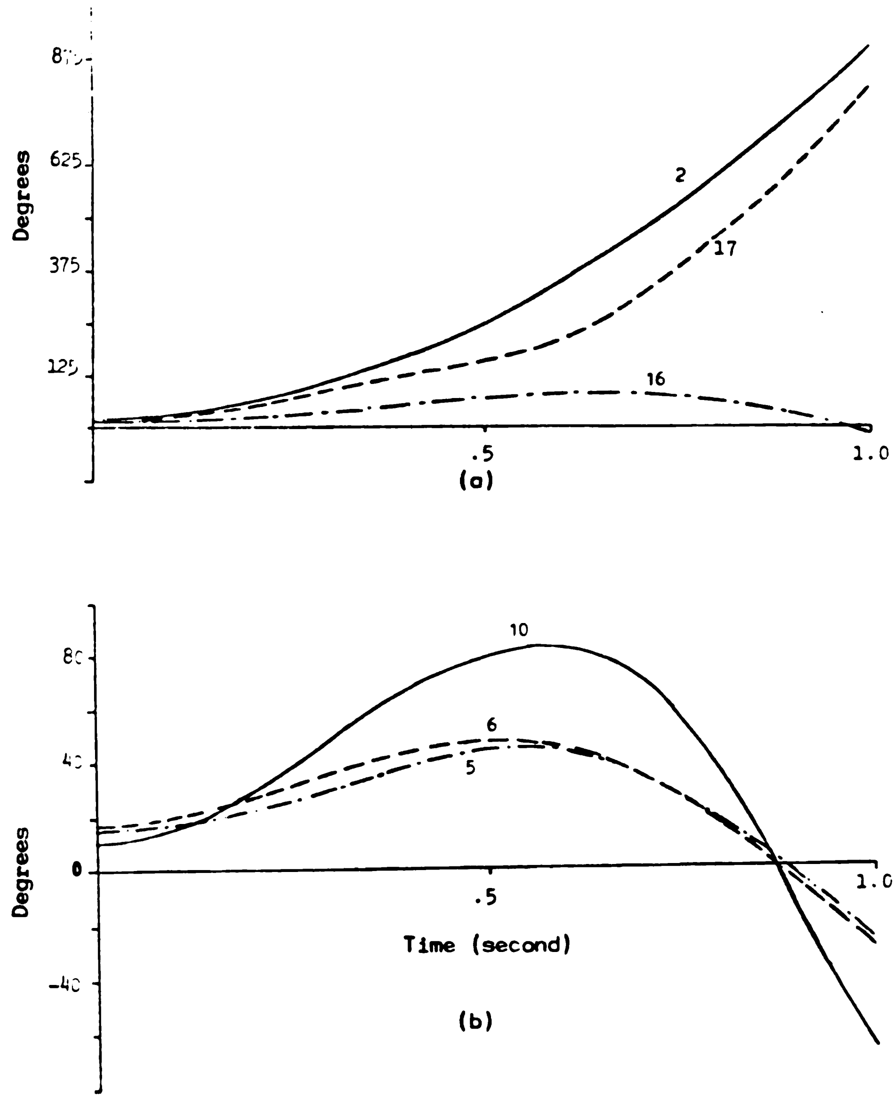

Figure 5.3 Swing curves. Clearing time = .3000 seconds.
a) Generators 2, 16 and 17
b) Generators 5, 6 and 10

the swing curves for generators 5, 6, 10, 17, 16 and 2, for fault clearing times of t_c=.21, .24 and .30 seconds, respectively. When the fault is cleared at t_c=.21, all the generators stay stable, and although the peak of swing curves of generator 2 reaches approximately 126°, ($\vartheta_2 > 90°$), it ultimately decelerates and forms a stable group with the rest of the system. Figure 5.2, however, illustrates that for a longer clearing time (t_c=.24 sec) generator 2 accelerates and pulls away from the rest of the system and hence by the definitions of Chapter 4 forms the <u>critical group</u>. As a further step, Figure 5.3 illustrates that for t_c=.3 second both generators 2 and 17 lose synchronism with respect to the rest of the system but the group consisting of these two generators, which did not lose synchronism simultaneously, is not considered as the critical group. To further confirm the fact that the critical group consists of generator 2 solely, a special program based on the Davidon-Fletcher and Powell optimization technique, developed by Systems Control, Inc. (SCI) was used. This algorithm minimizes a scalar one-dimensional quantity, the mismatch function ($F(\vartheta)$, which is a measure of closeness to an equilibrium point. The scalar quantity [4]

$$F(\vartheta) = \sum_{i=1}^{n} f_i^2(\underline{\vartheta})$$

where $f_i(\vartheta) = M_i\dot{\omega}_i = P_i - P_{ei} - \frac{M_i}{M_T} P_{COA}$ is identically zero for

$\dot{\omega}_i=0$, $i=1,2,\ldots,n$. Therefore, at a true equilibrium point $F(\vartheta)=0$ and increases as the trajectories move away from the equilibrium state. Starting from the post-fault stable equilibrium point where $F(\vartheta)=0$ (bottom of the valley in Figure 2.4), the mismatch power reaches its maximum at a point ϑ^{ss} on the boundary connecting all the unstable equilibrium points. Starting from ϑ^{ss}, the same function is minimized in every angle direction to obtain an approximation, $\hat{\underline{\vartheta}}^u$ to the actual unstable equilibrium point $\underline{\vartheta}^u$. $\underline{\vartheta}^u$ is then the result of a minimization load flow technique using $\hat{\underline{\vartheta}}^u$ as its starting points [4].

Table 5.1 illustrates the post-fault s.e.p. and the appropriate u.e.p. closest to the faulted trajectory for both the Cooper and Raun cases. From the third and fourth columns of Table 5.1, it is clearly seen that the ϑ_2^u in Cooper and $(\vartheta_5^u, \vartheta_6^u)$ in Raun exceed 90°, indicating the generators of the critical group. Note that for the Cooper case the critical group and critical generator are identical. For Raun this result indicates (5,6) is the critical group but results in Chapter 4 indicates (5) is the critical generator.

The critical boundary or the LKEC for Cooper is based on the minimum over time after t_c of

$$KE_2 = \frac{M_2}{2M_T} \sum_{\substack{j=1 \\ j\neq 2}}^{17} M_j(\omega_2-\omega_j)^2$$

Table 5.1. The equilibrium points for Cooper and Raun cases

Post-fault s.e.p. (Degrees)		Machine	Unstable Equilibrium Points (Degrees)	
Cooper	Raun		Cooper	Raun
-5.11	-4.92	1	-5.91	-1.41
21.77	22.26	2	150.04	46.63
5.36	5.60	3	3.55	9.68
-4.51	-8.34	4	-9.86	-23.95
15.28	18.87	5	18.06	163.55
16.75	21.57	6	20.42	144.87
-1.41	-1.53	7	-9.31	-15.96
-4.88	-4.76	8	-9.52	-7.98
9.33	8.91	9	.86	-6.62
10.37	12.85	10	19.64	47.77
-4.03	-1.17	11	-5.17	10.28
11.39	13.90	12	21.28	49.58
-6.93	-6.61	13	-16.54	-25.80
-5.29	-5.08	14	-14.83	-23.62
.52	-2.12	15	-5.66	-17.61
14.87	17.78	16	23.34	63.55
17.98	19.43	17	34.78	50.06

This critical generator kinetic energy is observed in Figure 5.4 and the results are summarized in Table 5.2.

For a relatively large clearing time, the kinetic energy existing between the critical generator and the rest of the system is large indicating the inability of the post-fault network to reverse the motion of the accelerated generator (the critical generator). Consider the first row of Table 5.2 where the fault is cleared at t_c=.3 sec. The post-fault network is able to absorb only a small portion of the kinetic energy at clearing (approximately 8%) and the minimum of the critical boundary is reached very shortly after the clearing time (at t_B=.35 sec), indicating the fact that the critical generator is only slightly decelerated (a point of inflection on the critical generator trajectory). The critical generator is accelerated after crossing the boundary as seen in increasing kinetic energy shown in Figure 5.4 and thus the critical generator and system loses stability. The results in Figure 5.4 and Table 5.2 indicate as clearing time is reduced, a higher percentage of the critical generator's kinetic energy at the clearing time is absorbed by the post-fault network. Eventually an instant of clearing time is reached for which all of the clearing kinetic energy of the critical generator is absorbed by the post-fault network and the minimum of the critical generator kinetic energy $KE_2(t_B)$ reaches zero indicating stability. The maximum clearing time at which this kinetic energy minimum $KE_2(t_B^*)$ is zero is the critical clearing time. It

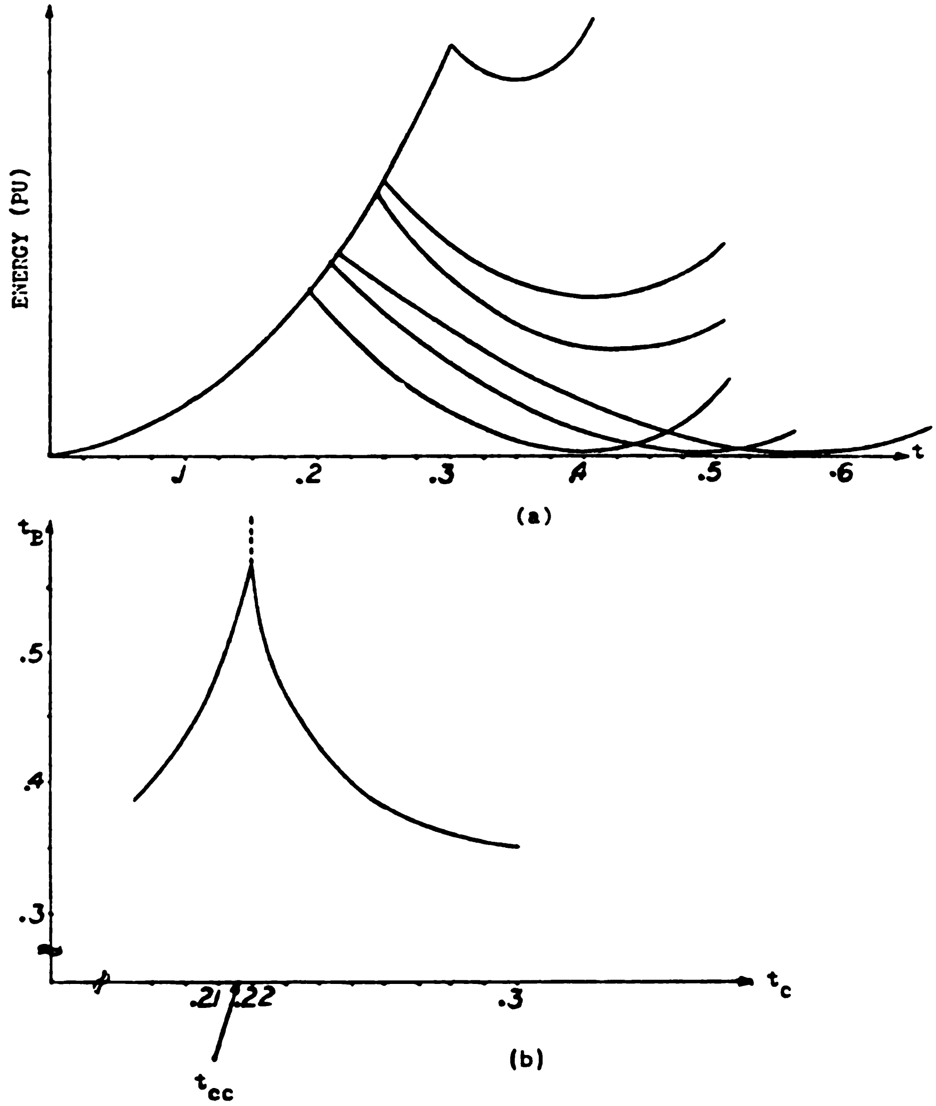

Figure 5.4 Determination of critical clearing time for Cooper via LKEC.
a) Kinetic energy vs. time
b) Boundary time vs. clearing time

Table 5.2 Local Kinetic Energy Condition for Cooper

t_c	$KE_2(t_c)$	t_B	$KE_2(t_B)$
.3	12.74	.35	11.73
.25	8.92	.40	4.63
.24	8.23	.42	3.10
.22	6.94	.56	.12
.21	6.33	.48	.14
.19	5.19	.4	.1

t_B: time at which the minimum of LKEC occurs

t_c: clearing time

should also be noted that the critical generator trajectory for this particular clearing time (t_{cc}) achieves the kinetic energy minimum at a latest time (t_B) than all the trajectories for which the fault was cleared at $t_c < t_{cc}$ since for $t_c < t_{cc}$ the machine receives less initial energy and takes a shorter time to decelerate and turn around. The crossing of the kinetic energy boundary also occurs earlier for $t_c > t_{cc}$ than at $t_c = t_{cc}$ since the excess kinetic energy that cannot be absorbed is a measure of the velocity of that generator as it crosses the boundary. Therefore, based on observation of the time t_B at which the crossing of the critical boundary happens, one is able to predict the critical clearing time as the t_c for which t_B is maximum. The other method of predicting t_{cc} is the maximum t_c for which $KE_2(t_B) \approx 0$. For the Cooper case it is estimated that the actual critical time is $t_c \in (.21, .22)$ seconds based on both criteria for selecting t_{cc}; accurate results are possible if the simulation is performed with a smaller integration step.

RAUN CASE: For the generators of the Raun critical group, a similar analysis to that of generator 2 of the Cooper Case is performed. Tables 5.3a and 5.3b summarize the results obtained by monitoring the individual machine kinetic energy for generators 5 and 6, respectively, shown in Figure 5.5. From Table 5.3a it is clearly observed that, as the clearing time decreases toward the actual critical clearing time (which is not known at this time), the minimum

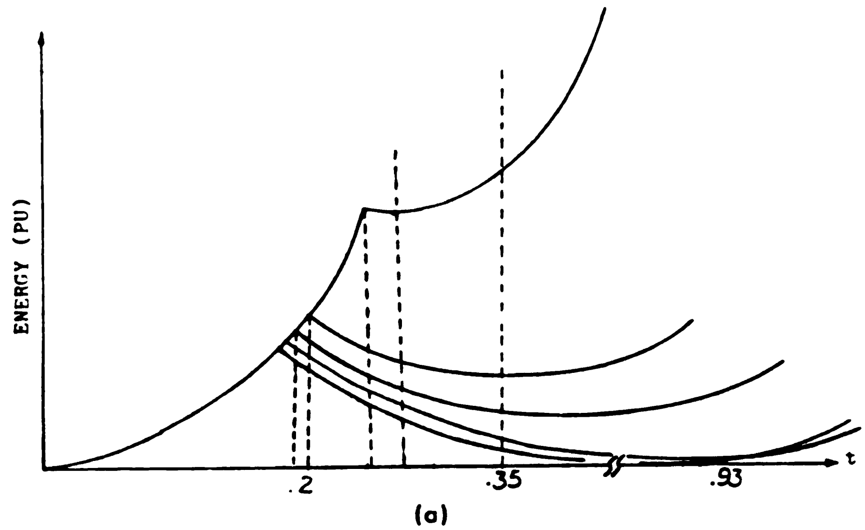

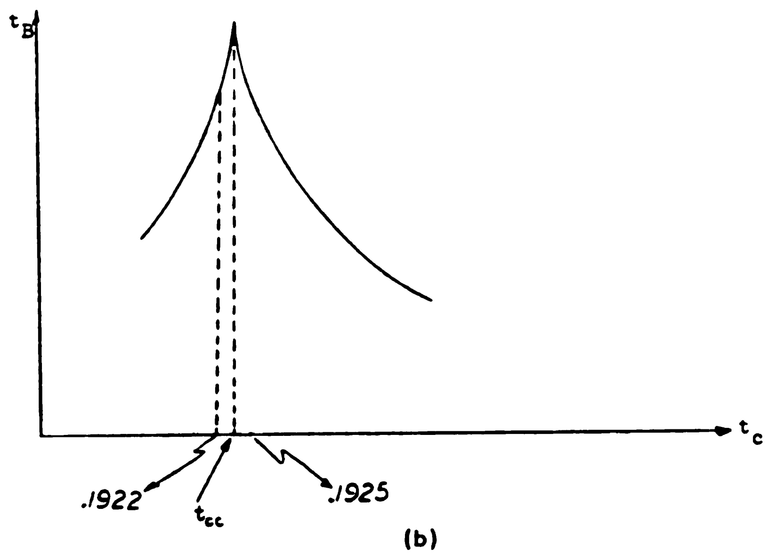

Figure 5.5 Determination of critical clearing time for Raun via LKEC.
a) Kinetic energy vs. time
b) Boundary time vs. clearing time

Table 5.3a. Local Kinetic Energy Condition for Generator 5 (Raun)

t_c	$KE_5(t_c)$	t_B	$KE_5(t_B)$
.25	2.10	.27	2.08
.2	1.53	.35	1.17
.195	1.47	.415	.98
.1925	1.444	.9300	.2
.1922	1.44	.8835	.008
.192	1.438	.816	.019

Table 5.3b. Local Kinetic Energy Condition for Generator 6 (Raun)

t_c	$KE_6(t_c)$	t_B	$KE_6(t_B)$
.25	19.84	.30	14.56
.2	11.44	.42	1.55
.195	10.88	.515	.40
.1925	10.61	.5375	.11
.1922	10.57	.5209	.115
.192	10.50	.504	.93

of the critical boundary decreases until it reaches its minimum value at $t \in (.8835, .9300)$. Note that again by observation of column three or four of Table 5.3a one is able to estimate the critical clearing time $t_{cc} \in (.1922, .1925)$. Further, it is seen that t_B reaches a minimum for $t_c \in (.1922, .1925)$, confirming t_{cc} lies in this range.

From Table 5.3b where the LKEC for generator 6 is considered, it is observed that again the minimum of $KE_6(t)$ decreases sharply as the clearing time approaches the critical clearing time and stays almost flat for the $t_c < t_{cc}$. The critical clearing time based on the third and fourth columns of this table are again estimated to be in the interval $t_{cc} \in (.1922, .1925)$. However, the time at which the minimum of $KE_6(t_B)$, that is, the time at which the velocity of generator 6 reverses direction and is as close as possible to the velocity of the rest of the system, is shorter than that of generator 5. The phenomenon indicates that more time is needed to drain out the excess clearing kinetic energy of generator 5 than that of generator 6. In other words, although both generators 5 and 6 lose synchronism with respect to the stationary group, generator 5 is strongly coupled to the rest of the system, after 6 has become weakly coupled and becomes weakly decoupled at a later time. This further confirms the fact that the true mechanism of stability is dictated by generator 5 rather than 6.

It should be noted that the prediction of the critical clearing time in the middle of the interval (.1922, .1925) agrees with transient stability simulation results. This accuracy of the prediction of critical clearing times is greater than for the kinetic energy stability condition based on (5,6) group kinetic energy approaching zero where t_{cc} was predicted to occur in (.19, .1922). The accuracy of these results is similar to that in [16] based on setting the critical energy V_{Cr} in

$$V_i(t_c) = KE_i(t_c) + PE_i(t_c) \le V_{Cr_i}$$

based on the peak potential energy $PE(t_B)$. This algorithm [16] is based on the individual machine energy function.

The algorithm based on the local kinetic energy stability condition and the potential energy [16] based on individual machine energy function are far more accurate than methods based on total system energy described in Chapter 2 by a factor of 5 and up to 200. Thus, it appears that algorithms for individual generator energy function should be pursued further to find efficient computational methods that do not require simulation of the transient stability model.

5.3 Local Equal Area Condition

The second method for determining the boundary of stability for a multi-machine power system is based on the well-known "equal area criterion" (EAC) of one-machine infinite bus systems. The "Local Equal Area Condition"

(LEAC) is an extension of EAC in the sense that a particular machine of the critical group is considered against the rest of the generators in the power sysem. Then by comparison of the energy transaction between this particular generator and the rest of the system during and after the fault period, a decision on the stability of the entire power system is made. In order to clarify the subject, the concept of EAC is revisited and is investigated in a suitable manner.

For the one-machine infinite bus model, consider the power angle representation of Figure 5.6 illustrating the behavior of the single machine against the infinite bus during the transition from one state to another. The area A_1 in Figure 5.6a, which is obtained from the mismatch of power existing between the mechanical input and the faulted electrical output is compared with a critical energy A_2. The critical energy A_2 is the amount of decelerating energy produced by the power mismatch of the post-fault network. Note that for $t_c < t_{cc}$ the rotor angle position peaks when $A_1=A_2$ and starts to decrease and oscillate afterwards. If the system is damped, then the rotor angle also damps out and assumes the post-fault steady-state angle.

$\Delta E(t)=-A_1(t)+A_2(t)$ is defined to be a function of rotor angle position which in turn is a function of time as follows

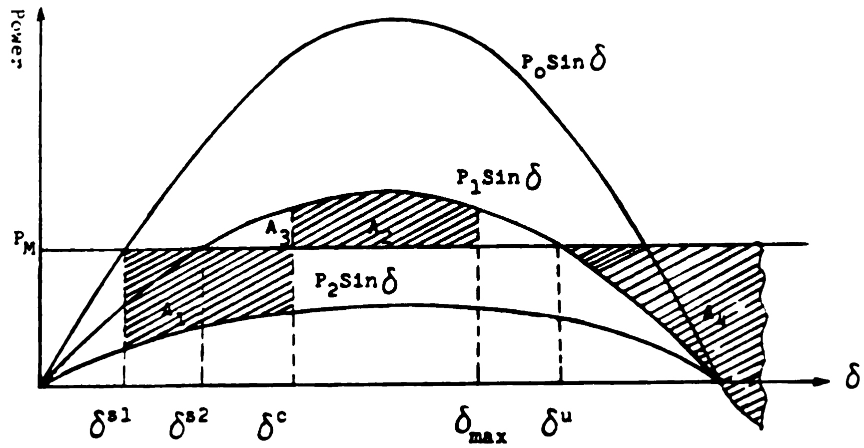

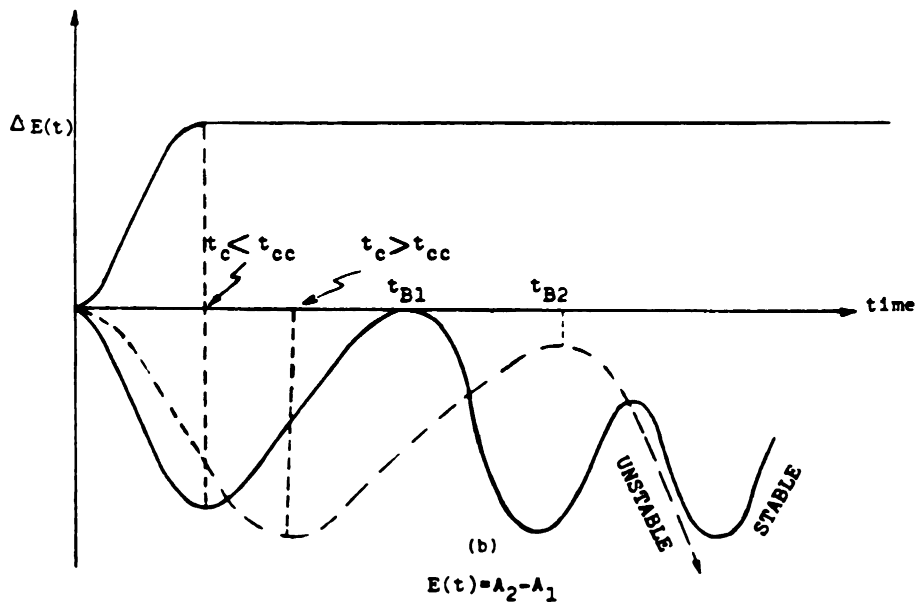

Figure 5.6 Equal area criteria.
a) Power angle representation of one-machine infinite bus
b) Variation of energy difference vs. time

$$A_1(t) = \begin{cases} +\displaystyle\int_{\delta_{s1}}^{\delta(t)} (P_M - P_2 \operatorname{Sin}\delta)\,d\delta & \delta(t) < \delta_c \\ 0 & \delta(t) \geq \delta_c \end{cases}$$

$$A_2(t) = \begin{cases} 0 & \delta(t) < \delta_c \\ -\left[\displaystyle\int_{\delta_c}^{\delta(t)} (P_M - P_1 \operatorname{Sin}\delta)\,d\delta\right] & \delta(t) \geq \delta_c \end{cases} \qquad (5.5)$$

Note that $\Delta E(t) = -A_1(t)$ becomes more negative as t and $\delta(t)$ increase. $\Delta E(t)$ captures the accelerating energy on the machine that is stored in the form of kinetic energy of the inertia of that machine. The acceleration is due to the fact that the faulted transmission network is too weak to hold the ma ine compared to the mechanical input power that performs work $P_M(\delta(t) - \delta_{s1})$ in accelerating the generator. $\Delta E(t) = -A_1(t_c) + A_2(t)$ for $t > t_c$ where $-A_1(t_c)$ is the total accelerating (negative) energy and $A_2(t)$ is the total decelerating energy at $t > t_c$ provided by the post-fault network that is more than capable of coping with the accelerating torque P_M.

Figure 5.6b depicts the quantity $\Delta E(t) = A_2 - A_1$ as a function of time. In the fault period $\Delta E(t) < 0$, and reaches its minimum value at the clearing time. At t_c, the network is switched to assume the post-fault network and hence for $t_c < t_{cc}$ $\Delta E(t)$ increases until it becomes zero (at t_{B_1}). Note that t_{B_1} is also the time at which the rotor angle position is maximum ($\delta(t_B)=\delta_{max}$).

The quantity $\Delta E(t)$ has an oscillatory response for $t_c < t_{cc}$ once $t > t_{B_1}$ reflecting the oscillations in $\delta(t)$ for $t > t_{B_1}$. Note that in the presence of damping, the oscillatory response of $\delta(t)$ and $E(t)$ damps out. In contrast, for $t_c > t_{cc}$, the quantity $\Delta E(t)=-A_1(t)$ decreases with time and then increases $(\Delta E(t)=-A_1(t_c)+A_2(t))$ for $t > t_c$. However, in this case $\mathrm{Max}(\Delta E(t)) < 0$ and occurs where $\delta(t)=\delta^u$ at $t=t_{B2}$. Thus, the decelerating energy capability of the post-fault network $A_2(t_{B2})$ is less than the acceleration energy $A_1(t_c)$. Since $\Delta E(t_{B2})=-A_1(t_c)+A_2(t_{B2}) < 0$ is a measure of the net decelerating energy and the kinetic energy remaining in the machine's inertia and since $\Delta E(t)$ remains negative and never reaches zero for all $t > 0$, the machine angle $\delta(t)$ never changes its direction of motion and continues to increase for $t > t_{B2}$. Thus, $\Delta E(t)=-A_1(t_c)+A_2(t_{B2})+A_4(t)$ for $t > t_{B2}$ where

$$A_4(t) = \begin{cases} 0 & \delta(t) < \delta^u \\ -\displaystyle\int_{\delta(t_{B2})=\delta^u}^{\delta(t)} (P_M-P_1\sin\delta)\,d\delta & \delta(t) > \delta^u \end{cases}$$

where $A_4(t) < 0$. Thus, for $t_c > t_{cc}$, $\Delta E(t)$ reaches a maximum less than zero at $\delta(t_B)=\delta^u$ and then decreases to a more negative value for $t > t_{B2}$.

It should be noted that increasing t_c for $t_c < t_{cc}$, t_{B1}, where $\Delta E(t_{B1})$ and thus kinetic energy is zero, increases since more accelerating energy $A_1(t_c)$ is put into the system and thus it takes a larger angle excursion. $\delta_{Max}=\delta(t_{B1})$ and thus a longer time for $\Delta E(t_{B1})=A_1(t_c)+A_2(t_B)=0$. For $t_c > t_{cc}$, t_{B2} decreases for increasing t_c since there is a larger excess accelerating and thus kinetic energy $\Delta E(t_{B2})=-A(t_c)+A_2(t_{B2}) < 0$. Thus, the maximum t_{B1} and t_{B2} occurs when $t_{B1}=t_{B2}$ for $t_c=t_{cc}$. Thus, there are two indicators of t_{cc} by observing the maximum values of $E(t)$.

(a) the maximum value of t_c for which the maximum value of $\Delta E(t)$ over t is zero

(b) the maximum time t_{B1} for $t_c \leq t_{cc}$ or t_{B2} for $t_c \geq t_{cc}$ at which $\Delta E(t)$ reaches its maximum value which satisfies $t_{B1}=t_{B2}$ and $E(t_{B1})=E(t_{B2})$ for $t_c=t_{cc}$.

This equal area criterion is now extended to multi-machine systems by attempting to apply a similar equal area analysis to the energy associated with accelerating and decelerating torques between critical generator i and the rest of the generators $j\neq i$ in the system. The potential energy measure is in part contributed by the torques on machine i and all $j\neq i$ from the equivalent transmission lines connecting generator i to the rest of the generators in the system.

Consider a particular generator i, in the critical group (for example, the critical generator). Then it is hypothesized that the boundary energy existing between this generator and the rest of the generators in the power system determines a boundary of stability of the entire system. The quantity,

$$PE_i = \frac{1}{M_T} \sum_{\substack{j=1 \\ j \neq i}}^{n} (P_i M_j - P_j M_i)(\delta_{ij} - \delta_{ij}^s) + \sum_{\substack{j=1 \\ j \neq i}}^{n} C_{ij}(\mathrm{Cos}\,\delta_{ij} - \mathrm{Cos}\,\delta_{ij}^s)$$
$$- \int_{\delta_i^s + \delta_j^s - 2\delta_o}^{\delta_i + \delta_j - 2\delta_o} D_{ij} \mathrm{Cos}\,\delta_{ij}\, d(\delta_i + \delta_j - 2\delta_o) \qquad (5.6)$$

identifies this boundary energy once with the during-fault configuration for $0 < t < t_c$, to obtain A_1, and then using the post-fault network from $t \geq t_c$, to obtain A_2 as was done in (5.5) for the single-machine infinite bus case. By observation of the behavior of $\Delta E = -A_1 + A_2$ and also the time and magnitude of the peak of $-A_1 + A_2$ just as in the single-machine infinite bus case, the boundary of stability is determined. Before pursing the subject further, the following remarks and limitations are in order.

Remarks:

(a) The concept of equal area is justified only for the lossless systems.

(b) When the power system consists of two generators or one generator against an infinite bus, the acceleration energy of the single machine is totally consumed by the infinite bus, and hence the quantity $-A_1+A_2$ at most reaches zero. However, this phenomenon may not necessarily hold for the boundary energy. A part of the energy produced by the critical generator resides within the center of inertia of the rest of the system.

Hence, the partial boundary energy at most is an approximation to the equal area. The errors involved in the analysis are in part due to the losses of the transmission network and in part due to the nonconstancy of the flow of energy between the critical generator and the rest of the system or measured by 5.6 (a and b above).

As a further justification of the analogy between the EAC and the LEAC, refer to Chapter 3. Note that in the analysis of this chapter the infinite bus assumptions are <u>not</u> considered and the real parameters of the network existing between the critical generator and the rest of the system are maintained.

For the Raun case, for both the inclusion and exclusion of the transfer conductances, several simulation runs for different clearing times were performed. Figure 5.7 through Figure 5.12 illustrate some of these results. Figure 5.7 depicts the partial potential energy across the boundary of generator 6, cleared at t_c=.18 seconds. It is clearly seen

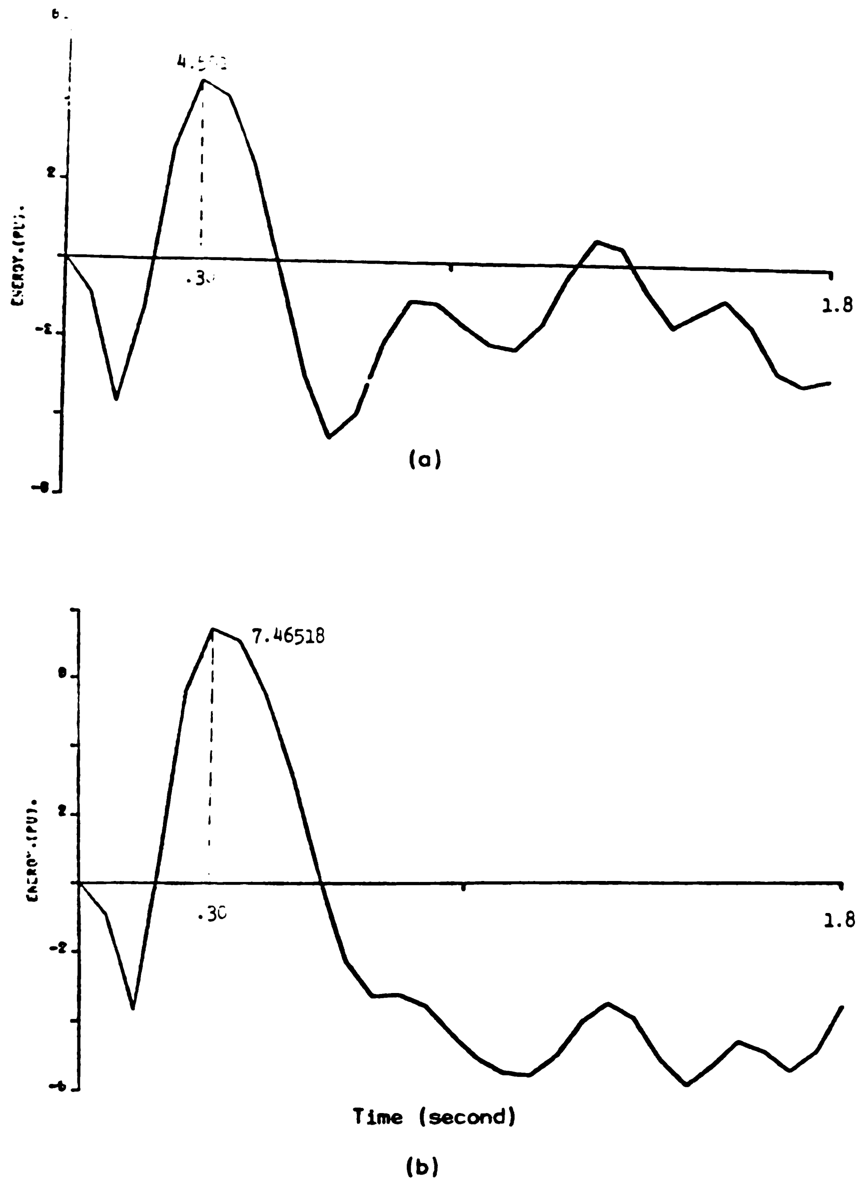

Figure 5.7 Equal area analysis (A_2-A_1). Raun case, 6-infinite bus. Clearing time = .18 seconds. a, b) Transfer conductance excluded and included, respectively

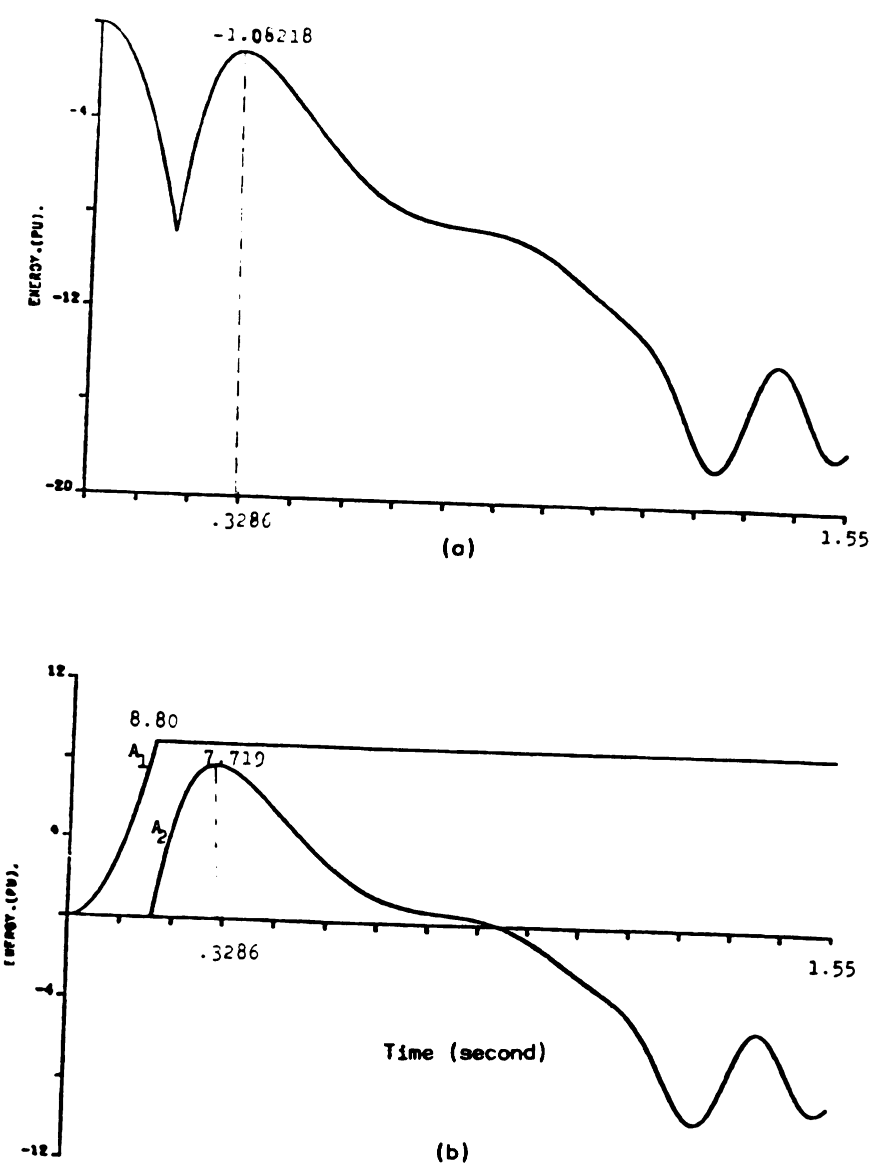

Figure 5.8 Equal area analysis. Raun case, 6-infinite bus. Clearing time = .1922 seconds.
a) $E(t) = A_2(t) - A_1(t)$ vs. time (transfer conductance included)
b) Areas A_1 and A_2 vs. time (transfer conductance included)

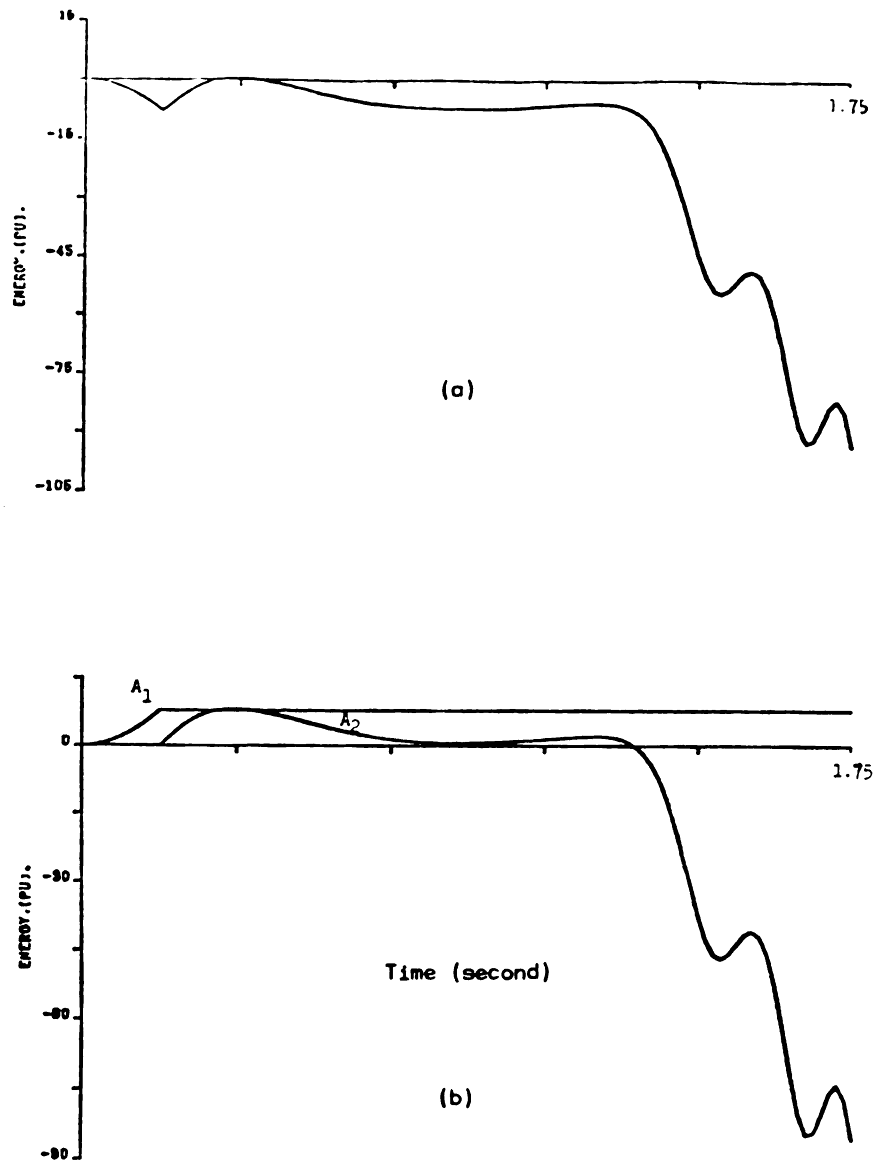

Figure 5.9 Equal area analysis. Raun case, 6-infinite bus. Clearing time = .1925 seconds.
a) $E(t) = A_2(t) - A_1(t)$ vs. time (transfer conductance excluded)
b) Areas $A_1(t)$ and $A_2(t)$ (transfer conductance excluded)

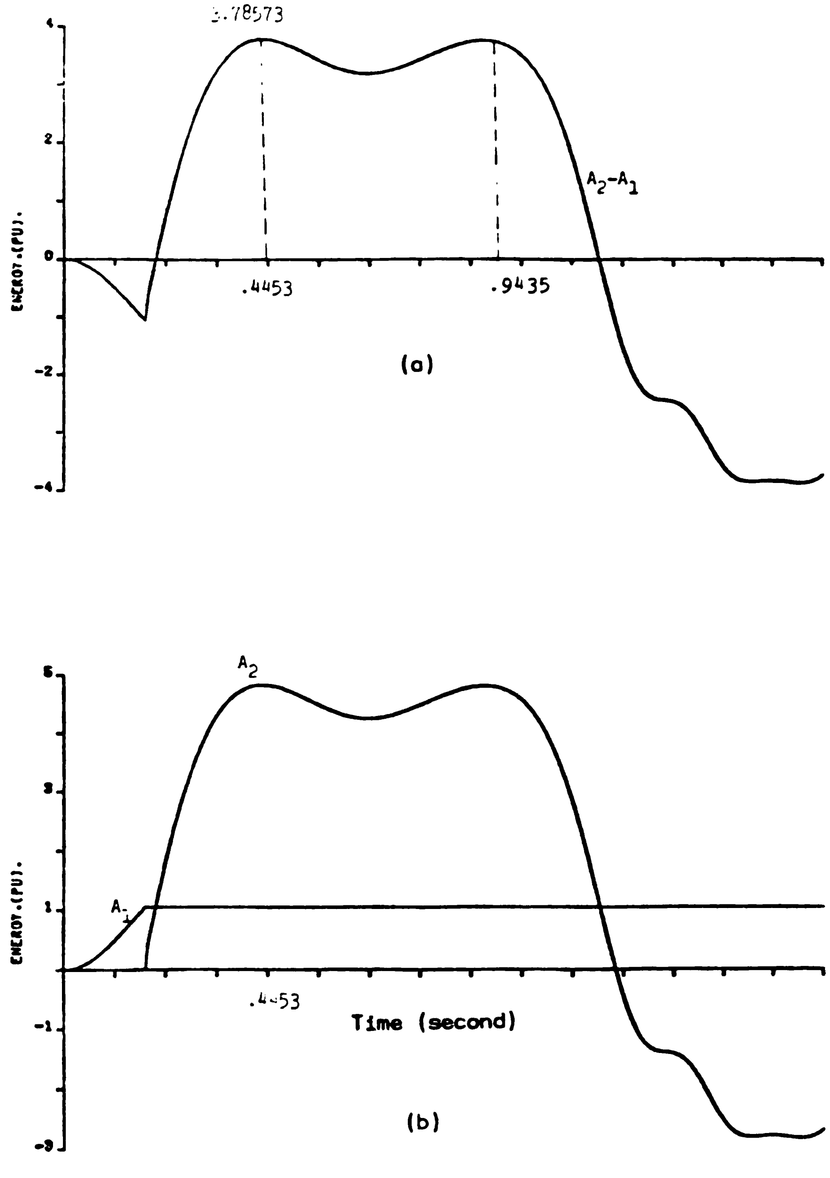

Figure 5.10 Equal area analysis. Raun case, 5-infinite bus. Clearing time = .1922 seconds.

a) $E(t) = A_2(t) - A_1(t)$ vs. time (transfer conductance included)

b) Areas $A_1(t)$ and $A_2(t)$ vs. time (transfer conductance included)

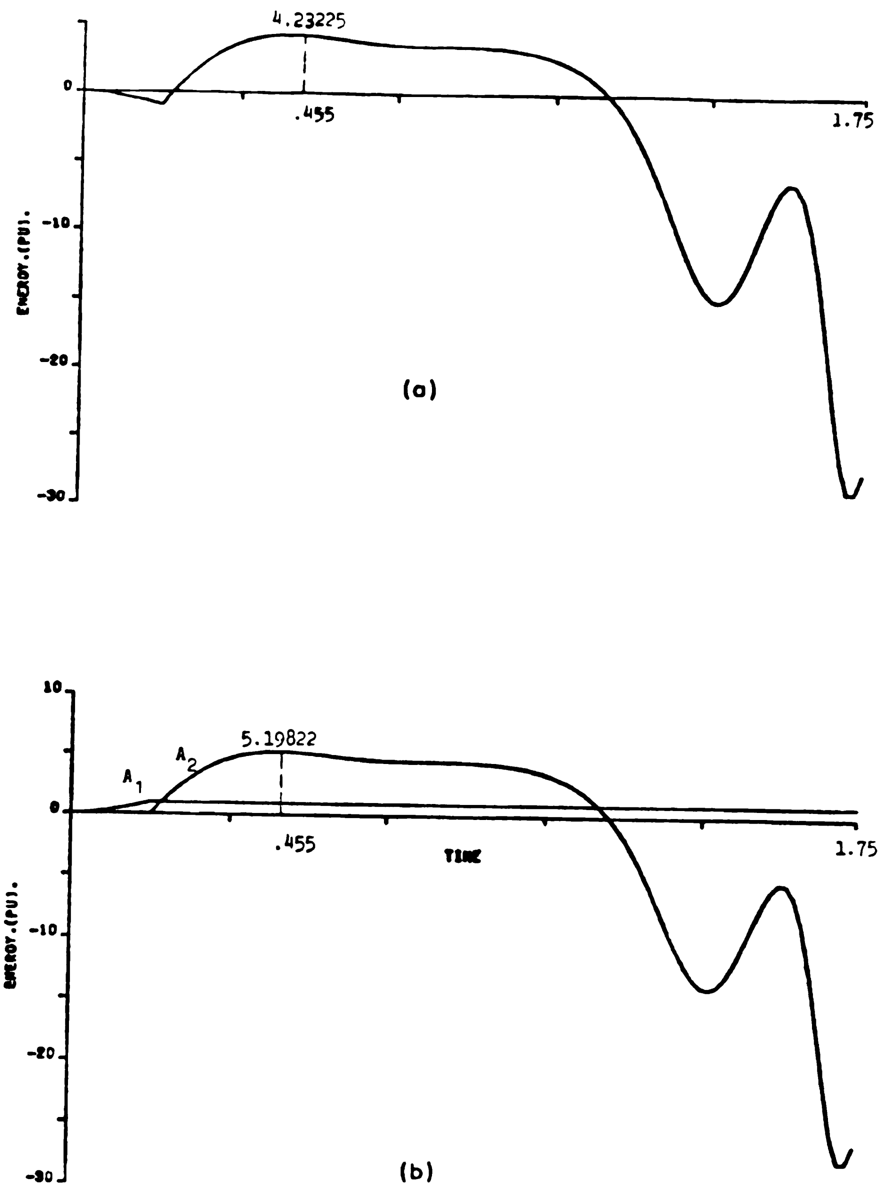

Figure 5.11 Equal area analysis. Raun case, 5-infinite bus. Clearing time = .1925 seconds.

a) $E(t) = A_2(t)-A_1(t)$ vs. time (transfer conductance included)

b) Areas $A_1(t)$ and $A_2(t)$ vs. time (transfer conductance included)

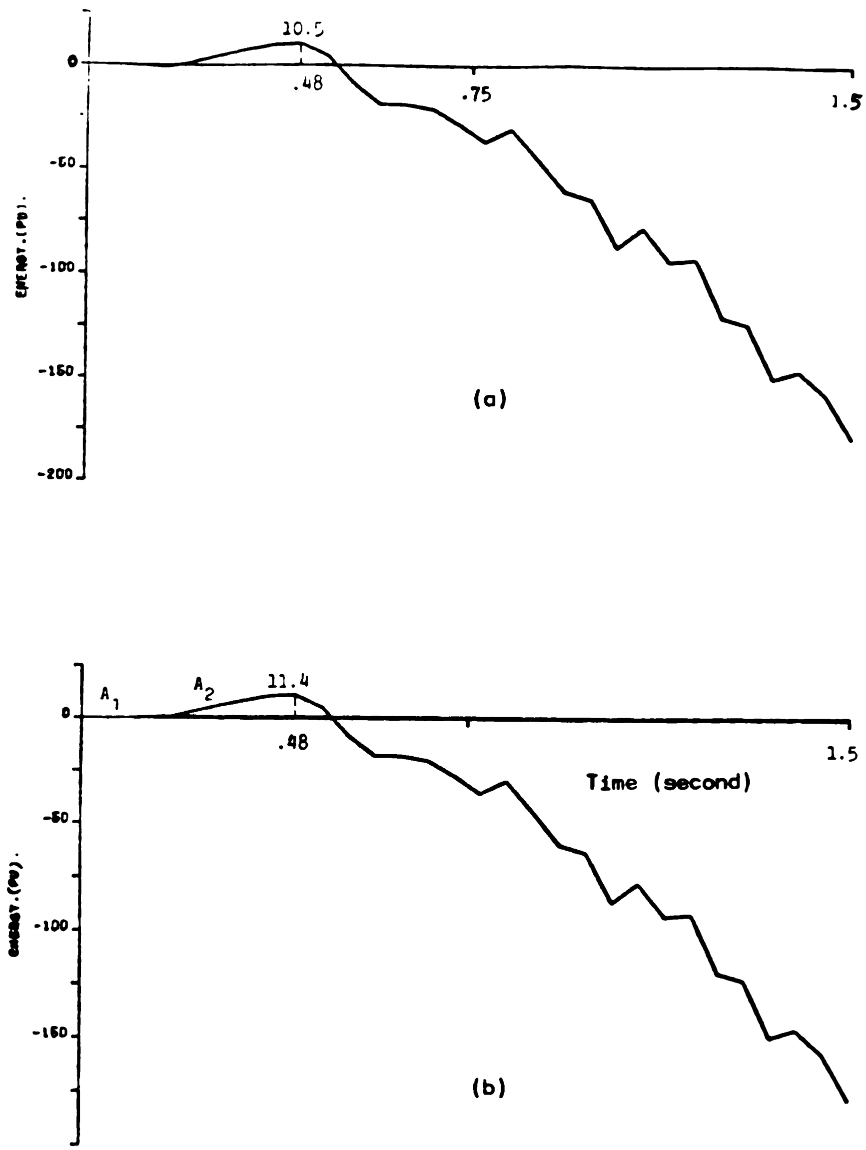

Figure 5.12 Equal area analysis. Raun case, 5-infinite bus. Clearing time = .24 seconds.
a) $E(t) = A_2(t)-A_1(t)$ vs. time
b) Areas $A_1(t)$ and $A_2(t)$ vs. time (transfer conductance excluded)

that the $\Delta E(t)$ for this case is oscillatory confirming the stability of the system. However, in contrast to the case of equal area criterion of one-machine infinite bus, the peak of $\Delta E(t)$ is not zero. As was discussed earlier, this phenomenon was expected. Note that the oscillatory behavior holds for both cases where the transfer conductance is and is not included. This observation certainly shows that for the qualitative analysis the concept of the equal area criterion can be extended for a multi-machine case. Figure 5.8, where the fault is cleared at t_c=.1922, illustrates the oscillatory behavior of generator 6 while in Figure 5.9, t_c=.1925, a sharp negative decrease in $\Delta E(t)$ is observed after t_{B2} indicating loss of stability.

Figures 5.10 through 5.12 depict the generator 5 potential energy boundary for t_c=.1922, .1925, and .24 seconds, respectively. The oscillatory behavior is only observed for t_c=.1922 seconds while the negative sharp decrease after t_{B2} is seen for both t_c=.1925 and t_c=.24 indicating loss of stability. In comparison of the behavior of generator 5 with that of generator 6, it is seen that the peak of $\Delta E(t)$ for generator 5 takes place at a later time than that of generator 6. Although the potential energy boundary of both generators predicts $t_{cc} \in$ (.1922, .1925), but the fact that the peak of $\Delta E(t)$ for generator 5 occurs at a later time confirms that the deciding generator is the critical generator.

Although the LEAC is an approximation to EAC, the results obtained by this method match perfectly with that of the LKEC of section 5.2. This technique is far from practical implementation; however, it sheds light on the importance of the consideration of an individual machine in determination of stability. Both the LKEC and LEAC as well as the algorithm of [16] are far more accurate than previous methods [13] for the cases studied. It should be pointed out that more exhaustive testing of the three algorithms is required to assure that they are robust in the sense that there are no special cases where they might fail to predict retention or loss of stability. The second major area of further work is to develop computationally efficient algorithms based on these conditions that do not require step-by-step integration of the system differential equations. Two approaches could be pursued in eliminating the need to integrate the differential equations; the first is to develop a Taylor series approximation for the system trajectory based on the pre-fault state δ_{s1} faulted network, post-fault network, and clearing time; the second is to develop a measure that will somehow predict the maximum angular swing for each generator based on the same information that is required for the Taylor series approximation. If either of these techniques is successful and if there are no special cases where the conditions developed in this chapter and in [16] fail, then the promise of a direct method for transient stability assessment may be realized.

CHAPTER 6

REVIEW, CONCLUSION, AND TOPICS FOR FUTURE INQUIRY

This final chapter is devoted to summarizing the results of the previous chapters and indicating the avenues for future investigations.

6.1 Chapter Review

The first part of Chapter 1 was devoted to the introduction of the concept of transient stability and its importance in preserving the quality of electric service. It was pointed out that in response to occurrence of a large disturbance the operating state of the power system will transit to a new operating point. In this transition the dynamic behavior and thus the stability of the system is determined via a step-by-step integration of the synchronous machine's rotor angles.

It was argued that in both planning and operation of a power system it is necessary to perform a set of transient stability simulations for several postulated contingencies. However, the increasing size of the power system interconnection, the need for consideration of a more detailed model of the power system and inclusion of such components as power system stabilizer in the power system model limits the use of the present transient stability analysis. Hence, the investigation of direct methods of Lyapunov for transient stability analysis of the power system was initiated as an alternative. A historical perspective for this investigation is provided by the consideration of the energy function development from 1947 to date. In the later part of the chapter it was concluded that the results obtained (regions of stability) by direct methods are conservative (small compared to the real value). It was then hypothesized that the true region of stability for the system is determined by a region of stability for a particular individual machine and this consideration removes part of the conservativeness.

In Chapter 2, the behavior of a power system during a transient is discussed. Based on this understanding, a two-dimensional (equal area) and a three-dimensional (3-D potential energy surface) example were presented. Finally, a discussion of an algorithm based on the potential energy boundary surface [4] and a u.e.p. algorithm based on energy accounting [13,14] were presented. A justification for the use of the classical transient stability model and an associated energy function concluded the chapter. This chapter is essential in presenting the ideas of the preceding chapters.

The first part of Chapter 3 was devoted to arguing that the fault splits the system into two coherent groups. The system kinetic and potential energy functions were divided into within-group and between-coherent group components. Then the assumptions of coherency were applied to the transient energy function of Chapter 2 (and not to the dynamics of the system), to develop an aggregated transient energy function (ATEF). It was shown that the energy function no longer had the within-group kinetic or potential energy components. The kinetic and potential energy components of ATEF were shown to measure the kinetic energy produced by the relative movement of the center of inertia of the two groups, and the potential energy of the equivalent transmission network connecting the two groups. Furthermore, the analysis indicated that the ATEF indeed is analogous to the equal area criterion. However, it was concluded that the region of stability identified by ATEF yields optimistic results because aggregating the generator groups in the energy function has the effect of stiffening the network connecting the groups and increasing the potential energy between groups. The transient energy function of the system, analytically split into within- and between-group energies, was then investigated. Based on the analysis of within-group and between-group energies at fault clearing time (t_C) and at the time (t_B) where the trajectory reaches the boundary of a region of stability, it was observed that kinetic energy between groups is zero at some $t_B > t_C$ if the system is stable but is not zero at the fault clearing time. This observation is used in a new algorithm that assumes the minimum between-group kinetic energy after fault clearing at t_c that exceeds critical clearing time (t_{cc}) is the excess energy at fault clearing that causes instability. This excess kinetic energy is subtracted from the clearing energy to obtain a new threshold for clearing energy at which the fault is cleared. The results of this algorithm are quite encouraging and far more accurate on this example than other methods that utilize total system energy. In the last part of this chapter it was again concluded that the consideration of the individual machine energy will estimate a still larger region of stability.

In Chapter 4, two hypotheses are discussed; i.e., (a) a single generator within an accelerated group dictates the stability of the accelerated group and thus the stability of the entire system and (b) that kinetic energy and potential energy of this critical generator indicate a kinetic and potential energy boundary, respectively. If these boundaries are exceeded, then the region of stability for the individual machine is crossed and the stability of the accelerated group and hence the entire system are lost. It is further discussed that the partial kinetic energy and partial potential energy existing between the critical generator and the rest of the system contain the individual machine's energies and thus are an indication of the individual machine's energy. The second section of this chapter investigates the individual machine energy functions from the perspective of the invariance theory. The need for a physical basis for using the individual machine energies as a criterion of stability is pointed out since it is shown that the individual generator energy function is not a Lyapunov function. Hence the latter part of the chapter is devoted to the argument that, if the maximum magnetic energy coupling, available to decelerate the machine, is exceeded, then this particular generator and the accelerated group both lose stability. The algorithm in [16] is argued to measure this maximum magnetic energy for deceleration by determining the maximum potential energy over time for a fault on trajectory. This maximum potential energy is then used as a threshold on the individual generator's kinetic and potential energy at clearing to determine a boundary of stability.

A method for determining the critical generator that dictates the stability of the accelerated group, which is the single generator or group of generators that lose synchronism together at the smallest clearing time, is then indicated. The critical generator in this accelerated group is then argued to be the last generator in the accelerated group to cross its potential energy boundary that partially decouples the strong connection between this generator and the rest of the system.

In Chapter 5, two algorithms based respectively on a "Local Kinetic Energy Condition" and "Local Equal Area Condition" existing between the critical generator and the rest of the system is introduced and justified based on physical arguments. The Local Kinetic Energy Condition states that the kinetic energy of the critical generator approaches zero at some time after fault clearing if the system is stable. This condition is based on the physical reasoning that, if the critical generator is observed to reverse the direction of motion caused by the fault, then the system is stable. This reversal of the direction of motion can but not necessarily occur if the kinetic energy approaches zero. Thus, a zero of kinetic energy is assumed to indicate a reversal of the direction of motion although such a change in direction of motion need not occur in all cases. If the multimachine system is analogous to the single-machine infinite bus, then a zero in kinetic energy followed by an increase in kinetic energies will always indicate a reversal of the direction of motion of the critical generator and thus retention of stability.

The Local Equal Area Condition is based on the fact that the accelerating potential energy becomes increasingly negative during the fault period and decreases toward zero for the deceleration in the post-fault period. The Equal Area Condition requires the potential energy to reach a maximum value of zero at some time after fault clearing and then oscillate to some steady state value if and only if the system is stable. This condition indicates all the fault acceleration energy caused by the difference in torques between generators during the fault on period is extracted by differences in decelerating torque between generators in the post-fault period. A loss of stability is indicated by a potential energy time record that has a maximum that is less than zero after which the energy decreases rapidly.

This Local Equal Area Condition is observed to be the potential energy analog of the Local Kinetic Energy Condition. The algorithms are then implemented and tested on the Reduced Iowa System consisting of 17 generators and 163 buses. Simulation results are presented and indicate the extreme accuracy of the algorithms and their significant promise for the future.

6.2 Topics for Future Research

Based on the development of the first five chapters, it is concluded that, in using the direct methods of transient stability, the energy behavior of a particular individual machine (critical generator) is the determining factor in accurately estimating the region of stability (critical clearing time). It is believed that the contents of the preceding chapters serve as a basis for understanding why and how an accelerated group of generators lose stability. The results of Chapters 3, 4 and 5 are extremely promising and could be further investigated as follows:

(1) development of a method for determining the accelerated group and the critical generator without simulating the system for the particular fault and analyzing the individual generator energy function time records

(2) development of computationally efficient algorithms for implementing the algorithms based on the Local Equal Area Condition, Local Potential Energy Condition, or the Local Kinetic Energy Condition without simulation of the system and thus integration of the differential equations. Three approximations

- Taylor series
- cosine function
- faulted rms coherency measure

exist that could be used to obtain the information about the system state trajectory required to implement these algorithms without simulation.

(3) extensive verification of the algorithms developed on several different example systems and extensive fault cases to determine if there are special cases for which these algorithms fail

(4) extension of the algorithms to energy functions which do not assume constant impedance load models and networks aggregated to internal generator buses. Constant current, constant power, and equivalent dynamic load models could be considered. The network model utilized may be the actual network rather than the aggregated network back to generator internal buses

(5) extension of the algorithms developed in this thesis to nonclassical transient stability models.

This work will take continued effort over several years to obtain practical and widely accepted algorithms for direct stability assessment, but it is believed that the foundation for this development finally exists after 35 years of effort.

7. BIBLIOGRAPHY

1. V. Venikov, "Transient Processes in Electrical Power Systems," MIR Publishers, Moscow, 1977.

2. A. A. Fouad, "Stability Theory-Criteria for Transient Stability," Conference Paper, Presented at "Systems Engineering for Power: Status and Prospects." Heniker, New Hampshire, Aug. 17-22, 1975.

3. R. L. Sullivan, "Power System Planning," McGraw-Hill, Inc., 1977.

4. T. Athay, V. R. Sherket, R. Podmore, S. Virmani and C. Pnech, "Transient Energy Stability Analysis," Systems Engineering for Power: Engineering Operating State Control. U.S. Department of Energy, Publication No. CONF-790904-PL.

5. P. C. Magnuson, "The Transient-Energy Method of Calculating Stability," IEEE, PES 1947, volume 66, pp. 747-755.

6. P. D. Aylett, "The Energy-Integral Criterion of Transient Stability Limits of Power Systems," IEEE, July 1958, pp. 527-536.

7. A. H. El-Abiad, K. Nagappan, "Transient Stability Regions of Multimachine Power Systems," IEEE on PES, Feb. 1966, pp. 169-179.

8. F. S. Prabhakara, A. H. El-Abiad, "A Simplified Determination of Transient stability Regions for Lyapunov Methods," IEEE, PAS-94, March/April 1975.

9. K. Uyemara et al., "Approximation of an Energy Function in Transient Stability Analysis of Power Systems," Electrical Engineering in Japan, Vol. 92, No. 6, pp. 96-100, Nov./Dec. 1972.

10. C. J. Tavora, O. J. M. Smith, "Equilibrium Analysis of Power Systems," IEEE, PAS, pp. 1131-1137, May/June 1972.

11. N. Kakimoto, M. Hayashi, "Transient Stability Analysis of Multimachine Power system by Lyapunov's Direct Method," Conference on Decision and Control, 1982.

12. N. Kakimoto et al., "Transient Stability Analysis of Electric Power System via Lure Type Lyapunov Function, Parts I and II," Tran. IEE of Japan, Vol. 98, No. 516, May/June 1978.

13. A. A. Fouad, "Transient Stability Margin as a Tool for Dynamic Security Assessment," Prepared for EPRI, RP 1355-3.

14. S. E. Stanton, "Assessment of the Stability of a Multimachine Power System by Transient Energy Margin," Ph.D. Dissertation, Iowa State University, Ames, Iowa, 1982.

15. A. A. Fouad, S. E. Stanton, "Transient Stability of a Multi-machine Power System, Part II: Critical Transient Energy," IEEE, PES, Winter 1981.

16. A. N. Michel, A. A. Fouad, Vijay Vittal, "Power System Transient Stability Using Individual Machine Energy Functions," Iowa State University, to appear in IEEE Transaction of Circuits and Systems.

17. G. C. Gupta, "Transient Security Assessment of Power Systems by Pattern Recognition and Lyapunov's Direct Method," Purdue University, Aug. 1976.

18. P. M. Anderson and A. A. Fouad, "Power System Control and Stability," Iowa State University Press, Ames, Iowa, 1977.

19. C. J. Tavora and O. J. M. Smith, "Characterization of Equilibrium and Stability in Power Systems," IEEE Transaction, Vol. PAS-91, 3, pp. 1127-1145, May/June 1972.

20. J. L. Willems, "Stability Theory of Dynamical Systems," John Wiley and Sons, Inc., New York, 1970.

21. M. A. Pai, "Power Systems Stability, Analysis by the Direct Method of Lyapunov's," North-Holland Publishing Company, 1981.

22. O. I. Elgerd, "Electric Energy Systems Theory," McGraw-Hill, Inc., New York, 1971.

23. M. A. Pai, "Transient Energy Analysis of Large Scale Power Systems, A Tutorial Survey," Presented at University of Illinois, Feb. 1980.

24. R. K. Miller and A. N. Michel, "Ordinary Differential Equations," Academic Press, New York, 1982.